SINTERING OF 316L AND 434L STAINLESS STEELS AND THEIR BASED COMPOSITES

By
Pradyot Datta

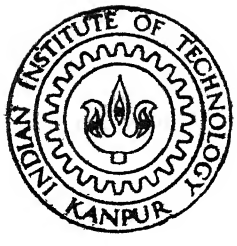

Department of Materials and Metallurgical Engineering
INDIAN INSTITUTE OF TECHNOLOGY KANPUR
June, 1998

SINTERING OF 316L AND 434L STAINLESS STEELS AND THEIR BASED COMPOSITES

A Thesis Submitted

in Partial Fulfilment of the Requirements

for the Degree of

Master of Technology

by

Pradyot Datta

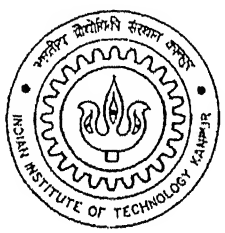

to the

DEPARTMENT OF MATERIALS AND METALLURGICAL ENGINEERING

INDIAN INSTITUTE OF TECHNOLOGY KANPUR

June, 1998

MME-1990-M-DAT-SIN

This thesis is dedicated to

MY PARENTS....

CERTIFICATE

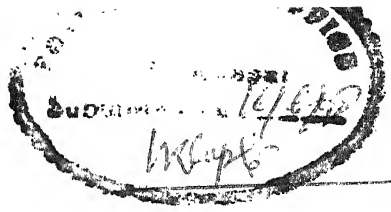

It is certified that the work contained in the thesis entitled **Sintering of 316L and 434L Stainless Steels and Their Based Composites** by **Pradyot Datta**, has been carried out under my supervision and to the best of my knowledge this work has not been submitted elsewhere for a degree.

13-6-98

Dr. G. S. Upadhayaya
Professor
Department of Materials and
Metallurgical Engg.
Indian Institute of Technology,
Kanpur.
June,1998

Acknowledgements

I am taking this privilage to tender my deepest reverence and heartiest gratitude to my thesis supervisor Prof. G.S. Upadhyaya for his earnest involvement, competent guidance and lively impetus without which it would not have been possible to complete this venture.

I want to express my gratitude to M/S K.P. Mukherjee, S.K. Jain and S.C. Soni for their everyday help for this work. Thanks are due to my labmates also.

I must not forget to thank my all friends who have always stood by me during hour of need and whose presence around me gives inspiration to take on venture like this. Special thanks are due to Anirban and Kousik. I also want to thank Sudip, Dhiman, Rajib, Tanmoy, Dobriyal, Suwasji and Pavitrada for their charming presence which made my entire stay at IIT Kanpur meaningful.

Last but not the least, it is appropiate to remember the sacrifices, patience, tolerence and moral support of my brothers and sister without which I could not have reached to this stage of my life.

Pradyot Datta
IIT, Kanpur
June, 1998.

Abstract

Among various grades of stainless steels used in powder metallurgy, 316L austenitic and 434L ferritic grades are the most widely used ones. In the present investigation, 316L and 434L stainless steel powders were cold compacted and sintered in hydrogen, nitrogen or in vacuum atmosphere.

P/M 316L stainless steel has good mechanical strength as well as corrosion resistance; its strength can be further increased by increasing N_2 content. Effect of N_2 content and particle size on the sintered properties of 316L have also been studied.

Although some work has been reported on sintered austenitic and ferritic steels, but no work is available for austenitic-ferritic duplex stainless steels. Significance of developing such alloys is their outstanding combination of properties which results from microstructural composition of ferrite and austenite. With this in view, premixes of 316L and 434L with varying proportions (20-80w/o) were mixed followed by cold compaction and sintering. It is expected that ternary additions will improve sintered properties. So, 2 mass % copper was also mixed with the premixes.

To impart wear resistance and high densification Cr_3C_2 (10v/o) and CrB (0-4w/o) were mixed respectively with the straight stainless steels.

Powders were cold compacted using a pressure of 600MPa and then were sintered in the temperature range of 1150°C to 1350°C for 1hr in H_2 atmosphere.

Sintered density, densification parameter, microhardness, grain size, coerccivity and magnetic saturation were measured. TRS, wear testing and corrosion weight loss in 1(N) H_2SO_4 for an exposure time of 360 hrs were also carried out for some selected samples.

Improved densification was observed in 434L after 1350°C sintering, 316L-40w/o 434L after 1350°C and composites with at least 2w/o CrB after 1250°C. TRS value was maximum

for 316L-60w/o 434L composite whereas sliding wear loss was minimum for straight 316L. Copper addition in 316L-434L composites was found to increase densification and to decrease microhardness, coercivity, magnetic saturation and corrosion resistance of all the composites. But copper addition was found to increase corrosion resistance of straight stainless steels.

Contents

List of Figures

3.6 Magnetic properties variation of 316L and 434L stainless steels sintered at 1250°C in different atmospheres.

3.7 Particle size distribution of various stainless steel powders.

3.8 Properties of 316L (AMETEK) and 316L(ANVAL) sintered at 1350°C in H_2 for different periods.

3.9 Optical microstructures of 316L (AMETEK) and 316L(ANVAL) sintered at 1350°C for 1 hr in H_2. AMETEK - (a) + 230 mesh, (a) + 270 mesh; ANVAL - (c) + 230 mesh, (d) + 270 mesh.

3.10 Properties variation of 316L-434L composites sintered in H_2 at different temperatures.

3.11 Optical microstructures of 316L-434L composites sintered at 1350°C in H_2. (a) 0w/o 434L, (b) 20w/o 434L, (c) 40w/o 434L, (d) 60w/o 434L, (e) 80w/o 434L, (f) 100w/o 434L.

3.12 Sliding wear loss of 316L-434L composites sintered at 1350°C in H_2 with respect to sliding distance.

3.13 Scanning fractographs of 316L-434L composites sintered at 1350°C in H_2. (a) 60w/o 434L and (b) 80w/o 434L.

3.14 SEM pictures of worn out surfaces of sintered stainless steels and their composites after sliding wear testing for 1650 m. (a) 0w/o 434L, (b) 20w/o 434L, (c) 40w/o 434L, (d) 60w/o 434L, (e) 80w/o 434L, (f) 100w/o 434L.

3.15 Magnetic properties variation of 316L-434L composites sintered at different temperatures in H_2.

3.16 Corrosion weight loss variation of 316L-434L composites in 1(N) H_2SO_4 after various exposure times. Sintered at 1350°C for 1 hr in H_2.

3.17 Properties variation of 2 mass % copper containing 316L-434L composites sintered at 1350°C in H_2 for 1 hr.

3.18 Optical microstructures of 316L-434L composites with 2 mass % copper sintered at 1350°C in H_2 for 1 hr. (a) 0w/o 434L, (b) 20w/o 434L, (c) 40w/o 434L, (d) 60w/o 434L, (e) 80w/o 434L, (f) 100w/o 434L.

3.19 Corrosion weight loss variation of copper containing 316L-434L composites in 1(N) H_2SO_4 after various exposure times (sintered at 1350°C in H_2 for 1 hr).

3.20 Properties variation of 316L and 434L stainless steels containing 10v/o Cr_3C_2 sintered at different temperatures in H_2.

List of Tables

Chapter 1

Literature Review

1.1 Introduction:

Stainless steels are iron base alloys that contain a minimum of approximately 11% Chromiur Few stainless steels contain more than 30% Cr or less than 50% Fe. They achieve the stainless characteristics through the formation of an invisible and adherent chromium ric oxide surface film. This oxide forms and heals itself in the presence of oxygen. Oth elements added to improve particular characteristics include Ni, Mo, Cu, N_2, S, Se. Carbo usually present in amounts ranging from less than 0.03% to over 1% in certain martensit grades. Figure 1.1 provides a useful summary of some of the composition and propert linkages in the stainless steel family [1]. Table 1.1 gives designations, grades, compositio of some widely used stainless steels. With specific restrictions in certain types stainle steels can be fabricated and shaped by P/M techniques. The main applications are in th automotive, marine, and aerospace industries, house hold applications, office supplies, leisu and recreation, medical instruments, hardware, jewelry [2]. The reason for its use in all case is same, economics. As maintenance costs per hour increase, stainless steels can be used t reduce maintenance hours [3].

Stainless steels in the past have been divided into four main classes: Martensitic, which ar straight chromium grades that can be hardened by quenching; Ferritic, which are straigh chromium grades not hardenable by conventional quenching and Austenitic which contai sufficient nickel or nickel plus manganese to produce a face centered cubic structure [4] Finally, Duplex austenitic-ferritic stainless steels which have found increasing use as the constitute a set of materials which have properties that are compromise between those o purely ferritic steels, which tend to have low toughness and austenitic steels over which the

exhibit superior stress corrosion resistance [5]. Also the two phase alloy is not sensitiv to intergranular attack in various corrosive media. However, these steels have considerabl difficulties from the point of view of their manufacture, due to precision in the chemica composition and temperature control needed [5]. The existence of such difficulties serves t make P/M an attractive manufacturing option.

The production of sintered stainless steels parts demands more attention than othe sintered ferrous alloys, from powder selection up to final sintering, mainly in this last stag of the process due to influence of temperature and time on the sintering operation and o furnace atmosphere used during sintering. Sintered stainless steel components account fo just 3wt% [6] of the market for P/M iron and steel parts. Market has been limited for variet of reasons

i. Owing to its high alloy content the powder is expensive.

ii.Compressibility of fully prealloyed stainless steel powder is far inferior compared to tha of unalloyed iron powder as a result of solid solution hardening [6].

iii. Sintering conditions require more attention than those for standard sintered steels.

The compaction behaviour of stainless steel powders also depend to some extent on the powde manufacturing process or on the details of chemical composition. All ferrite martensite grade can practically transform to martensite after solidification even if only minute amount of ni trogen or carbon dissolved into the melt. Martensite must be transformed into ferrite b an annealing step to render the powder compressible. High densities can be achieved b sintering with shrinkage or by double pressing and double sintering.

During presintering chromium steels can absorb N_2 which adversely affects recompact ability. Surface oxide layer which forms during water atomization must be reduced durin sintering to achieve good ductility and strong sintering bonds [7]. The oxide is presumed t be predominantly chromium oxide containing silicon atoms. The plots (Figure 1.2) based o thermodynamic data give an estimate of the dew point required to reduce chromium oxide Dew point should be selected in such a manner so that chromium oxide can be reduced a prevailing sintering temperature and atmosphere.

Table 1.2 summarizes the mechanical properties of various grades of sintered stainles steels [8].

1.2 Powder Production

Currently stainless steel powders are produced by atomization process. Melting of raw metals is carried out in air or vacuum induction furnace. Low manganese concentrations (< 0.3%) and deoxidation with ferrosilicon to achieve 0.7 to 1% Si in the alloy prevent oxidation of the powder during water atomization. Typical water pressure for producing predominantly -80 mesh powder is about 14 MPa [9]. Gas (N_2, Ar) atomized stainless steel powders have particles spherical in shape. They have high apparent densities of about 5 g/cm^3 and excellent flow rates. Oxygen contents are less than 200 ppm. Chemical compositions are similar and identical to conventional wrought grades. Water atomized powders have apparent density ranging from 2.5 to 3.2 g/cm^3, adequate green strength and reasonably good compressibility. Dauzenberg and Gesell [10] reported an improvement in compactibility of Mo-containing austenitic stainless steel powder to about 0.12 Mg/m^3 when it was annealed in H_2 at 1050°C.

1.3 Sintering Variables

Powders are generally compacted at a pressure of 600 MPa to 1000 MPa to achieve green densities in the range of 5.9 Mg/m^3 to 6.9 Mg/m^3. However for certain grade of stainless steels like ferritic stainless steel, it is very difficult to get densities higher than 6.5 Mg/m^3 and pressure beyond 900 MPa does not improve density. Prior to the actual sintering operation the lubricant, which is used with the prealloyed powder to permit compaction of the powder and the ejection of the part from the die, must be removed [11,12]. Residual lubricant carbon deposits have highly adverse effects when stainless steel is sintered, resulting in lower corrosion resistance. Incomplete carbon removal results in an elevated level of carbon in the part. This, when coupled with relatively slow cool following sintering, results in sensitization. This is the precipitation of chromium rich carbides at the grain boundaries leaving the surrounded matrix depleted in chromium and subjected to corrosion attack. Complete lubricant removal is therefore critical if best corrosion resistance is to be attained [13]. Maximum lubricant burn off is achieved in the temperature range of 425°C to 540°C. Burn off is less controllable in dissociated ammonia [14].

Stousy [15]; and Ambs and Stousy [16] carried out a thorough investigation of the sintering of various stainless steel powders and gave ample details in establishing the sinterability of stainless steels. Shaw and Honeycombe [17] investigated the sintering behaviour of austenitic stainless steel powders. Imai and Hirotani [18] carried out sintering of 13Cr-ferritic steels,

austenitic and martensitic steels. Fleming [19] also reported sintering behaviour of various grades of stainless steel powders.

The sintering characteristics of different grades of stainless steel are more or less similar. Nickel decreases the sintering rate, whereas ferrite stabilizing elements like silicon, molybdenum increase it. The sintering rate is faster for ferritic stainless steel than austenitic one because of its bcc structure, where self diffusion is much faster than fcc austenitic stainless steel [20-21], for example in pure iron at 1183K $D\alpha/D\gamma$=330 [17]. Depending on the production methods, it is useful to anneal stainless powder in hydrogen atmosphere around 700-800°C to improve compressibility [10].

1.3.1 Effect of Sintering Temperature and Time

stainless steel parts are generally sintered at temperatures ranging from 1100-1500°C [22-26]. High temperature sintering gives improved mechanical and corrosion resistance properties. oxygen content and graphite additions are also factors in high temperature sintering. Density variation tolerances which yield acceptable parts after conventional sintering need to be tightened for sintering at such higher temperature range. Higher sintering temperature imparts better mechanical properties in stainless steels. Various authors [1,13,27-29] reported an increase in ultimate tensile strength and percentage elongation with increase in sintering temperature whereas yield strength and hardness show a decreasing trend. Low temperature sintering results in better dimensional control due to less severe shrinkage [30-31]. In spite of that one has to go for high temperature sintering when one needs higher densification.

Sintering time varies from one hour to several hours under suitable atmosphere. However, with an increase in sintering time both tensile and yield strength along with percentage elongation increase though the major change occur in the first thirty minutes to three hours. The effect of sintering time and temperature on tensile and yield strengths of 316L have been shown in Figure 1.3. The general conclusions are applicable to other grades of stainless steels.

After the reduction of surface oxides in the initial stage of sintering, particles bond together by solid state diffusion. This is followed by a gradual increase in the amount of bonding and an increase in grain size. The two phenomena occur simultaneously but their rate of growth is influenced differently by sintering time and temperature. As the bond areas increase, yield and tensile strengths increase.

1.3.2 Sintering Atmosphere

The atmosphere during sintering is a very critical factor for the properties of sintered products. The available literatures [10,12,22,23,29,31,32,34-37] recommend the use of following sintering atmospheres for stainless steel powders.

- Argon
- Hydrogen
- Vacuum
- Dissociated Ammonia
- Nitrogen

Argon is a neutral and best sintering atmosphere for certain grades of stainless steels like 316L. Hydrogen is the most strongly reducing atmosphere of all commercially available sintering atmospheres. The principal disadvantage of using hydrogen is higher cost. Typically the ratio of hydrogen to water vapour determines the extent of surface chromium oxide reduction during sintering and cooling. But to maintain reducing conditions in actual practice a dew point of at least -35°C to -40°C is required in the furnace. As water vapour is formed during reduction, a sufficient amount of gas flow is required to continually remove this water, as well as the water that is formed by the reaction between the hydrogen and the oxygen introduced with the parts and through furnace openings. High temperature sintering in hydrogen atmosphere is sometimes used for processing 410L martensitic stainless steel. Typical processing conditions call for sintering at 1260°C for 45 minutes in 100% H_2 at a dew point of -35°C.

The acceptance and wide usage of vacuum sintering is increasing, largely because of energy conservations and ecological considerations. The vapour pressure of some elements (such as chromium) at the sintering temperature is near the pressure that can be achieved in commercial vacuum furnaces equipped with mechanical pumping systems [38]. Chromium evaporates if the furnace pressure falls below its vapour pressure and the corrosion resistance is seriously reduced. The required composition control is achieved by back filling the vacuum vessel with a suitable gas (Ar, N_2) to a partial pressure above the vapour pressure of any of the elements in the alloy. If argon is used as back fill gas, the mechanical properties are similar to those obtained in hydrogen [39,40]. When N_2 is used for backfilling, the

sintered properties are comparable to those achieved in dissociated ammonia. A circulating gas quench is recommended to provide desired high cooling rate and the gas composition should be same as that used for maintaining a partial pressure during heating or soaking.

When stainless steels are sintered in dissociated ammonia, a dew point of -45°C to -50°C is required to prevent oxidation. The oxidation/reduction curve for Cr_2O_3 (Figure 1.2) shows that lower dew points are required at lower temperatures if a reducing environment is to be maintained.

Many parts can be sintered successfully in nitrogen based atmosphere with as little as 3% H_2 in the atmosphere in contrast to the 75% in dissociated ammonia. Slow cooling results N_2 pick up because of reduced N_2 solubility below about 1095°C. Chromium nitride precipitates below this temperature.

1.3.3 Cooling Rates

Regardless of the sintering atmosphere the rate of cooling from sintering temperature has a significant role on the properties of sintered stainless steels. Depending on the rate of heat extraction different cooling rates are designated in literature [24,32] as follows ; slow cooling 20°C/min, medium or normal cooling rate 63°C/min and fast cooling rate 250°C/min. All stainless steels contain some carbon and when dissociated ammonia is used N_2 is also present. The amount of these elements normally present is beyond the limits of room temperature solubility. During cooling carbides and nitrides tend to precipitate in the form of fine particles. With extremely slow cooling such as furnace cooling, precipitation occurs preferentially at grain boundaries. As a result, there is a noticeable increase in strength and loss in ductility, even though the amount of precipitate is minimal. With normal cooling rates (10 to 30 min) used in typical P/M production, less precipitation occurs at grain boundaries. Consequently strength is lower but ductility is higher. Rapid cooling, such as obtained by water quenching, suppresses the precipitation of carbides and nitrides which produces maximum ductility.

1.4 Effect of Various Elements on Sintering of Stainless Steels and their Properties

1.4.1 Nitrogen

N_2 detoriates the corrosion resistance of stainless steels. N_2 containing atmosphere results in the absorption of considerable amounts of N_2 along with an increase in strength, a decrease in ductility and a decrease in corrosion resistance [41,42]. The corrosion always changes abruptly from relatively high corrosion resistance to low corrosion resistance at about 0.4% absorbed N_2 as shown in Figure 1.4. In order to avoid significant corrosion of sintered parts N_2 content should be no more than 0.4% and preferably no more than 0.3% [42]. As corrosion begins at the surface N_2 content of the surface should be controlled to obtain an optimum combination of corrosion resistance and mechanical properties. Zoning technique lowers N_2 pick up of stainless steels [43]. This technique permits introduction of N_2 in the furnace both before and after the hot zone using separate inlets. The mixtures range from 20% to 100% H_2. If the overall flow is kept same, it has been found that N_2 can be maintained at the 0.3% level with 40- 45% H_2 for zoned practice which is about half of what is required to the unzoned atmosphere approach. Theoretically, all chromium can be precipitated as lamellar chromium nitride if exposure to nitrogen or dissociated ammonia in the stability range of Cr_2N is long enough. This has been presented with the help of a schematic diagram shown in Figure 1.5 [44]. Cr_2N formation can be avoided if rapid cooling from sintering is done because rapid cooling maintains a lower N_2 absorption level and therefore avoids Cr_2N precipitation. N_2 containing atmosphere can be used for sintering stainless steels without affecting their corrosion resistance, provided high sintering temperature, low dew point and rapid cooling are employed.

1.4.2 oxygen

As water atomization is the most viable and cost effective route for production of stainless steel powder surface oxide formation is inevitable [45,46]. The oxides form on the powder surfaces usually make up the total O_2 content of the water atomized steel [47].
Melt temperature and O_2 content in the atomized chamber are also important factors for determining the O_2 content of the powder. Alloy composition has a strong effect on the oxide content. O_2 content is raised by Mn and Cr and is lowered by C and Si. O_2 decreases tensile strength. By mixing carbon with steel powders and sintering at vacuum O_2 content can be

reduced. Moreover material with added carbon shows best UTS elongation to fracture and impact energy when sintered at high temperature. The inter particle bonding with graphite and powder mixture is significantly enhanced due to the effective removal of surface oxides. It is supposed that the reduction of surface oxides in the presence of carbon takes place via the overall reaction C(S)+MeO→ Co(g)↑ + Me. Oxygen can also be removed during sintering beginning at the surface by selecting adequate dew points. At high dew points oxygen content of the part may get increased during sintering. In this case, oxide layers on the atomized particles are never reduced, bulk diffusion and sintering are slowed down and prior particle boundaries remain as it is. Such parts exhibit low sintered strengths. Moreover merely dew point selection does not guarantee lower oxygen content in the sintered parts. A dew point which is reducing during sintering may become oxidizing at some point during cooling as illustrated in Figure 1.6 [48]. It is important that the cooling rate is fast enough to prevent oxidation because a bright appearance may not be sufficient evidence of a good dew point and cooling rate, as detrimental oxide layers are too thin to be seen.

1.4.3 Carbon

Carbon is normally present in amounts ranging from 0.03% to over 1.0% in certain martensitic grades. To retain low carbon content after sintering (for certain austenitic grade steels) which ensures maximum corrosion resistance and machinability, carbon pick up must be avoided. The solid lubricant used for pressing must be completely removed by presintering because stearates and waxes are a source of carbon. Other common sources of carbon include soot, residual lubricant in the furnace and traces of previous furnace atmosphere. Dissociated ammonia and hydrogen atmospheres develop a carburizing potential when small amounts of residual carbonaceous materials present in the furnace. Care must be taken to ensure that the furnace is clean and that the atmosphere is pure. Carbon content also determines the amount of various phases in stainless steel. Figure 1.7 shows the influence of carbon content upon the phases in an Fe-Cr alloy containing 20% Cr [37]. Moreover because of decreasing carbon solubility with decreasing temperature grain boundary precipitation of carbon as Cr-rich carbide ($M_{23}C_6$) with attendant Cr depletion occurs during cooling in the sintering furnace for materials with carbon contents exceeding 0.03%. The Cr depleted regions will exhibit inferior corrosion resistance.

1.4.4 Chromium

Chromium content determines the corrosion resistance of stainless steels and it varies from 11 to 30% to various stainless steel grades [49,50]. The higher is the Cr content the higher is the corrosion resistance. However Cr impoverishment due to improper sintering conditions can affect the corrosion resistance of steels severely. It will be appreciated however that a substantially drier gas would have to be used in practice for reduction of Cr_2O_3 to proceed. Such a reaction proceeds more quickly in the presence of iron, presumably because the metallic Cr formed is taken into solution. During sintering in vacuum, the pressure should be maintained in such a fashion so that Cr can not get distilled off.

1.4.5 Nickel

Nickel content may vary from 0% to 10-14% [50,51] in stainless steels. In certain martensitic grade steels there stays no nickel at all. In certain austenitic grade steel Ni may be present as high as 10.5% to 14% [49]. However for austenitic stainless steels Ni increases the compressibility of powders up to at least 4% [52]. Ni improves corrosion resistance of stainless steels and controls various phases in it. Moreover addition of elemental nickel powder activates the sintering process and increases density by decreasing total and open interconnected porosity due its high diffusion rate. It can also reduce interconnected porosity by forming liquid phase which changes pore morphology and thereby increases corrosion resistance. Furthermore, a sufficient stable passivation layer can be expected as a result of moderate cathodic activity and low cathodic overpotential [53].

1.4.6 Tin

Recently developed tin containing stainless steels have shown less sensitivity to nitride precipitation and improved corrosion resistance. Beneficial effect of tin is that it attributes to an enrichment of surfaces of both the water atomized powder and the sintered part from it, presumably as a result of low solubility of tin in solid stainless steel. It can also form stable acid resistant passive films in a crevice and may cause cathodic surface poisoning, but its major beneficial effect is believed to lie in its formation of an effective barrier to N_2 diffusion [54]. Moreover presence of tin facilitates reduction of silicon oxide. So, the beneficial effect of tin on corrosion resistance may come from lower O_2 contents as well as its electrochemical properties (high hydrogen overvoltage) and good acid resistance of its oxide [55].

1.4.7 Copper

Cu contributes a lot to improve the corrosion resistance of stainless steels [56-57]. If Cu content increases, strength of the material decreases. Porosity is affected both by the compacting pressure and the Cu content [56]. In the later case, the increase in volumetric fraction of pores is induced by swelling during sintering of Fe-Cu which is responsible for distribution of pore areas over a wide range. But in an increase of sintering time, Cu content does not lead to any appreciable spherodization of pores. As far as Cu is concerned the microstructure characterization shows that it is homogeneously diffused in base 316L stainless steel. At highest Cu content(9wt%) as solubility limit is reached, some free Cu may remain after sintering. Cu can reduce N_2 content of steel by acting as a shield for N_2 diffusion. % Elongation and UTS both decrease with increase in Cu content. So it is possible to optimize the processing of Cu alloyed sintered stainless steel.

1.4.8 Silicon

Introduction of Si in austenite stainless steel powder produces duplex stainless steel [58-59] with mixed austenite-ferrite structure. The volume fraction of induced ferrite phase increases with increasing Si content [58]. Si is chosen as an additive to promote the densification rate because of its strong effect in introducing and stabilizing the ferrite phase in the microstructure. Si powder activates the sintering process through the introduction of eutectic liquid and formation of liquid δ ferrite [60]. Generally the sintered density increases with increasing Si content and sintering temperature. Density is higher for those sintered in vacuum than those sintered in H_2. This is because of reduction of surface oxides by the reaction
$Si + SiO_2 \rightarrow 2SiO(g)\uparrow$. The reduced and clean surface will enhance the rate of sintering as the reaction between Si and stainless steel powder enhance. Hardness also increases monotonically with the increase in Si content as it is an effective solid solution hardener and strength of ferrite [~350Hv(25g)] is higher than that of austenite [~230Hv(25g)] [59] in duplex stainless steel. Tensile strength increases with increasing Si content owing to higher hardness and strength of ferrite (Figure 1.8). At the same time % elongation decreases with increasing Si content since bcc ferrite is inherently less ductile than fcc austenite. The corrosion resistance in 10% $FeCl_3$ solution increases with increasing ferrite volume fraction, the austenite phase being attacked preferentially in this medium. High temperature oxidation resistance of these alloys is greatly improved by increasing the Si content as both the internal oxidation and the growth of oxide scale are inhibited by Si enrichment in the sub layer of the scale located

at the alloys interface. But high Si content accelerates precipitation of sigma phase, which detoriates toughness.

1.5 Magnetic Properties

The magnetic behaviour of stainless steels varies considerably ranging from paramagnetic (nonmagnetic) in fully austenitic grades, to hard or permanent magnetic behaviour in the hardened martensitic grades to soft magnetic properties in ferritic stainless steel. Although their magnetic properties are not generally as good as conventional magnetic alloys, they have been successfully used for magnetic components that must withstand corrosive environments. In addition some stainless steels like ferritic stainless steels may be cost effective alternative to silicon iron components due to their high electrical resistivity.

Like other properties, magnetic properties of a P/M are also determined by sintering[61]. Sintering time and temperature should be adjudged carefully to achieve desired level of densification as magnetic induction is a function of sintered density [62,63]. This is because higher sintered density minimizes the effects of macrodefects (i.e residual porosity) to enhance magnetic induction. It also promotes domain wall mobility and thereby causes improvement of magnetic permeability. Accordingly, magnetic properties are directly related to sintering parameters which is very much evident from Table 1.3 [64]. Sintered density is not the sole factor to determine the magnetic behaviour of stainless steels. On the contrary, it has been reported that attempts should not be made to increase sintered density by any means because that may ruin the magnetic properties. It is clear from Table 1.4 that Cu infiltration in a 410L steel has resulted in a very high level of densification and at the same time has ruined virtually all magnetic characteristics of this magnetic material. This is the natural consequence of the presence of non magnetic copper constituent within the structure of ferritic stainless steel.

Residual interstitial elements like carbon, oxygen and nitrogen may have significant impact on coercive force and magnetic permeability as they are structure sensitive properties and microstructures are largely dependent on the above mentioned properties [65,66]. As a result H_2 atmosphere can maximize magnetic properties by reducing those impurities to a very low level [67,68].

1.6 Corrosion Behaviour of Sintered Stainless Steel

Corrosion resistance of any stainless steel is the primary reason of its selection. The passivity of stainless steel is based on an optimum chromium content of at least 12% [69]. However the corrosion resistance of the alloys can be improved considerably when the chromium content is increased to over 16% [70]. But the improved corrosion resistance of these steels does not depend on an increased electrochemical nobility of the alloys themselves compared with that of more common steels. On the contrary, stainless steels are, due to their high chromium content, less noble than steels without chromium [71]. Corrosion resistance of stainless steel is a sum of 'properties' of which the 'ease of passivation' and the 'stability of passivation' are perhaps the most important ones.

As earlier explained stainless steels can exist both in active and in passive states. A uniform corrosion is therefore possible only if the surface of the alloy is activated and not able to passivate again. So depending upon the appearance of the corroded metal it is possible to classify corrosion by the forms in which it manifests itself. First of which is pitting corrosion. This type of corrosion occurs always at localized points or areas. This is, of course, only natural considering the fact that the passive film and the base metal is attacked and further that such attacks are successful only at points with an inferior or defective passive film. Generally, the pitting corrosion occurs due to concentration differences or increased chloride contents in the environment [72]. Another form of corrosion is crevice corrosion. It is the result of intense localized corrosion which frequently occurs within crevices and other shielded areas of the surfaces exposed to corrosives. As the passivity requires continuous repairing of the passive film by some oxidizing elements such as dissolved oxygen, so it is possible that stainless steels become active beneath a deposit or in a crevice where a small volume of stagnant solution is present. This is attributed to the fact that the replenishment of the consumed oxygen is too slow to maintain passivity resulting in localized corrosion [73-75].

Another form of corrosion of serious concern is intergranular corrosion i.e. localized attack at and adjacent to the grain boundaries with relatively little corrosion of the grains. Intergranular corrosion of stainless steels is usually observed in welded construction and more often concentrated among welds. Sometimes faulty heat treatment can lead to relatively uniform intergranular corrosion [76]. Stress corrosion results from a corrosion attack on stressed constructions. This kind of corrosion is favoured by high temperature, chloride containing atmosphere and by alternating evaporation and condensation phenomena on chloride containing surfaces, no matter how small the chloride content is. Stress corrosion cracking very seldom happens in service in sintered stainless steels as sintered material is seldom used

in heavily stressed conditions unless we manufacture tubes or sheets [30].

1.6.1 Role of Iron Contamination

Iron contamination affects the corrosion property of any stainless steels severely. This is because iron particle forms galvanic cell with the passive stainless steel and corrodes anodically in preference to the stainless steel. The build up of initial corrosion product forms a crevice in which oxygen depletion causes acidification of solution inside the part [77]. Iron or iron base powder may contaminate during powder production or during manufacturing sintered part. It may also come during handling or transportation. Corrosion due to such contamination can be avoided if sintering conditions result in alloying of iron in stainless steel matrix [78].

1.6.2 Role of Interstitial Elements

Carbon, oxygen and nitrogen are the major interstitial elements present in stainless steel matrix. Virtually all the properties including corrosion resistance are dependent on these three elements. Stainless steel's corrosion resistance is compromised by nitrogen oxygen or carbon (NOC) when chromium is depleted by NOC precipitates [79]. Precipitation can be avoided if concentration of NOC is maintained below equilibrium. However for nitrogen and carbon it is not always possible to have an amount less than equilibrium. As fast cooling can arrest carbon and nitrogen in solution at concentrations that are not at equilibrium, equilibrium precipitates can not form because lower temperature does not allow atoms like chromium in iron, carbon nitrogen *etc* to rearrange themselves for precipitate formation. The exact solubility limits of carbon and nitrogen depend upon the specific chemistry of the material in question and numerous other factors. As a rule of thumb carbon should be below 0.03% and nitrogen should be below $2500ppm$ [79]. Carbon and nitrogen deplete chromium from the matrix by forming chromium rich carbides ($M_{23}C_6$) and nitrides (M_2N). They form preferentially at grain boundaries. In case of oxygen, as it is present primarily as silicon oxides in the surface, chromium depletion occurs due to reduction of surface silicon oxides during sintering in any atmosphere. Whatever be the cause of chromium depletion it has significant effect on the corrosion resistance of stainless steel. This chromium depletion not only reduces the amount of chromium available to form protective chromium oxide films but also sets up a galvanic couple between chromium depleted region and chromium containing region due to change in chemical potential.

1.6.3 Role of Sintered Density

Though the effect of density on the corrosion resistance is unclear, it is widely believed that the corrosion resistance of P/M stainless steels increases with increasing sintered density [80]. The common explanation is that higher is the sintered density, lesser is exposed surface area over which chromium depletion can occur during sintering by vaporization [81]. In addition,the presence of pores gives rise to crevice corrosion which is enhanced by decreasing density due to the greater amount of pores [82,83]. Contrary to this, Pao & Klar [77] suggested that low density is beneficial from corrosion point of view. They interpreted this effect in terms of facilitated oxygen diffusion in the low density specimens with their larger pore sizes which retards oxygen depletion and acidification. It may be summarized that positive effect of density on corrosion resistance is derived from short term potentiodynamic polarization measurements whereas negative relationships are derived from long term salt immersion tests [84].

1.7 Stainless Steel Based Particulate Composites

1.7.1 Various Processes for Producing Particulate Composites

It has long been known that alloys may be greatly strengthened by introducing a suitable second phase dispersoid in the matrix. Conventional precipitation hardening has been widely used for strengthening purpose. But it has certain disadvantages as it demands the alloy system to show increasing solubility of the second phase with increasing temperature, and the tendencies for overaging to occur with a loss of strength if alloys are heated much above their aging temperature [85,86]. In order to overcome this problem and to prepare very intimate mixture of matrix and dispersoid which is essential to bring out effectiveness of dispersoids, P/M technique is the most suitable one. Various techniques such as surface oxidation [87], internal oxidation [88], reduction technique [89], shotting technique [90], salt decomposition [91], mechanical mixing [92], mechanical alloying [93-94], have been developed to produce particulate or dispersion strengthened alloys. Among all mechanical alloying is one of the most attractive methods because very flexible combination of dispersoids and matrix are possible for the production of composites. In this process the ductile particles are repeatedly flattened, fractured, welded and rewelded [94,95]. The force of the impact deforms the particles entrapped between two grinding balls, and creates new surfaces. The clean surfaces are welded together on forceful contact. Subsequently, higher forces of the mill

promotes increased deformation. Inter-dispersion of the ingredients by this repeated cold working and fracture, ultimately, produces uniform distribution of dispersoids in the matrix [93.95-97].

1.7.2 Austenitic Stainless Steel Based Particulate Composites

Sands *et al* [98] investigated the effect of Al_2O_3, ZrO_2, ThO_2, and TiO_2 additions on a P/M austenitic stainless steel. Alumina content was varied from 5 to 15% whereas other contents were kept fixed to 10v/o. It was reported that higher alumina content was not beneficial to UTS at elevated temperature and a maximum UTS was reported for 5% Al_2O_3. Titania containing alloy had superior strength and creep resistance as compared to the other dispersion strengthened alloys. Better creep resistance of TiO_2 containing alloy was attributed to the lower solubility of TiO_2 in Fe, Cr, Ni, oxides which were present in the stainless steel. Various volume percent of Y_2O_3 (0-8%) had been taken by Lal *et al*[99] as a dispersoid to study their effects on the properties of 316L. It was observed that the sintered porosities were superior for Y_2O_3 containing composites as compared to straight 316L under identical sintering conditions. This was attributed to the chemical interaction of surface oxide Cr_2O_3 on 316L surface with Y_2O_3 dispersoid. It was also observed that 316L-4v/o Y_2O_3 gives maximum tensile strength and ductility. Hardness increases with increase in Y_2O_3 but oxidation resistance decreases with increase in Y_2O_3 addition. Petersen [100] investigated with 316L containing 10 v/o Al_2O_3 or Cr_3C_2. CrB (0-2w/o) was used as an sintering additive. She obtained 99% of the theoretical density for 316L-10v/o Cr_3C_2 composite containing 2w/o CrB when sintering temperature was 1250C°. In this case highest density was achieved with maximum addition (2w/o) but for the composites containing Al_2O_3 and CrB increasing the amount of CrB from 1w/o to 2w/o did not lead to increase in density. Composite with Cr_3C_2 and 2w/o CrB got higher density due to the formation of large amount of liquid phase. She found that sintering temperature had strong effect on strength of the composites. At 1150°C CrB addition had no effect at all on the tensile strength of the composites. But at 1250°C it increased up to 1w/o CrB addition for both the composites. Moreover addition of 1w/o CrB improved elongation for Al_2O_3 containing composite whereas the same was impaired for Cr_3C_2 containing composite. In the later case ductility was poor because of the presence of brittle Cr_3C_2. Besides, M_2B boride based eutectic phase also caused loss in ductility.

In a recent study, Tandon and German [101] investigated the effect of boron addition in 316L. They used up to 1w/o of boron either in elemental form or in combined form for their work. The improved performance of boron doped 316L was attributed to the presence of

eutectic liquid phase at the grain boundaries at a relatively low temperature of 1240°C. The eutectic melt was rich in Mo, Cr, B. They obtained near about full density by sintering at 1240°C for 15 minutes in H_2 atmosphere. But when the temperature was raised to 1250°C a sharp fall in tensile strength was noticed. It was concluded that the process was very much sensitive to sintering temperature typical for supersolidus sintering and the degradation of tensile strength was attributed to rapid grain growth and formation of a brittle phase along the grain boundaries. The authors also observed superiority of NiB as an additive over CrB_2 or FeB when added with 316L. This was explained in terms of pore sizes and their distribution. For NiB addition pores were small and uniformly dispersed throughout the matrix resulting in homogeneous microstructure. However, for either CrB_2 or FeB addition inhomogeneous microstructures were generated with large pores and undesirable precipitate network along the grain boundaries. Another important observation was that 0.5% addition of NiB or elemental boron with 316L exhibited similar tensile strengths because both could produce same type of homogeneous microstructures up to that point. But when the addition was increased to 1w/o, elemental boron doped 316L showed higher tensile strength and % elongation than NiB addition as the homogeneity of microstructure was retained in the former case. The authors also observed that stainless steel with 0.5w/o added boron was more corrosion resistant than stainless steels with no boron. The difference in pitting behaviour of the two alloys was due to the presence of small pores in the steel with no boron compared to the stainless steel containing 0.5w/o boron which did not evidence any pores.

1.7.3 Ferritic Stainless Steel Based Particulate Composites

Al_2O_3, ZrO_2, MgO, Y_2O_3, TiO_2, Nbc, in ferritic stainless steel have been used as dispersoids by various research workers [102-112]. Imai and Hirotani [17] developed 13% Cr-1% Si-0.05% Al-Al_2O_3 composites. The stainless steel powder and 15v/o Al_2O_3 were mixed heated in H_2 at 1100°C compacted at 500 MPa, presintered at 800°C for 2 hours and then were sintered at 1350°C for 4 hours in H_2. The sintered alloy consisting 15v/o Al_2O_3 showed a marked superiority in tensile strength, being about 4 times stronger than cast alloy, at 1150°C though the elongation was decreased.

Daikoku *et al* [102-103] followed mechanical mixing route for developing two Al_2O_3 strengthened ferritic stainless steels using liquid phase sintering. Both steels showed higher creep strength than that of wrought steels without Al_2O_3. Borok *et al* [104] developed Kh13M2 steel (13Cr-2Mo) strengthened with Al_2O_3. With 3% Al_2O_3 rupture stress of this alloy at 700°C was increased approximately 50%. Denisenko and Asbroeck [105] added 2%

TiO_2 in Fe-13Cr steel to obtain better creep strength. The research workers in the aircraft engine group of General Electric Company (U.S.A) conducted a series of investigation [106-111] aimed at improving the strength of Fe-Cr-Al-Y alloy by dispersion strengthening. Long time hot corrosion testing indicated that alloy 2541 (ODS-Fe-25Cr-4Al-1Y) was extremely corrosion resistant.

Mukherjee and Upadhyaya [112] investigated 434L ferritic stainless steel particulate composites with different volume fraction of Al_2O_3 (0-8v/o). They obtained an optimum overall properties for ferritic stainless steel with 4-6v/o Al_2O_3. They also showed higher yield strength, ultimate compressive strength and tensile strengths for Al_2O_3 containing composites as compared to straight ferritic stainless steel. The authors further studied 434L-Al_2O_3 composites by adding transition metal (Nb,Ti)[113] and obtained higher tensile strength and ductility for transition metal containing composites as compared to straight composites.

1.8 Scope of Present Investigation

316L and 434L are two important members of stainless steel family because the former being austenitic is used widely due to its proven corrosion resistance whereas the latter being ferritic is used in the cases where strength is of prime importance along with moderate to good corrosion resistance. It is therefore, worthwhile to study the properties of these materials.

It is necessary to select sintering atmosphere judiciously because densification is largely dependent on sintering atmosphere. Hydrogen has been selected as sintering atmosphere because of its reducing capability not only provides protection from further oxidation but also can reduce any existing oxides. Many researchers have tried with H_2 due to this reason. N_2 and Vacuum sintering have also been performed.

As the N_2 content in 316L stainless steel obtained from two sources were different, it was planned to study their properties based on similar size powders and processed under similar conditions.

It is also aimed to study the sintered properties of austenite/ferrite duplex stainless steels. These steels are characterized by an outstanding combination of strength, toughness and corrosion resistance. Furthermore, due to lower nickel content duplex stainless steels are much cheaper than comparable austenite grades. They have therefore, found applications in off-shore constructions, heat-exchangers, gas and oil pipe lines as well as in the chemical

industry. So far no work is reported on such materials produced through powder metallurgy route. Considering this fact it was considered worthwhile to study this material.

Addition of copper in powder metallurgy stainless steel parts enhances sintering rate because of the presence of liquid phase at the sintering temperature. No work on the effect of such addition in 316L- 434L composites is yet reported.

Literature survey reveals that at least a temperature of 1300°C is essential to achieve good densification in sintered stainless steel. It is well known that liquid phase sintering is viable alternative to lower the processing temperature. Chromium boride addition has been reported to give rise liquid phase even at as low temperature as 1250°C[101]. Cr_3C_2 addition in stainless steel - CrB composites has been aimed for to impart better wear resistance.

Table 1.1

NOMINAL COMPOSITIONS OF SOME OF THE MORE COMMON STAINLESS STEELS

American AISI Type No	% Cr Chromium	% Ni Nickel	% C Carbon	% Mn Manganese	% Si Silicon	% Other N Nitrogen: Mo Molybdenum Ti Titanium: Se Selenium Nb Niobium: S Sulphur
201	16-18	3.5-5.5	0.15 max	5.5-7.5	1 max	N 0.25 max
202	17-19	4-6	0.15 max	7.5-10	1 max	N 0.25 max
301	16-18	6-8	0.15 max	2 max	1 max	-
302	17-19	8-10	0.15 max	2 max	1 max	-
302B	17-19	8-10	0.15 max	2 max	2-3	-
303	17-19	8-10	0.15 max	2 max	1 max	S 0.15 min
303Se	17-19	8-10	0.15 max	2 max	1 max	Se 0.15 min
304	18-20	8-12	0.08 max	2 max	1 max	-
304L	18-20	8-12	0.03 max	2 max	1 max	-
305	17-19	10-13	0.12 max	2 max	1 max	-
308	19-21	10-12	0.08 max	2 max	1 max	-
309	22-24	12-15	0.2 max	2 max	1 max	-
309S	22-24	12-15	0.08 max	2 max	1 max	-
310	24-26	19-22	0.25 max	2 max	1.5 max	-
310S	24-26	19-22	0.08 max	2 max	1.5 max	-
314	23-26	19-22	0.25 max	2 max	1.5-3 max	-
316	16-18	10-14	0.08 max	2 max	1 max	Mo 2-3
316L	16-18	10-14	0.03 max	2 max	1 max	Mo 2-3
316Ti	16-18	10-14	0.08 max	2 max	.75 max	N 0.10 max Mo 2-3 Ti 5(C+N) min 0.07 max
317L	18-20	11-15	0.03 max	2 max	1 max	Mo 3-4
321	17-19	9-12	0.08 max	2 max	1 max	Ti (5× C) min
347	17-19	9-13	0.08 max	2 max	1 max	Nb+Ta(10× C) min
348	17-19	9-13	0.08 max	2 max	1 max	Ta 0.1 max, Co 0.2 max
403	11.5-13	-	0.15 max	1 max	0.5 max	-
405	11.5-14.5	-	0.08 max	1 max	1 max	Al 0.1-0.3
409	10.5-11.75	-	0.08 max	1 max	1 max	Ti (6× C) 0.75 max
410	11.5-13.5	-	0.15 max	1 max	1 max	-
414	11.5-13.5	1.25-2.5	0.15 max	1 max	1 max	-
416	12-14	-	0.15 max	1.25 max	1 max	S 0.15 min
416Se	12-14	-	0.15 max	1.25 max	1 max	S 0.15 min
420	12-14	-	over 0.15	1 max	1 max	-
430	14-18	-	0.12 max	1 max	1 max	-
430F	14-18	-	0.12 max	1.25 max	1 max	S 0.15 min
430F Se	14-18	-	0.12 max	1.25 max	1 max	Se 0.15 min
431	15-17	1.25-2.5	0.2 max	1 max	1 max	-
440A	16-18	-	0.6-0.75	1 max	1 max	Mo 0.75 max
440B	16-18	-	0.75-0.95	1 max	1 max	Mo 0.75 max
440C	16-18	-	0.95-1.2	1 max	1 max	Mo 0.75 max
442	18-23	-	0.2 max	1 max	1 max	-
446	23-27	-	0.2 max	1.5 max	1 max	N 0.25 max

Table 1.2 : Typical mechanical properties of various sintered stainless steels. Ref 9

P/M MATERIAL DESIGNATION AISI	DENSITY g/cm^3	MECHANICAL PROPERTIES (TYPICAL VALUES) YS N/mm^2	UTS N/mm^2	E %	H ROCKWELL
303	6.4	230	270	1	62 B
	6.4	275	300	7	60 B
	7.0	120	390	20	45 B
304	6.4	260	290	1	61 B
	6.6	275	400	10	68 B
	7.0	120	390	22	45 B
314	6.4	240	290	1	59 B
	6.6	275	475	10	69 B
	7.0	160	375	16	45 B
410	6.7	440	600	1	26 C
	7.0	100	360	20	53 B
420	6.7	810	850	0.5	30 C
434	7.0	200	350	14	55 B
432	6.9	350	470	2	78 B

Table 1.3 : Magnetic properties of P/M stainless steels. Ref 64

PM	Compacting pressure (tsi)	Green density (g/cm^3)	Sintered density (g/cm^3)	B_{100} (x 10^3 G)	B_r (x 10^3 G)	H_c (Oe)	μ_{max} (x 10^3)	Resistivity μ.cm
410L	35	6.31	6.75	11.12	4.72	2.56	0.955	90.44
	45	6.57	6.99	11.65	4.08	3.45	0.627	89.94
430L	35	6.13	6.62	10.54	4.68	2.56	0.993	100.38
	45	6.40	6.88	11.23	4.77	2.74	0.963	93.82
434L	35	6.09	6.51	10.05	5.43	2.11	1.327	109.56
	45	6.39	6.79	11.02	5.69	2.27	1.317	103.55

Table 1.4 : Influence of copper infiltration on magnetic properties of P/M 410L stainless steel. Ref 64

Condition	Green density (g/cm^3)	Sintered density (g/cm^3)	B_{15} (×10^3 G)	B_r (×10^3 G)	H_c (Oe)	μ_{max} (×10^3)
As-sintered	6.51	6.98	8.32	4.74	2.34	1.09
Sintered & copper infiltrated	6.53	7.73	0.41	0.07	2.15	0.6

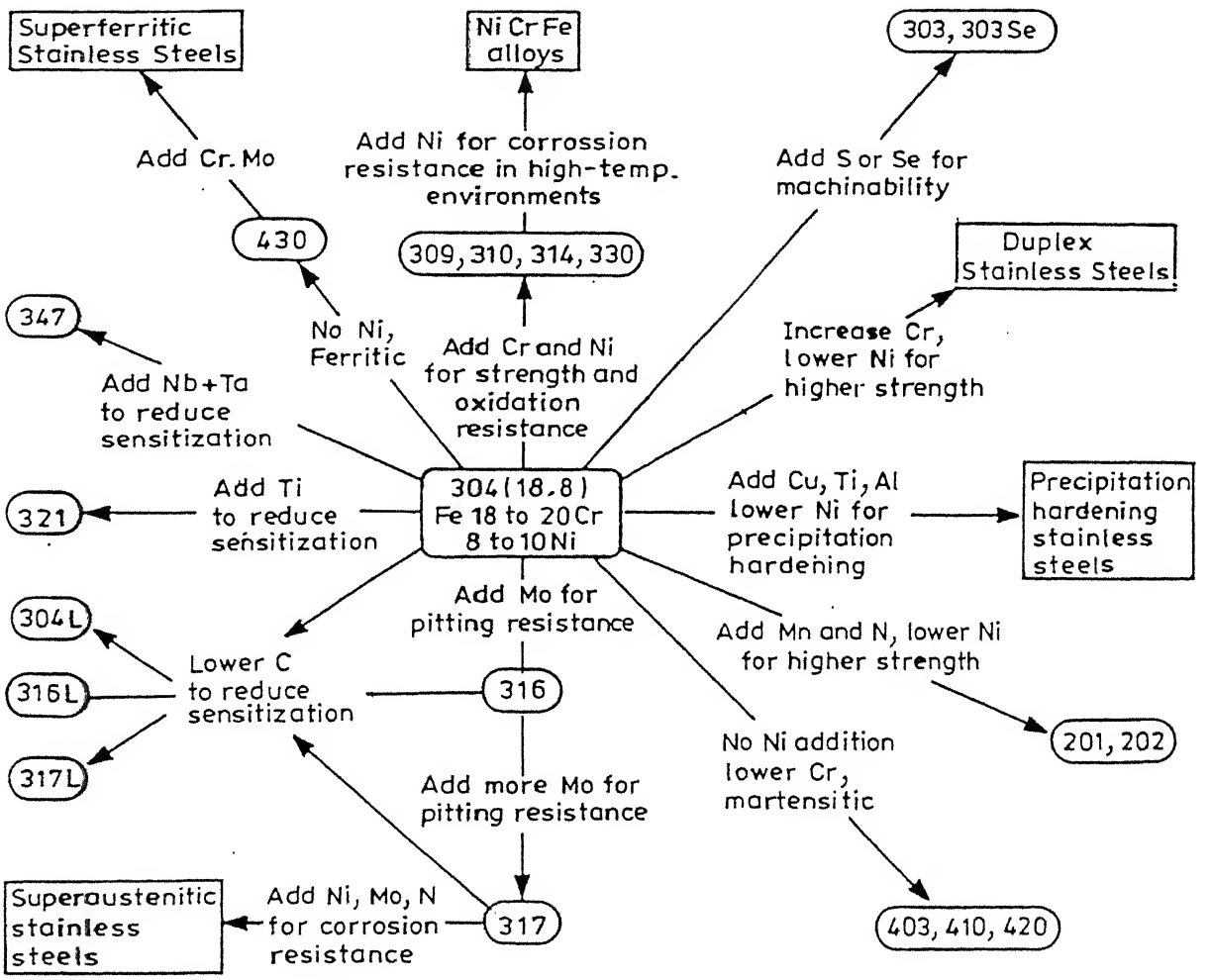

Fig 1.1 Compositional and property linkages in the stainless steel family. Ref-1

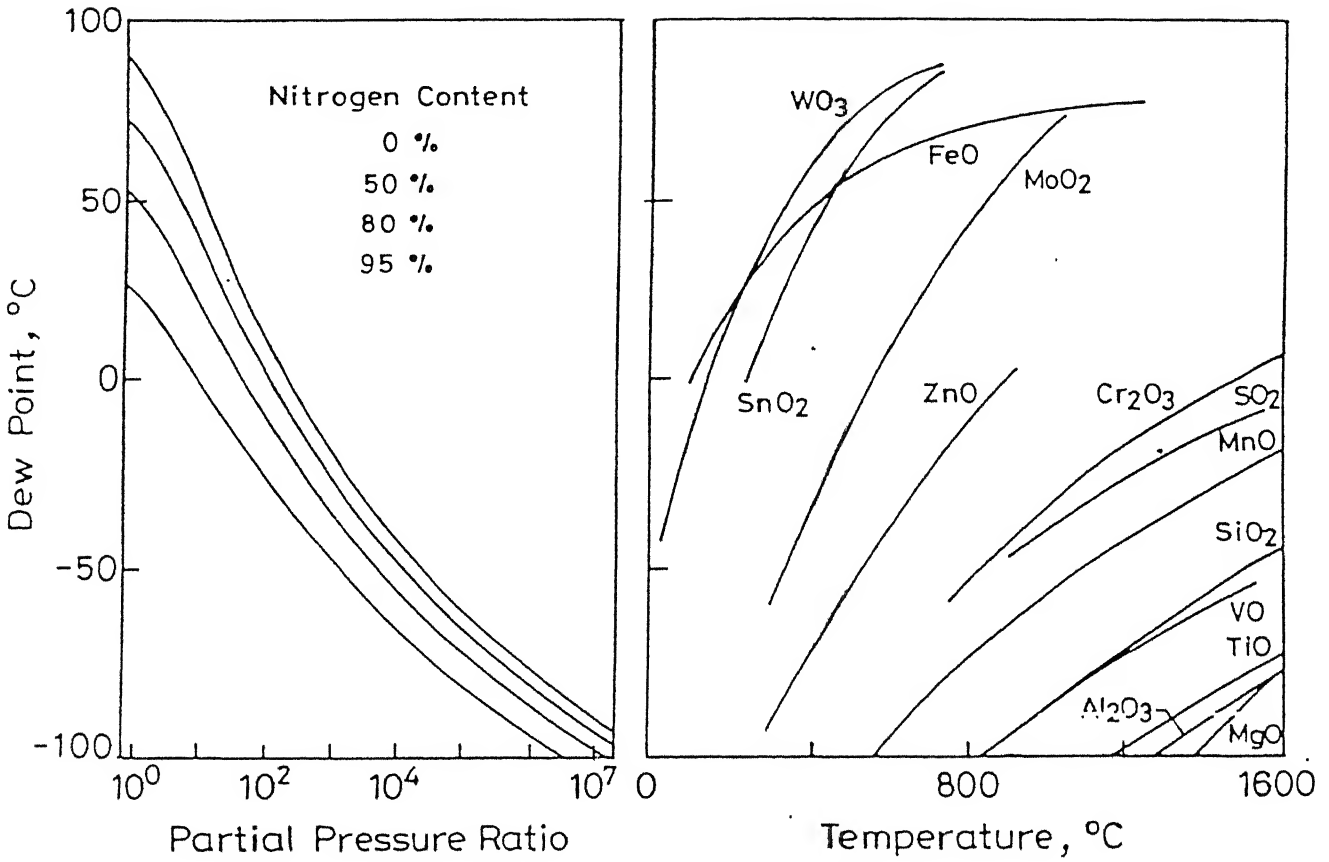

Fig. 1.2 Dew point requirements for oxide reduction of various elements. Ref.6

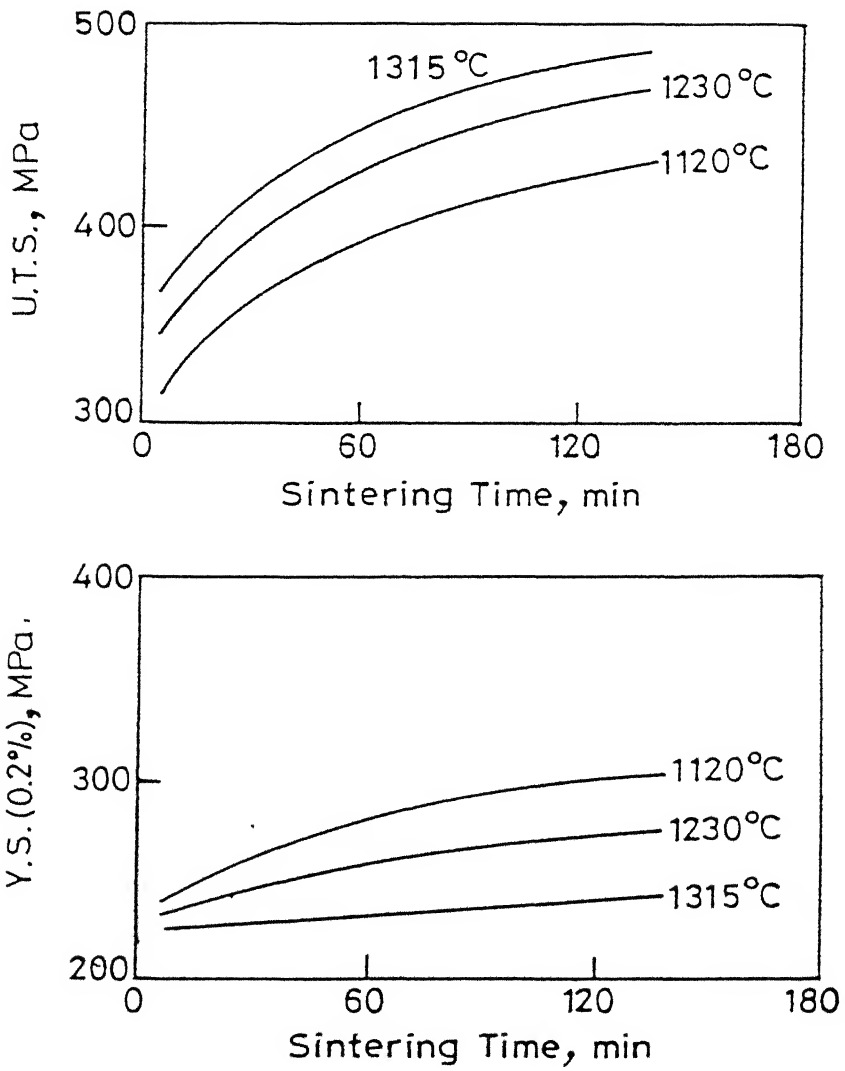

Fig. 1.3 Effect of sintering time on tensile and yield strength of 316L stainless steel sintered at different temperatures in dissociated ammonia. Ref.1

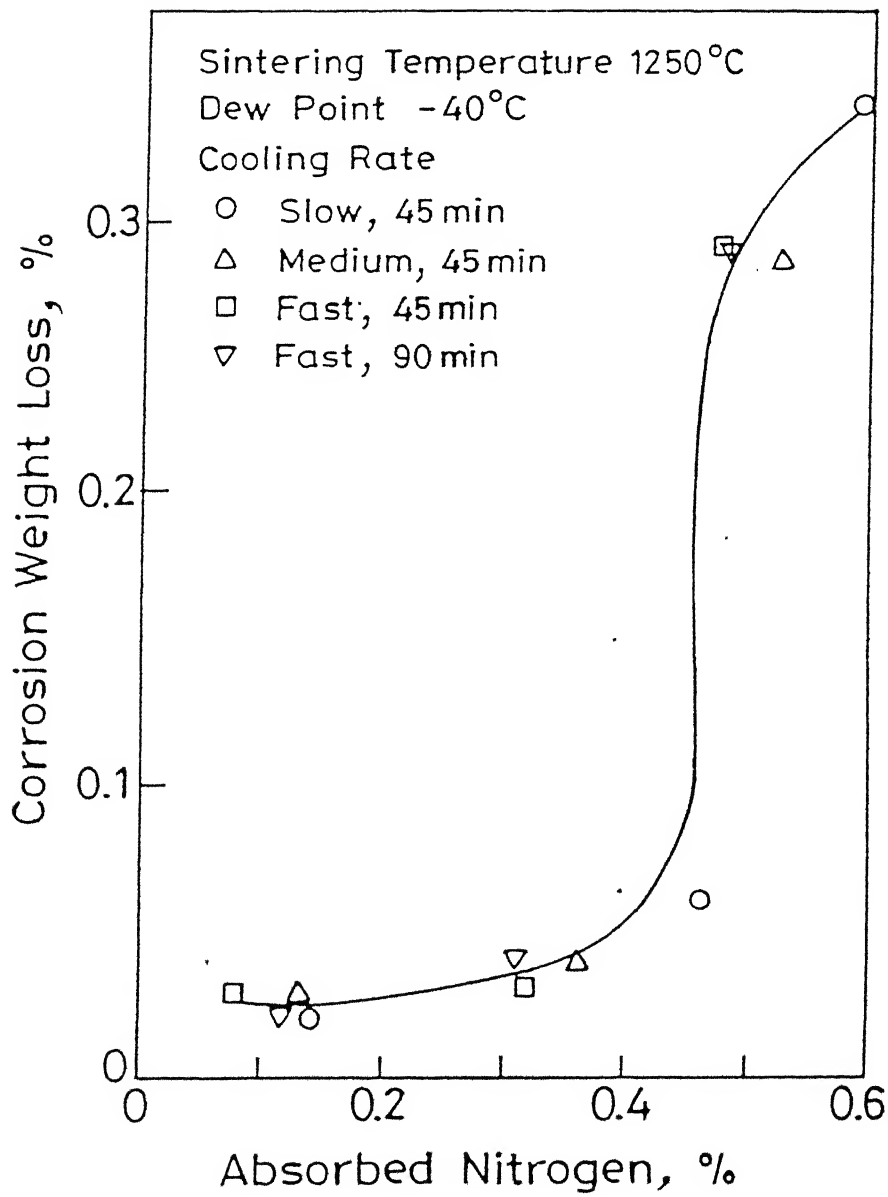

Fig. 1.4 Effect of N_2 content in 316L stainless steel on corrosion weight loss. Ref-43

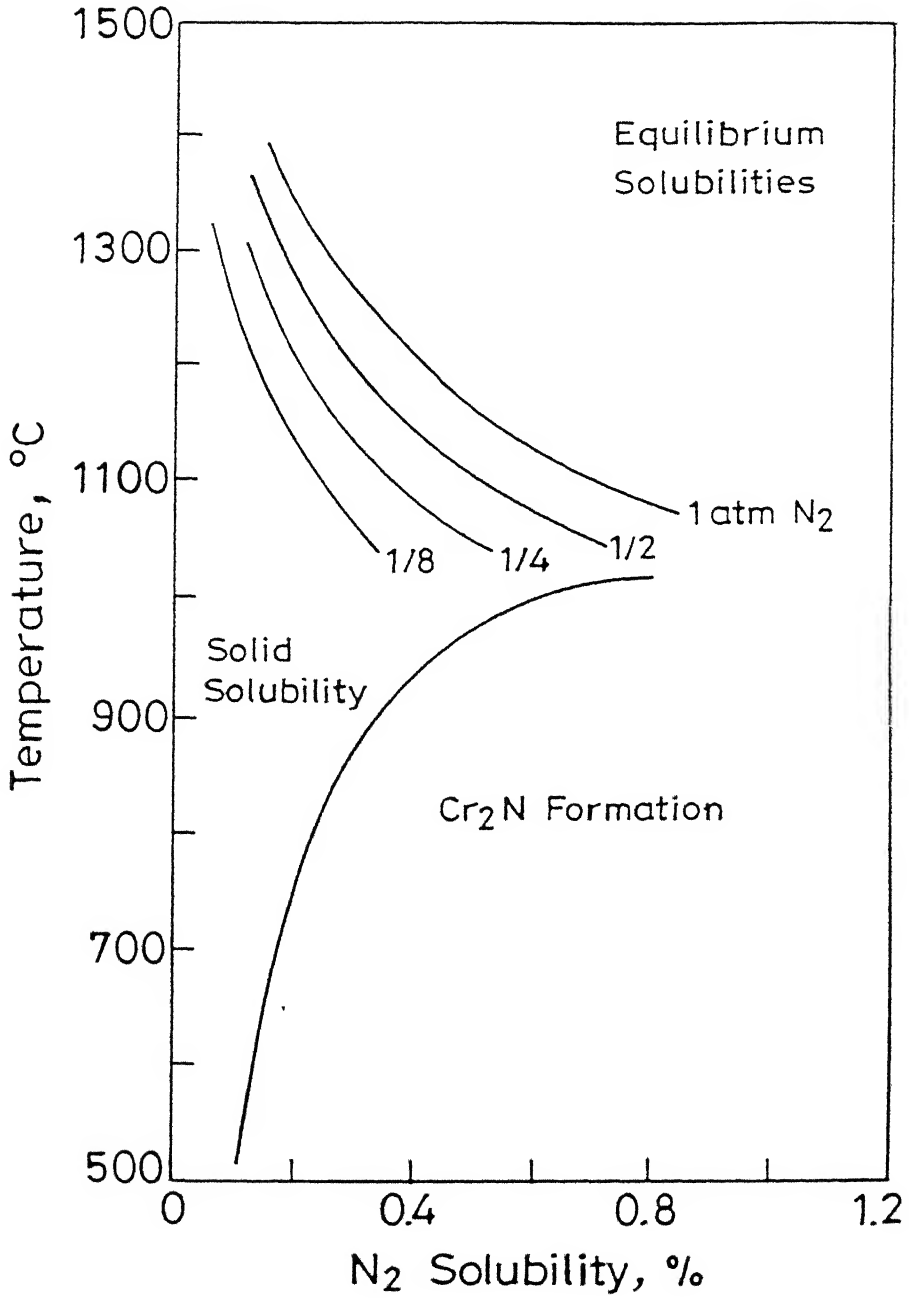

Fig. 1.5 A Schematic equilibrium diagram for estimated nitrogen solubility and Cr_2N formation boundary in austenite stainless steel. Ref.24

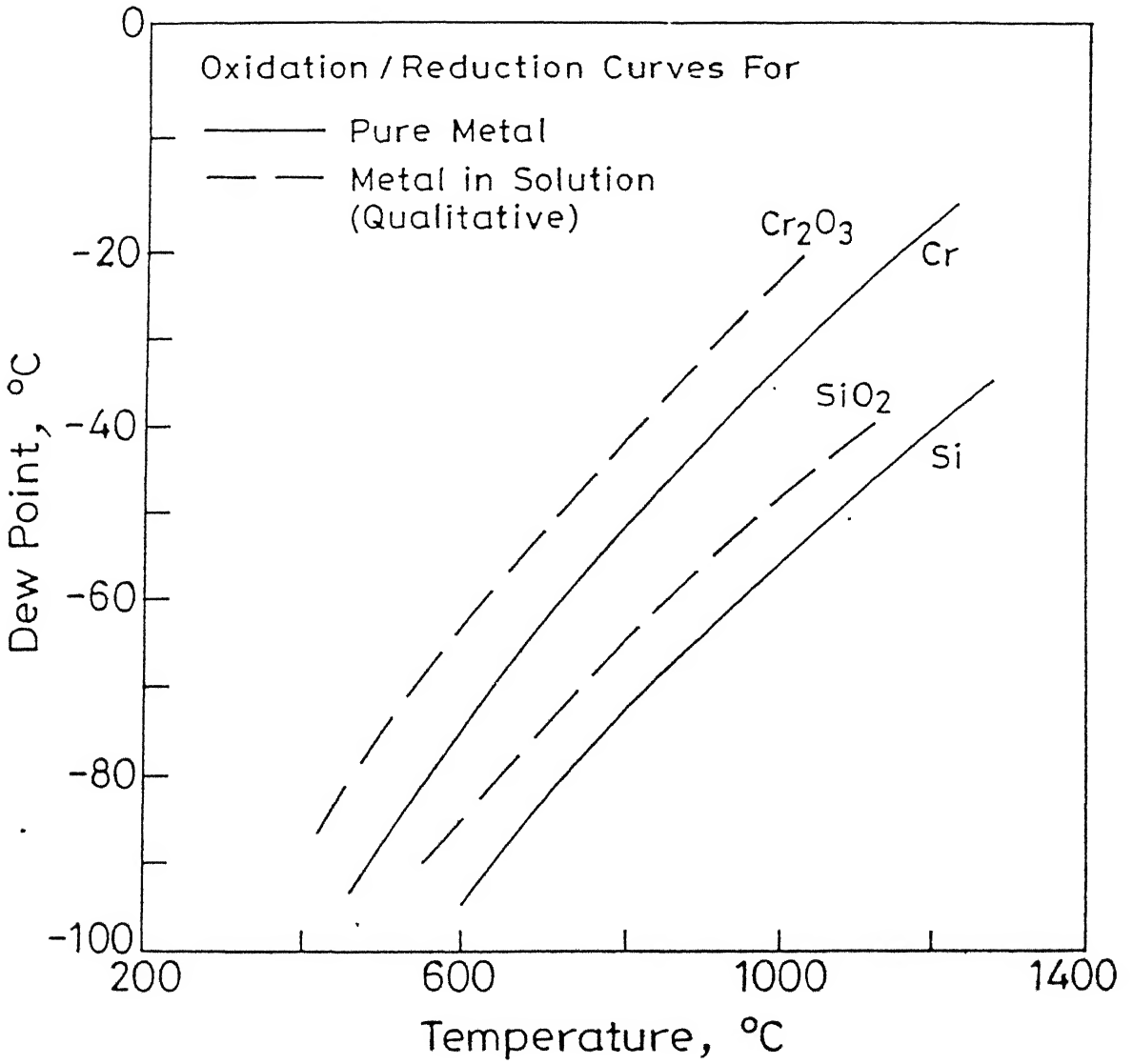

Fig. 1.6 Dew point vs. sintering temperature for oxidizing and reducing reaction for Cr_2O_3 and SiO_2 in hydrogen. Ref.48

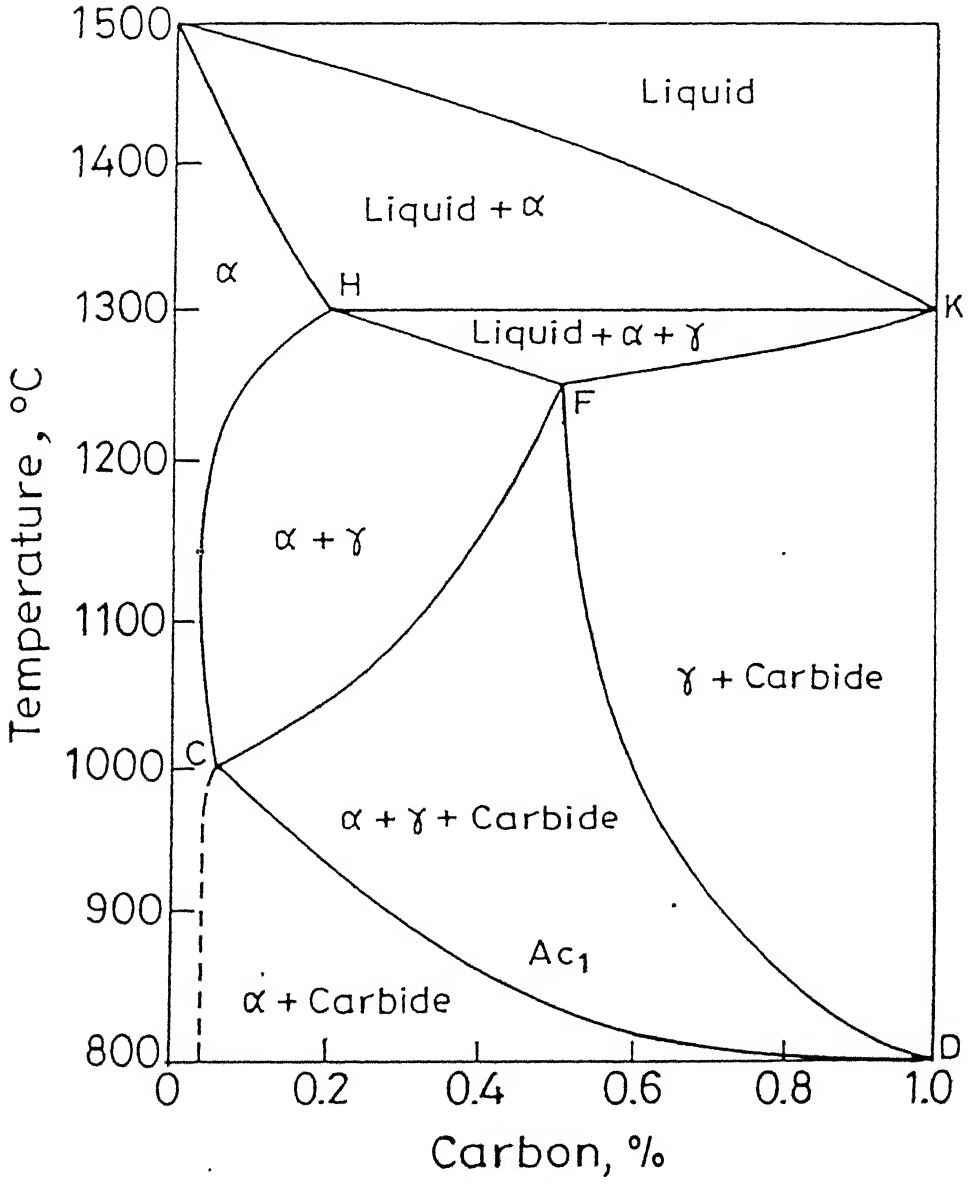

Fig. 1.7 Influence of carbon content on various phases of stainless steel with 20% Cr. Ref. 37

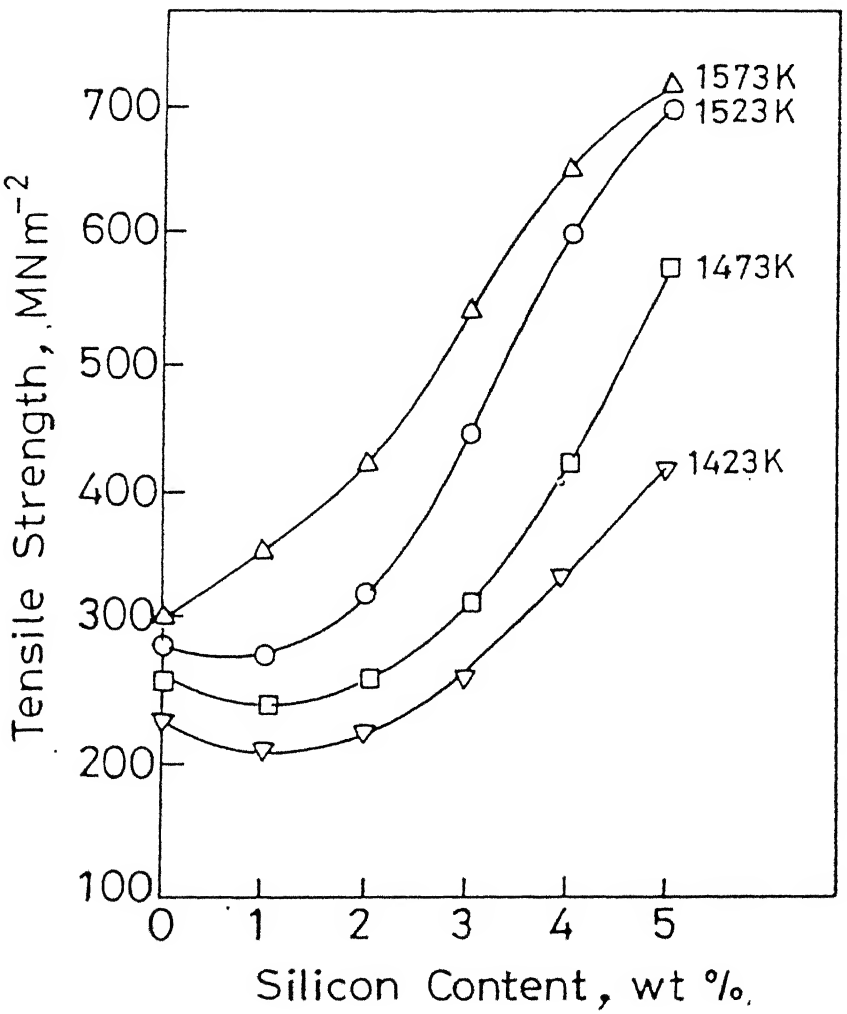

Fig. 1.8 Effect of silicon content on tensile strength of 304L stainless steel sintered at different temperatures in H_2. Ref. 58

Chapter 2

Experimental Procedure

2.1 Raw Materials

The characteristics of the different powders used in the present investigation are as given bellow :

Austenitic Stainless Steel (316L) Powder: Two types of 316L powders manufactured by two different manufacturer are used in this investigation. Both the powders were water atomized and annealed. Chemical compositions and properties of both the powders are as follows :

A : Manufacturer : AMETEK, USA

Chemical composition

C	0.025	Apparent density	2.9g/cm^3
Ni	12.97	Flow	37sec/50g
Cr	16.51	Sieve Analysis	
Mo	2.48	+100	3.9
Si	0.93	+140	13.5
Mn	0.21	+200	29.7
S	0.008	+230	20.6
P	0.01	+270	23.1
N	0.044	+350	3.8
Fe	Balance	-350	3.5

B : Manufacturer : ANVAL, SWEDEN

Chemical composition

C	0.023	Apparent density	4.5g/cm^3
Ni	10.6	Flow	27sec/50g
Cr	16.8	Sieve Analysis	
Mo	2.11	+100	0.4
Si	0.56	+140	1.6
Mn	1.20	+200	2.1
S	0.008	+230	7.6
P	0.029	+270	61.6
N	0.07	+350	15.9
Fe	Balance	-350	7.8

In the present text, mere 316L would be treated as that lot manufactured by AMETEK, USA unless stated otherwise.

Ferritic Stainless Steel (434L) Powder : The stainless steel powder that was used in this investigation was 434L grade, water atomized and annealed manufactured by AMETEK Pennsylvania, USA. Its chemical compositions and properties were as follows :

Chemical composition

C	0.023	Apparent density	2.9g/cm^3
Cr	16.93	Flow	37sec/50g
Mo	1.00	Sieve Analysis	
Si	0.71	+100	2.9
Mn	0.24	+140	7.9
O	0.27	+200	28.4
S	0.013	+230	26.6
P	0.02	+270	28.1
N	0.024	+350	4.3
Fe	Balance	-350	0.6

Copper Powder : The copper powder was supplied by AMRUT Industries & Products. Mumbai, and had the following characteristics :

Chemical composition

Cu	99.6		
Acid insoluble matter	0.05		
As	0.002	Apparent density	1.4g/cm^3
Pb	0.008	Mesh size	400 (32μm)
Fe	0.005		No Flow through Hall Flowmeter
Sulphide	0.005		

Chromium Carbide Powder :

Manufacturer : THIKOL, INC USA Apparent Density : 2.1 g/cm^3 No flow through Hall Flowmeter

Chromium Boride Powder :

Manufacturer : CERAC, INC, Milwalkee, USA Purity : 99.5% Particle size : < 42μm Apparent Density : 2.1 g/cm^3 No flow through Hall Flowmeter

2.2 Premix Preparation

Premixes of 316L and 434L were prepared in Turbula mixer, type 12C Nr921266 for half an hour. 434L content in different premixes were selected as 20, 40, 60, 80 weight percent respectively. Individual steels with 10v/o Cr_3C_2 premixes were also prepared by same procedure. 2 mass percent copper was manually mixed with each premixes of 316L and 434L along with straight compositions in a mortar and pestle. CrB was also manually mixed with the steels containing Cr_3C_2. CrB content in different premixes were selected as 0, 1, 2, 3 and 4w/o respectively. The details of the processing schedule is given in Figure 2.1 to 2.3 .

2.3 Room Temperature Compaction

Cylindrical green compacts of 12.76 mm diameter and approximately 5 mm to 7 mm height were made from the premix powder in a single acting hydraulic press at 600 MPa pressure. Manually operated hydraulic machine (Apex Construction Ltd, UK) of 20 tons capacity

was used for this purpose. The die made of high chromium high carbon steel was cleaned with acetone and was lubricated with zinc-stearate prior to each powder fill. For Transverse rupture strength the specimens of dimensions 25 mm length and 8 mm width having thickness of around 3mm to 4mm were prepared as per above procedure.

2.4 Sintering

Sintering experiments were carried out in a laboratory type silicon carbide resistance heated tubular furnace. The furnace tube had an internal diameter of 52 mm and capable of attaining a maximum temperature of 1400°C with a control of ±5°C over a length of 100 mm at the center. Dry hydrogen and nitrogen (dew point -35°C) were used as sintering atmosphere. The gases were allowed to pass through Lectrodryer containing activated Al_2O_3 for moisture absorption before finally passing through the furnace.

2.4.1 Sintering of 316L and 434L Steels

Requisite number of the green cylindrical compacts of straight stainless steel compositions were placed over an inconel boat and transferred in the center of the tubular furnace. Both ends of tubular furnace were sealed with SILASTIC adhesive/sealant to prevent any gas leakage. Commercially pure hydrogen after drying in Lectrodryer was used as sintering atmosphere. Straight 316L and 434L were also sintered in nitrogen atmosphere while the sintering time was kept 1 hour for all the cases. The sintering temperatures selected were 1150°C, 1250°C, 1350°C for both sintering atmospheres. Some 316L and 434L compacts were also sintered at 1250°C in vacuum. In order to study the effect of nitrogen content on 316L, two types of 316L with different N_2 contents and supplied by two different manufacturers (AMETEK, ANVAL) were sieved to get a particle size of +230 and +270. Compacts were made from those particles and was sintered at 1350°C in H_2 atmosphere in the same furnace. In this case sintering periods were 1 hour and 1.5 hour.

2.4.2 Austenitic/Ferritic Stainless Steel Composites Containing 2 mass % Copper

Green compacts in cylindrical form were sintered in hydrogen atmosphere in a silicon carbide heated tubular furnace as stated in earlier section. The sintering temperatures were main-

tained as 1150°C, 1250°C, 1350°C respectively while the sintering period was kept 1 hour for all the cases. When 2m/o Cu was added then the compacts were sintered only at 1350°C for 1 hour and in H_2.

2.4.3 316L And 434L Stainless Steel Composites Containing Cr_3C_2 And CrB

Green cylindrical compacts were sintered in silicon carbide heated tubular furnace at 1150°C, 1200°C, 1250°C, in H_2 for 1 hour.

2.5 Density And Densification Parameter

Densities of green and sintered cylindrical compacts were calculated from the mass and physical dimension measurements of the sample. The oil impregnation method was also used to measure density and a very little difference was detected in the values. In oil impregnation method, sintered pellets were impregnated with xylene under vacuum and the following formula was used for determining the sintered density [114]

$$Sintered\ density = \frac{a}{b-c}$$

a = Weight of compact in air(gms)
b = Weight of xylene impregnated compact in air(gms)
c = Weight of xylene impregnated compact in water(gms)

$$\%Sintered\ porosity = \frac{(Theoretical\ density - Sintered\ density) \times 100}{Theoretical\ density}$$

Densification parameter (Δ D) was expressed as follows

$$\Delta D = \frac{Sintered\ density - Green\ density}{Theoretical\ density - Green\ density}$$

Theoretical densities of the powders used in this investigation were taken as follows: [1.115-116]

316L(AMETEK)	8.0g/cm^3
316L(ANVAL)	8.0g/cm^3
434L	7.8g/cm^3
Copper	8.96g/cm^3
Cr_3C_2	6.68g/cm^3
CrB	6.05g/cm^3

Theoretical density of each of the premixes was determined from the rule of mixture taking the theoretical density of various elements at room temperature. This is an oversimplification as all the used premixes did not remain as mixture without undergoing any reaction.

2.6 Mechanical Properties

2.6.1 Microhardness

For to avoid interference of porosities to hardness value, microhardness was taken in the solid matrix of sintered compacts. It was measured on Vickers microhardness testing machine of Leitz make, using a load of 50g and at a magnification of 500X. In case of ferrite-austenite two phase structures microhardness was taken on both phases. About eight indentations were taken on each polished surface and the average value was reported.

2.6.2 Transverse Rupture Strength (T.R.S)

The test for three point loading was performed on a fixture where the sintered metal bar was kept on two WC rollers of 5mm diameter which were 15mm apart from each other (ASTM specifications B406-76). Another similar roller was kept in the middle of the bar.The load was applied gradually by M.T.S testing machine. The maximum rupture load at the failure point of the test piece was used in the following formula in order to determine (T.R.S) :

T.R.S (MN/m^2) $= \frac{3 \times Load(MN) \times Length(m)}{2 \times Width(m) \times (Thickness,m)^2}$

2.6.3 Wear Testing

Wear testing of selected sintered samples were performed using a Wear and Friction Monitor, Model TR-20 of Ducom, Bangalore make. This was done to find the abrasion resistance of materials.

2.6.4 Magnetic Property

Magnetic property like coercivity was measured by using a COERCIMETER of EMTR, Thane make. This was done to get an idea about the grain size of the material being investigated. Magnetic saturation of specimens was also measured by using a Sigmameter, Model SM-75 of Lab Physik Magnet, India make.

2.7 Corrosion Study

Corrosion behaviour of straight 316L and 434L and their composites sintered at 1350°C in H_2 was studied by weight loss method in 1(N) H_2SO_4 for 360 hours. corrosion behaviour was also studied for the samples where copper was added as an sintering additive under similar situations.

2.8 Microstructural Studies

Optical and SEM metallographic techniques were adopted to study the microstructural changes.

2.8.1 Optical Microscopy

The sintered cylindrical compacts were wet polished on the Lunn Major Unit of Struers make, over 220, 320, 500 and 1000 grit silicon carbide emery papers followed by fine wheel polishing with suspended 0.03μm size alumina powder in distilled water. The etchants with the following compositions were used [117].

1. $CuSO_4.5H_2O$ 12g
   HCl(concentrated) 60ml
   H_2O(distilled) 60ml

2. $CuCl_2$ 5g
   H_2O 100ml
   HCl 100ml
   CH_3OH 100ml

3. HNO_3 3ml
   HCl 10ml
   CH_3OH 100ml

4. $FeCl_3$ 5g
   HCl 50ml
   H_2O 100ml

It is interesting to note that optimum selection of etchant was very much dependent on sintering variables.

2.8.2 Grain Size Measurement

Grain size was measured directly on etched samples under a microscope Metallux-3 and mostly at a magnification of 200X. Size of the grains was measured directly from the scale attached with the microscope. This reading was a magnified value and divided by magnification to get the proper value. About 20 to 25 grains were measured at various fields and the average value was reported.

2.8.3 Scanning Electron Microscopy

The scanning micrographs of the fractured surfaces of the MPIF test specimens for measuring transverse rupture strength were taken. After sliding wear testing also scanning micrographs of worn surfaces were taken. Micrographs were taken using a JEOL, 840A scanning electron microscope.

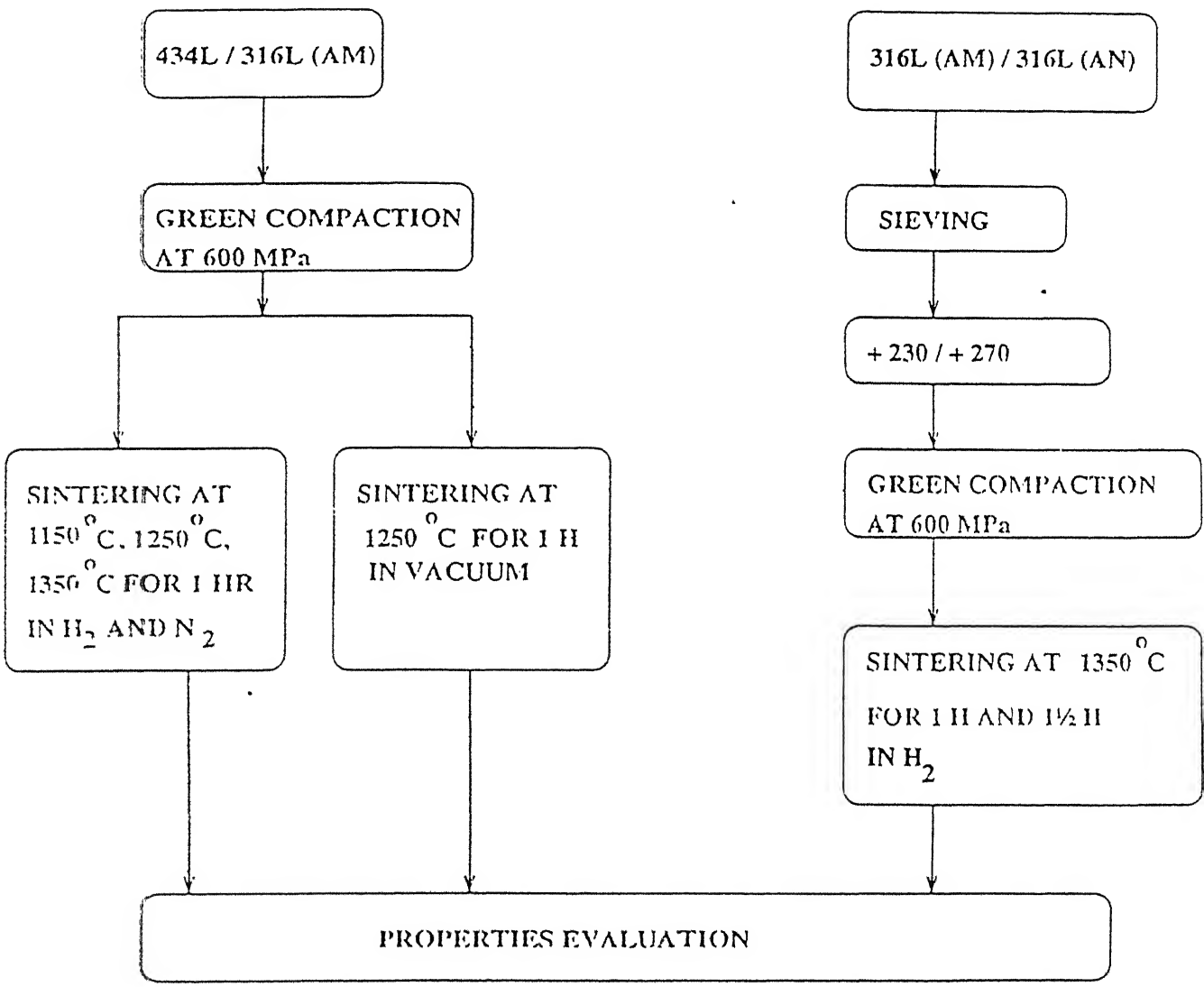

Fig. 2.1 P/M processing schedule.

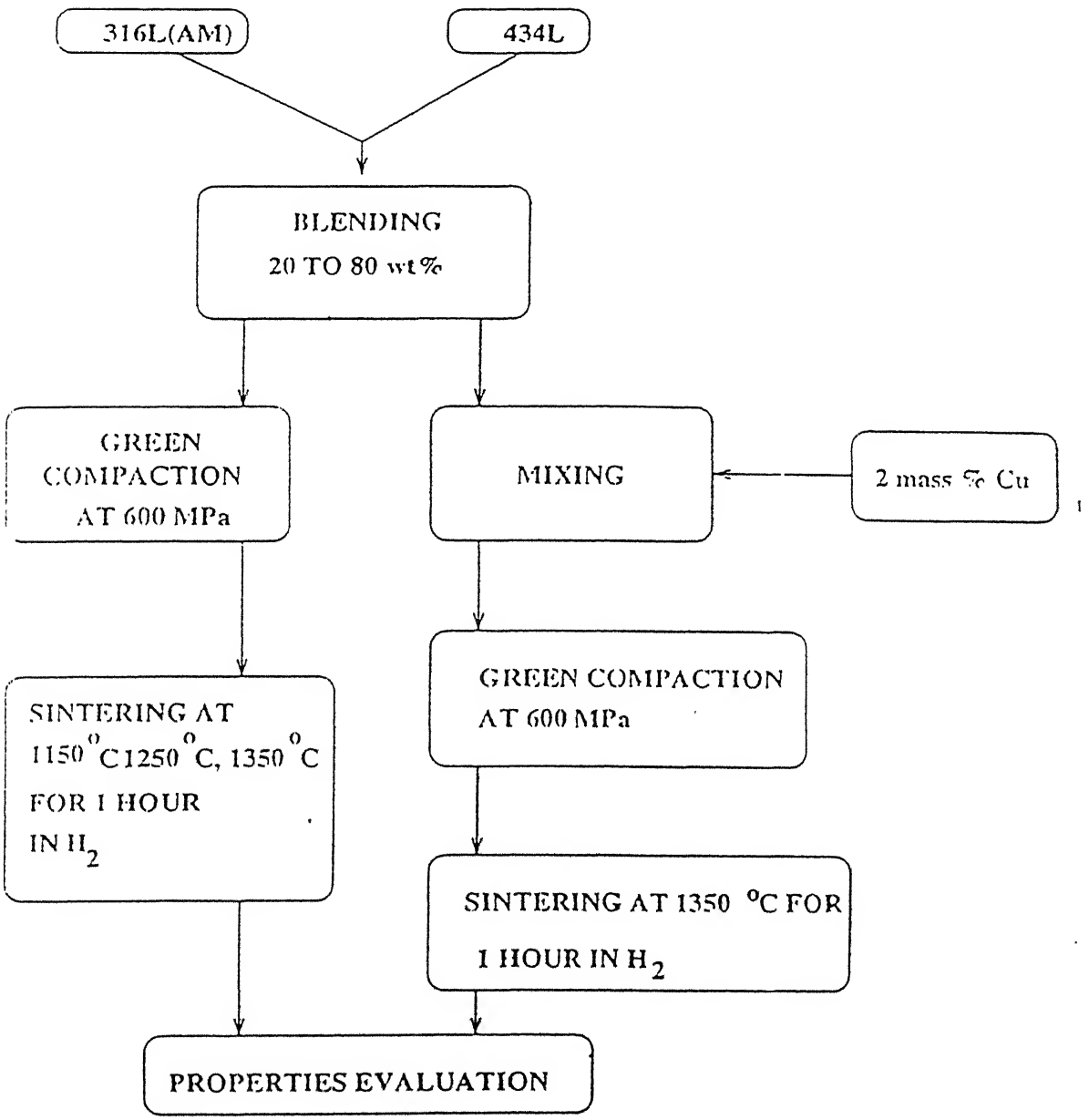

Fig. 2.2 P/M processing schedule for 316L - 434L composites.

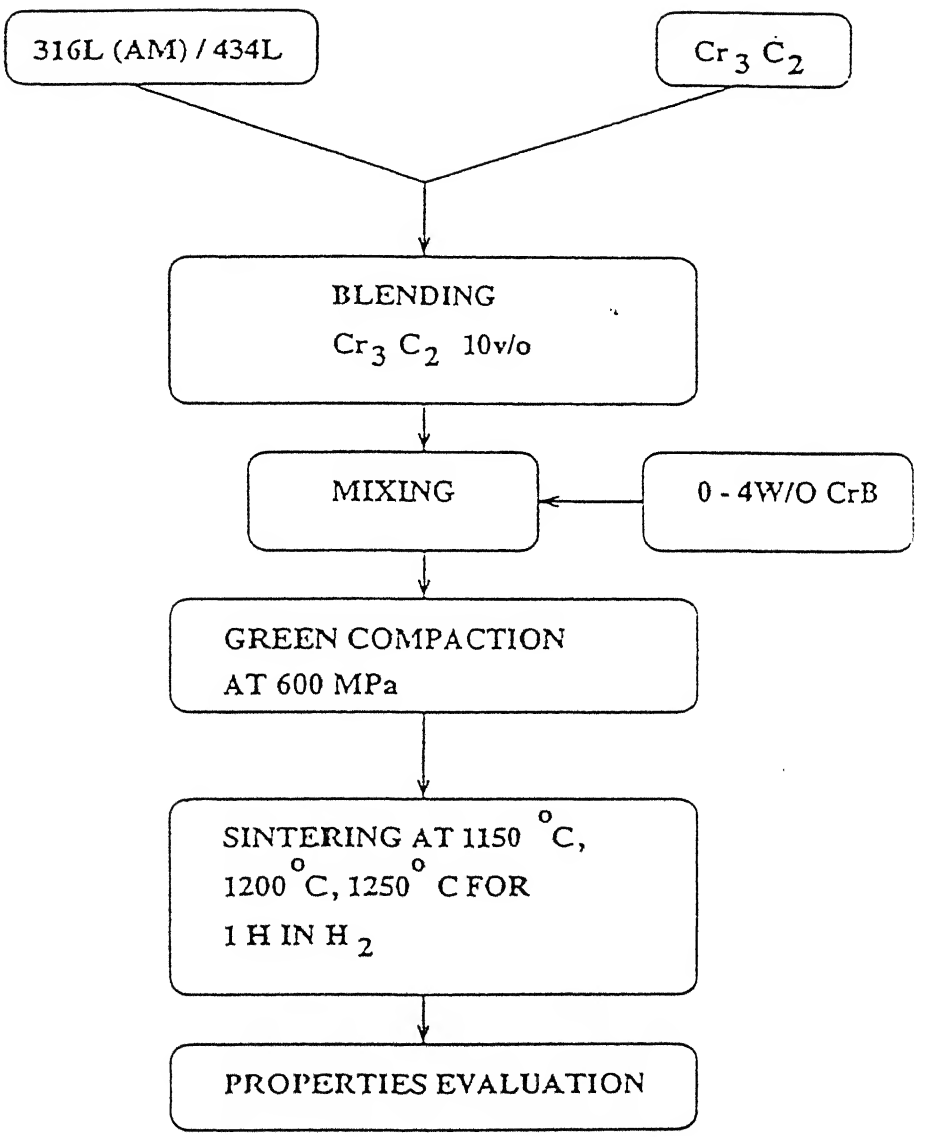

Fig. 2.3 P/M processing schedule.

Chapter 3

Experimental Results

This chapter describes the results of the investigation and has been divided into three sections. The first section deals with the results of sintering of 316L/ 434L while in second section results of sintering of 316L-434L composites and their Cu containing alloys are described. In the third section, results of sintering of 316L and 434L stainless steel composites containing Cr_3C_2 and CrB are described.

PART I

Sintering of 316L/ 434L Stainless Steels

3.1 Effect of Sintering Temperature

3.1.1 Sintered Density

Figure 3.1 shows the effect of sintering temperature on sintered density of both the stainless steels. It is clear that sintered density increases with increasing sintering temperature irrespective of the sintering atmosphere (*i.e* H_2 or N_2). Though at lower sintering temperatures difference in density is not much, but at higher sintering temperature, this difference is very much noticeable. Sintered porosity is consistent with that of sintered density for both steels and in both atmospheres. It is also clear from Figure 3.1 that sinterability of 316L is greater

than 434L. But at 1350°C sinterability of 434L is higher than that of 316L in either H_2 or in N_2. This observation is also reflected in densification parameter.

3.1.2 Microhardness

Figure 3.1 reflects that microhardness decreases with increase in sintering temperature for both the steels, when sintered in H_2 atmosphere. This feature is more evident in 434L than in 316L. However, microhardness of 434L is much more higher than 316L up to 1250°C sintering when sintered in H_2. In N_2 sintering, variation in microhardness is not much in either case and in general a peak is observed at 1250°C.

3.1.3 Microstructures

Optical microphotographs of 316L and 434L are shown in Figure 3.2. Microstructures also qualitatively conform with the sintered porosity level obtained through calculation. Grain coarsening also noticeable in the Microstructures for both steels.

3.1.4 Magnetic Properties

Coercivity for 316L is zero irrespective of sintering temperature and atmosphere. Variation of coercivity for 434L with sintering temperatures is shown in Figure 3.3. It decreases with increase in sintering temperature and becomes almost zero at 1350°C. At 1150°C a very high value of coercivity is noticed for H_2 sintered specimens. Variation of magnetic saturation with respect to sintering temperature has also been shown in Figure 3.3. It is observed that magnetic saturation of 434L increases with increase in sintering temperature. Magnetic saturation for 316L is very very small (within 7 Gauss/g).

3.2 Effect of Sintering Atmosphere (H_2, N_2, Vacuum)

3.2.1 Sintered Density

Figure 3.4 shows that irrespective of steel grade sintered density is higher for H_2 atmosphere followed by N_2 and vacuum. Sintered porosity is also lowest for H_2 atmosphere. Figure 3.4

also shows that porosity level is higher for 434L than 316L in any sintering atmosphere.

3.2.2 Microhardness

Variation of microhardness with change in sintering atmosphere is also shown in Figure 3.4. It is observed that microhardness value for 316L is higher for N_2 atmosphere and the values are more or less comparable in other two sintering atmospheres. However, in case of 434L it is higher for H_2 atmosphere followed by N_2 and vacuum. Barring H_2 atmosphere microhardness values of 434L are less than that of 316L in other two atmospheres.

3.2.3 Microstructures

Figure 3.5 shows some of the microstructures of sintered 316L and 434L steels. Grain size variation is shown in Figure 3.4. For 316L, large grain is obtained in vacuum whereas in other two atmospheres grains have more or less similar sizes. For 434L small grained structure is obtained in case of N_2 sintering.

3.2.4 Magnetic Properties

Figure 3.6 shows the variation of coercivity in different sintering atmospheres. It increases when sintering atmosphere is changed from H_2 to either N_2 or vacuum. Coercivity is zero for 316L irrespective of sintering atmosphere except vacuum where a very small value is noticed. Magnetic saturation for 434L is highest at N_2 sintering atmosphere and it is more or less comparable at other two atmospheres. But for 316L some value (122 Gauss/g) of magnetic saturation is observed when sintered in vacuum whereas at other two atmospheres the value is as low as less than 5 Gauss/g.

3.3 Effect of N_2 Content and Particle Size of 316L

3.3.1 Sintered Density

Figure 3.7 shows the particle size distribution of stainless steels used in the present work. It is seen that particle size distribution of both the steels of AMETEK make has broad bands

where as the same is unimodal for 316L, ANVAL. Effect of particle size on sinterability is shown in Figure 3.8. It is observed that % sintered porosity is less with attendant high densification for samples based on +270 mesh ($> 53\mu$m) powder than that of +230 mesh ($> 63\mu$m). Figure 3.8 also shows that irrespective of the coarseness of particle, % sintered porosity decreases with increase in sintering period for either type of steel. However, this feature is more pronounced for ANVAL than AMETEK grade 316L for the particle size of +230 mesh. Moreover, densification of ANVAL grade of 316L is more at all sintering periods irrespective of particle size.

3.3.2 Microhardness

From Figure 3.8 it is found that, microhardness for the samples based on +230 mesh powder of ANVAL make is higher than that of AMETEK make when period is 1 hour. However when sintering time is increased to 1.5 hours no difference in microhardness is noticed. In case of samples based on powder +270 mesh, microhardness is lower for ANVAL make for either of the sintering periods.

3.3.3 Microstructures

Optical photomicrographs of 316L (AMETEK) and 316L (ANVAL) are shown in Figure 3.9. Figure 3.8 shows that increasing sintering period has no effect on grain size of 316L(ANVAL) irrespective of the initial particle size. But for 316L (AMETEK) it is shown that grain size increases with increasing sintering period for either of the particle sizes.

PART II

Sintering of 316L/ 434L Composites and their Copper Containing Alloys

3.4 Effect of Composition and Sintering Temperature

3.4.1 Sintered Density

Sintered density increases with increase in sintering temperature and the variation of sintered density with respect to temperature is shown in Figure 3.10. Consequently % porosity decreases leading to higher densification with increase in sintering temperature. However, the effect is not so visible between 1150°C and 1250°C. With respect to composition the % porosity variation is not much.

3.4.2 Microhardness

Figure 3.10 shows variation of microhardness of steels with respect to composition at various sintering temperatures. In general hardness decreases with increase in sintering temperature. But change in hardness with respect to composition is noticeable. In general, there is increasing trend of hardness with respect to ferritic stainless steel addition. Microhardness value of second phase which is either ferrite or martensite (details will be discussed in next chapter) has also been plotted in Figure 3.10. From microhardness values it is observed that the second phases of 316L-60w/o 434L and 316L-80w/o 434L alloys have got similar values after 1250°C as well as after 1350°C. For the latter case the value is lower than the former one.

3.4.3 Microstructures

Quantitatively measured grain sizes have been shown in Figure 3.10. Grain coarsening is also qualitatively confirmed from the microstructures (Figure 3.11). Pore rounding is noticeable in the optical microphotographs taken from the samples sintered at 1350°C where two phase structures of some of the composites are also revealed.

3.4.4 Transverse Rupture Strength

Figure 3.10 shows the T.R.S values of the composites. It is noticed that T.R.S value increases with increase in 434L content in 316L and reaches to a peak at 316L-60w/o 434L. Same test could not be performed for 316L and 434L because of their ductility.

3.4.5 Wear Testing

Sliding wear results has been shown in Figure 3.12. It reveals that wear loss is maximum for 434L and minimum for 316L. Wear loss of the composites are in between the straight stainless steels.

3.4.6 SEM Photographs

Figure 3.13 shows the scanning photomicrographs of fracture surfaces after T.R.S of 316L-60w/o 434L and 316L-80w/o 434L. The former shows dimples suggesting ductile fracture whereas the fracture surface of the latter shows mixture of dimples and cleavages.

Figure 3.14 shows the SEM photographs of the samples after wear testing. Scanning photomicrographs reveal the worn surface of the samples taken after wear testing. It is apparent that wear pictures of 20 and 40w/o 434L containing composites are similar. The same is the case for 60 and 80w/o 434L containing composites. Although the wear is more for 434L steel, it is not very evident from the SEM pictures. 316L appears to undergo some degree of plastic deformation but at the same time there is some material deposition over the surface.

3.4.7 Magnetic Properties

Variation of magnetic properties like coercivity and magnetic saturation have been shown in Figure 3.15. It is observed that coercivity decreases with increase in sintering temperature irrespective of the composition of the material though the intensity of fall is not equal for all compositions. In general coercivity decreases drastically when sintering temperature is raised from 1250°C to 1350°C for 40 to 80w/o 434L. Magnetic saturation increases with increase in sintering temperature irrespective of the alloy composition except 316L-20w/o 434L where

some decreasing trend is observed. Intensity in increase is highest for 60 and 80w/o 434L containing composites when temperature is raised from 1250°C to 1350°C.

3.4.8 Corrosion Behaviour Study

Percentage weight loss of the composites as well as the straight steels in 1(N) H_2SO_4 after various exposure times have been shown in Figure 3.16. It is observed that at all exposure times weight loss is maximum for 316L-20w/o 434L composite. At the same time no weight loss is noticed when 434L content of 316L is either 40w/o or 60w/o. Coming to the straight steels, it is observed that rate of weight loss for 316L is higher as compared to 434L where after 120 hours no further weight loss is taken place even after an exposure time of 360 hours.

3.5 Effect of 2 mass % Copper addition in 316L-434L Composites

3.5.1 Sintered Density

Effect of 2 mass % copper addition on sintered density has been shown in Figure 3.17. It is observed that sintered density increases with increase in 434L addition. Consequently porosity decreases with attendant densification as ferritic stainless steel addition increases.

3.5.2 Microhardness

Microhardness variation of copper containing composites (Figure 3.17) shows a peak at 316L-60w/o 434L composite. Presence of second phase (will be discussed in next chapter) is noticed only at 316L-80w/o 434L composite. Microhardness variation of both the phases has been shown in the same figure.

3.5.3 Microstructure

Figure 3.17 shows measured grain sizes of Cu containing composites whereas in Figure 3.18 optical photomicrographs have been shown. Presence of second phase is clear in 316L-80w/o

434L. Small and round pores are visible in the microstructures. Microstructures also confirm lesser amount of pores.

3.5.4 Magnetic Properties

Variation of magnetic properties has been shown in Figure 3.17. It is observed that coercivity increases up to 40w/o 434L followed by a down fall and becomes zero for straight 434L. But magnetic saturation increases with increase in w/o 434L in 316L-434L composites. A steep change is noticeable in magnetic saturation value when 434L content of the composites is increased to 60w/o from 40w/o.

3.5.5 Corrosion Behaviour Study

Percentage weight loss of Cu containing composites in 1(N) H_2SO_4 and at various exposure times has been shown in Figure 3.19. It is observed that weight loss increases with increase in exposure time as well as with increase in w/o 434L in 316L-434L composites. It is also observed that up to 40w/o 434L weight loss is not much between the exposure times of 24 hours and 360 hours. But for other two composites (60 and 80w/o 434L) the intensity of weight loss is high and for 80w/o it is highest.

PART III

316L and 434L Composites Containing Cr_3C_2 and CrB

3.6 Effect of Cr_3C_2 addition

3.6.1 Sintered Density

Figure 3.20 shows the effect of Cr_3C_2 addition on the properties of either 316L or 434L. It is observed that % porosity increases with Cr_3C_2 addition for both the steels at 1150°C. But at 1250°C, it either remains same as in the case of 434L or decreases as in the case of 316L.

3.6.2 Microhardness

Influence of Cr_3C_2 addition on the microhardness of either 316L or 434L has been shown in Figure 3.20. It is observed that Cr_3C_2 addition increases microhardness for 316L at both sintering temperatures but the same is lowered for 434L irrespective of sintering temperature.

3.6.3 Microstructures

Quantitatively measured grain sizes have been shown in Figure 3.20. It is observed that after 1150°C sintering grain size either remain same as in the case of 316L based composite or decreases as observed in 434L based composite. But after 1250°C sintering Cr_3C_2 addition has no effect on grain size of 316L whereas it increases in 434L. This observation is reflected in the microstructures shown in Figure 3.21A and Figure 3.21B.

3.6.4 Magnetic Properties

Coercivity is zero both for 316L based composite and straight 316L stainless steel. Virtually no difference in magnetic saturation value is observed before and after Cr_3C_2 addition in 316L as the value lies within 5 Gauss/g for both the cases irrespective of sintering temperature. Coercivity and magnetic saturation both decrease with Cr_3C_2 addition in 434L at any sintering temperature as shown in Figure 3.22.

3.7 Effect of CrB Addition in Stainless Steel 10v/o Cr_3C_2 Composites

3.7.1 Sintered Density

Effect of CrB addition on sintered densities of 316L-10v/o Cr_3C_2 Composite and 434L-10v/o Cr_3C_2 composite has been shown in Figure 3.23. It is observed from Figure 3.23 that CrB addition in 316L composite has little or no effect when sintered at 1150°C. But after sintering at 1200°C, about 90% of the theoretical density is achieved when addition is in the range of 3 to 4w/o. More pronounced effect of CrB addition is observed at 1250°C with 2w/o additive. In this case about 97% of the theoretical density achieved due to commencement

of liquid phase sintering. However, no further improvement in sintered density is observed at more than 2w/o CrB addition. However, for 434L based composites density variation with CrB addition as shown in Figure 3.23 is not much after sintering up to 1200°C. After 1250°C about 97% of the theoretical density is achieved at 3w/o CrB addition. This high level of density is the consequence of liquid phase sintering. Round grains in some of the microstructures shown in Figure 3.24 & Figure 3.25 also suggest commencement of liquid phase sintering.

3.7.2 Microhardness

For 316L based composites, microhardness is highest when CrB content is either 2w/o or 4w/o and sintered at 1250°C as shown in Figure 3.23. But for 434L based composites microhardness increases with increase in CrB content after sintering at 1250°C.

3.7.3 Microstructures

Optical microphotographs of some of the composites with CrB have been shown in Figure 3.24 and Figure 3.25. For both the composites grain growth is pronounced at 1250°C and at an additive content of 3w/o CrB.

3.7.4 Magnetic Properties

For 316L based composites coercivity is zero at all additions and at all sintering temperatures whereas magnetic saturation is within 5 Gauss/g. Variation of coercivity for 434L composites is shown in Figure 3.26. It is observed that coercivity is highest for the composite containing 3w/o CrB sintered at 1250°C. It is also observed from Figure 3.26 that magnetic saturation is lowest again at 3w/o CrB addition.

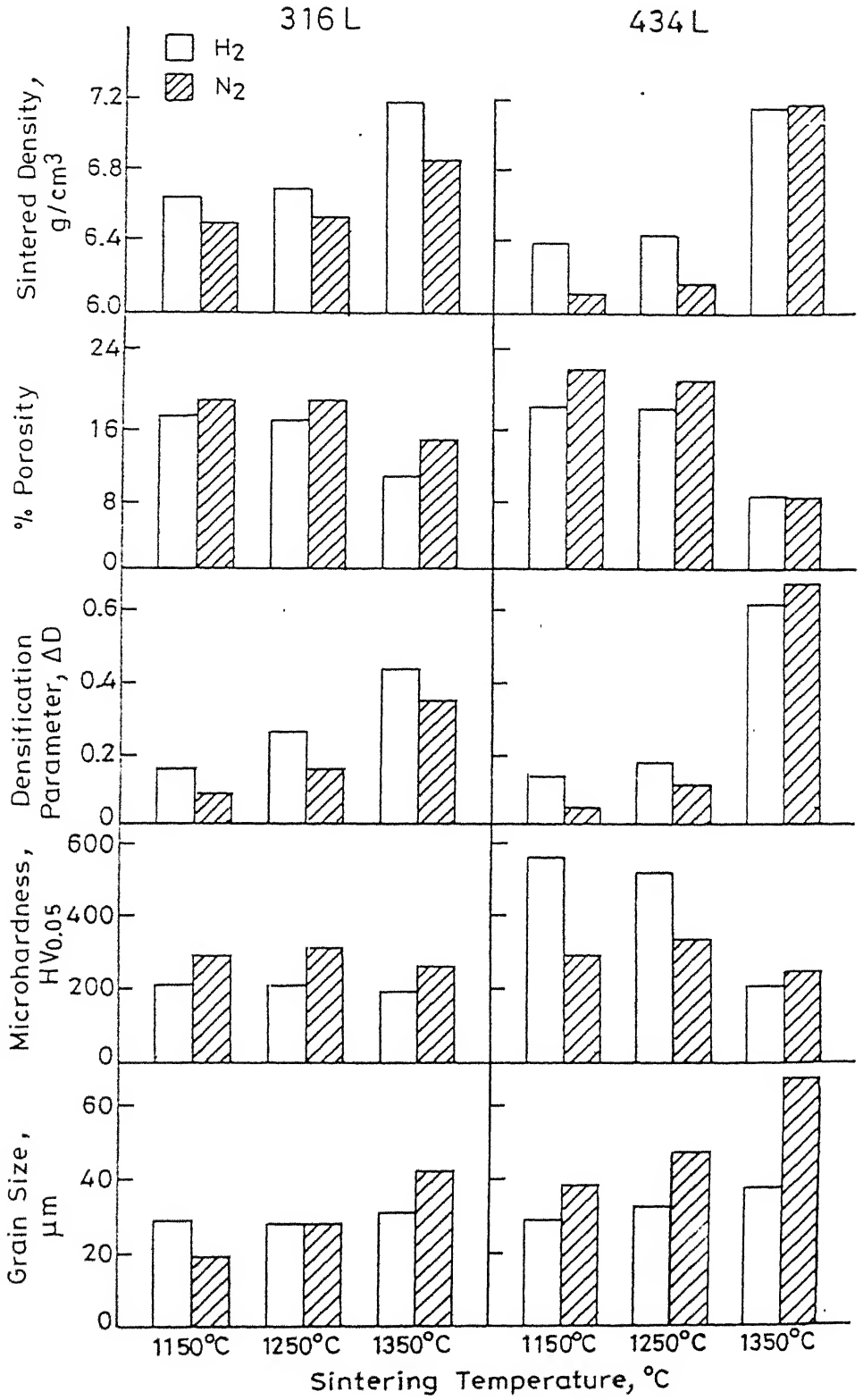

Fig. 3.1 Properties variation of 316L and 434L stainless steels sintered at temperatures in hydrogen and nitrogen respectively.

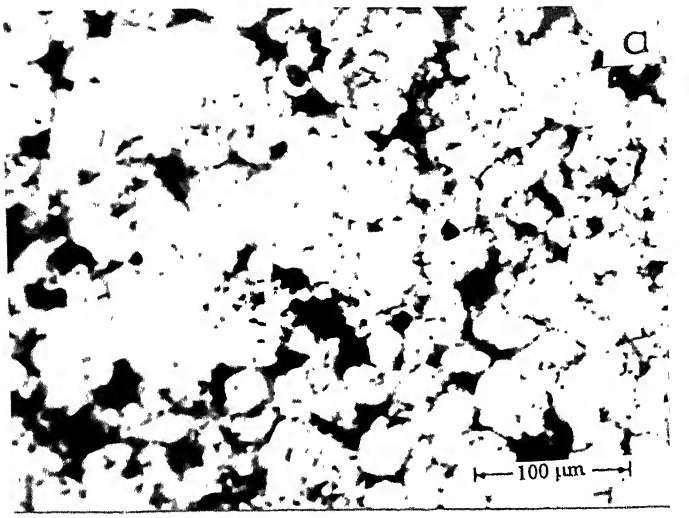
a
100 μm

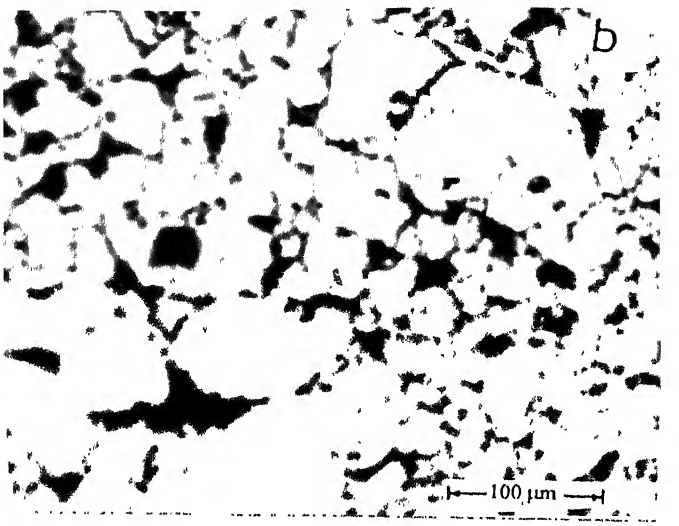
b
100 μm

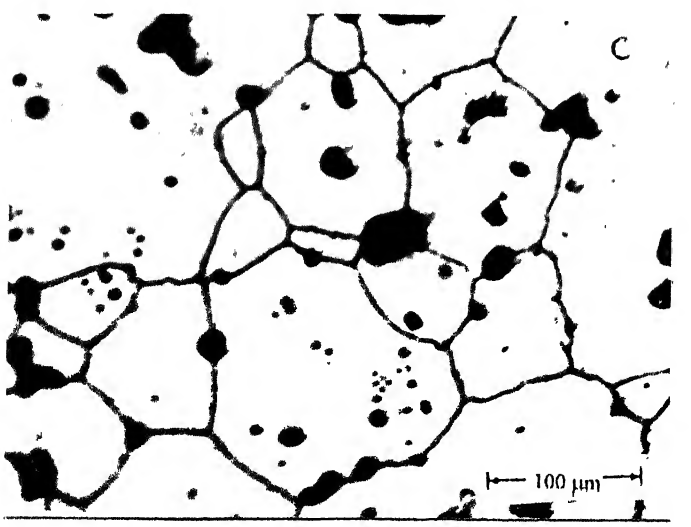
c
100 μm

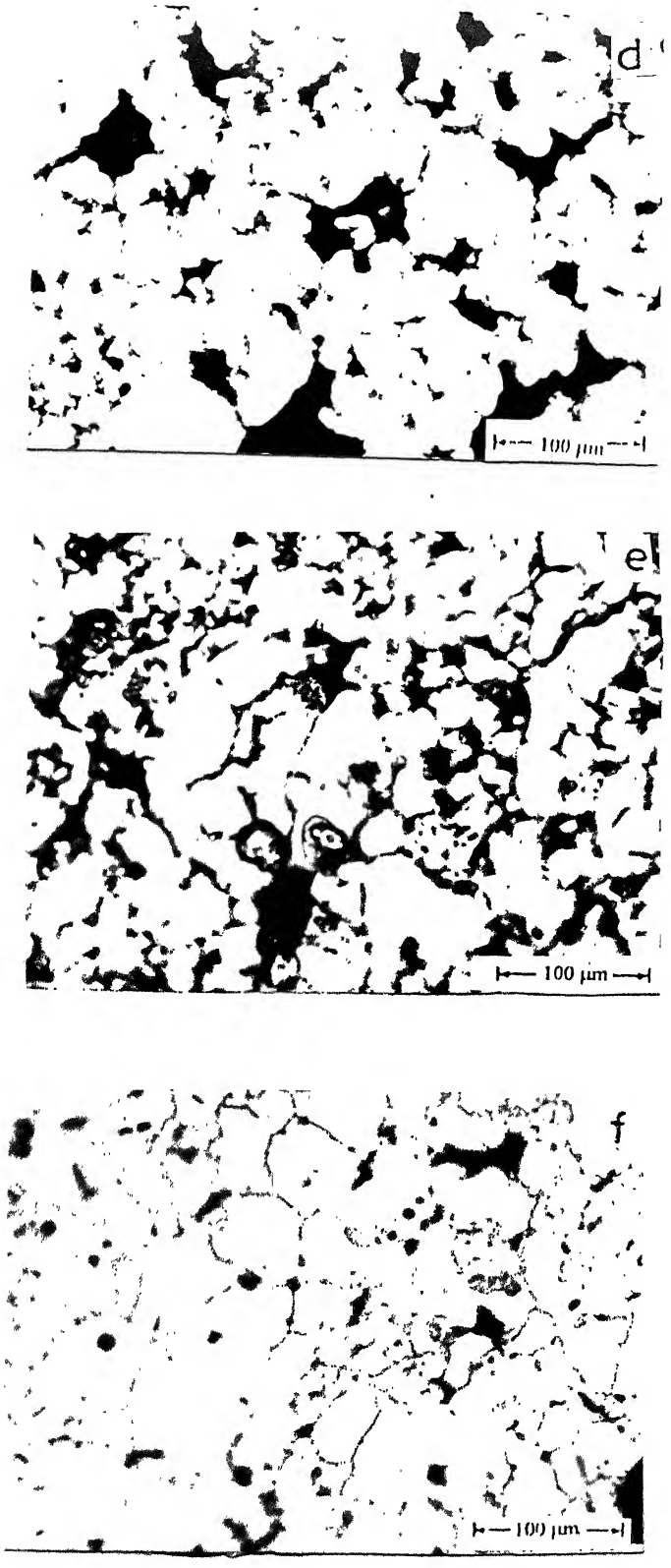

Fig. 3.2 Optical microstructures of 316L and 434L stainless steels sintered at different temperatures in H_2. 316L - (a) 1150°C, (b) 1250°C, (c) 1350°C; 434L - (d) 1150°C, (e) 1250°C, (f) 1350°C.

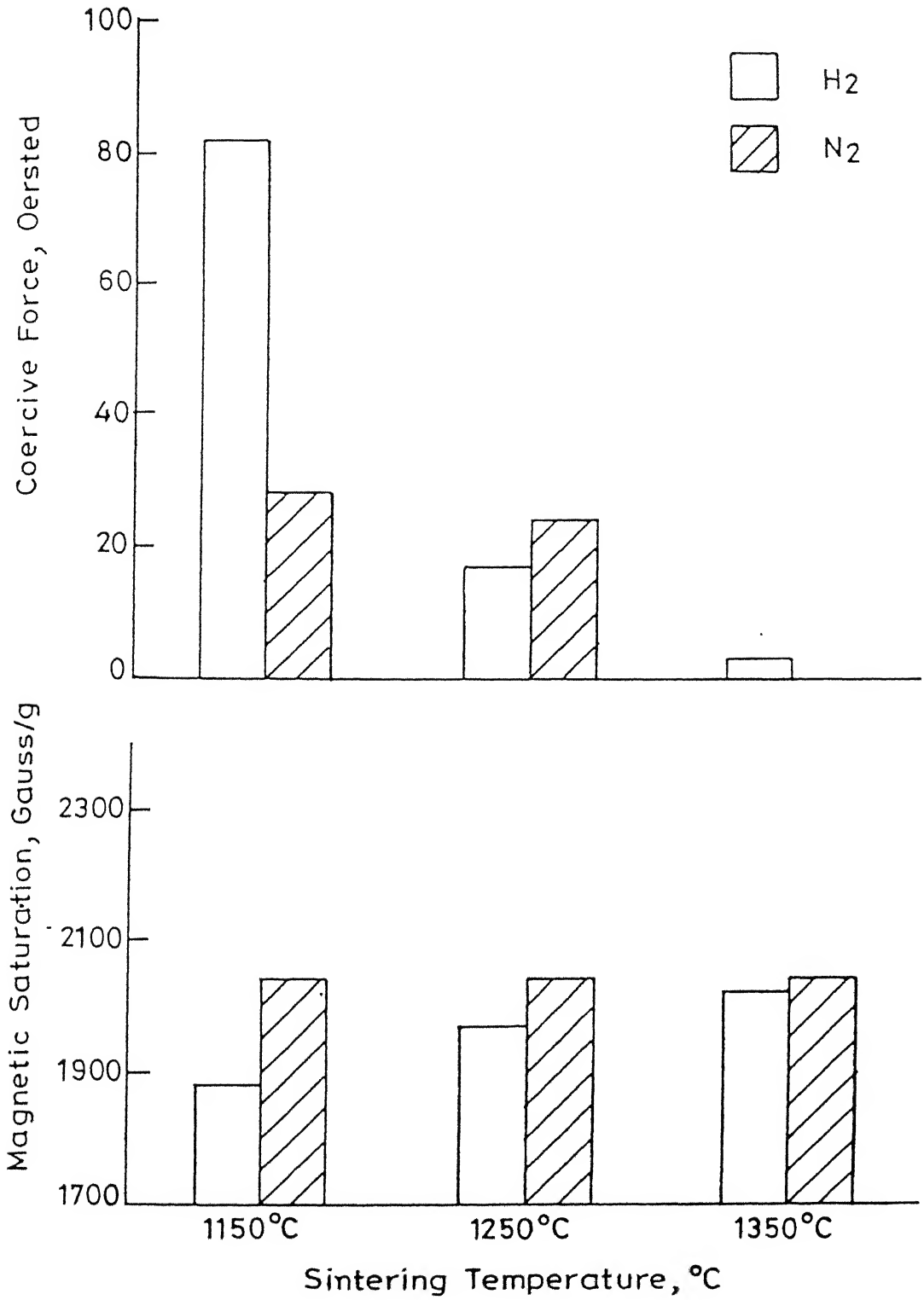

Fig. 3.3 Magnetic properties of 434L stainless steel sintered at different temperatures in hydrogen and nitrogen respectively.

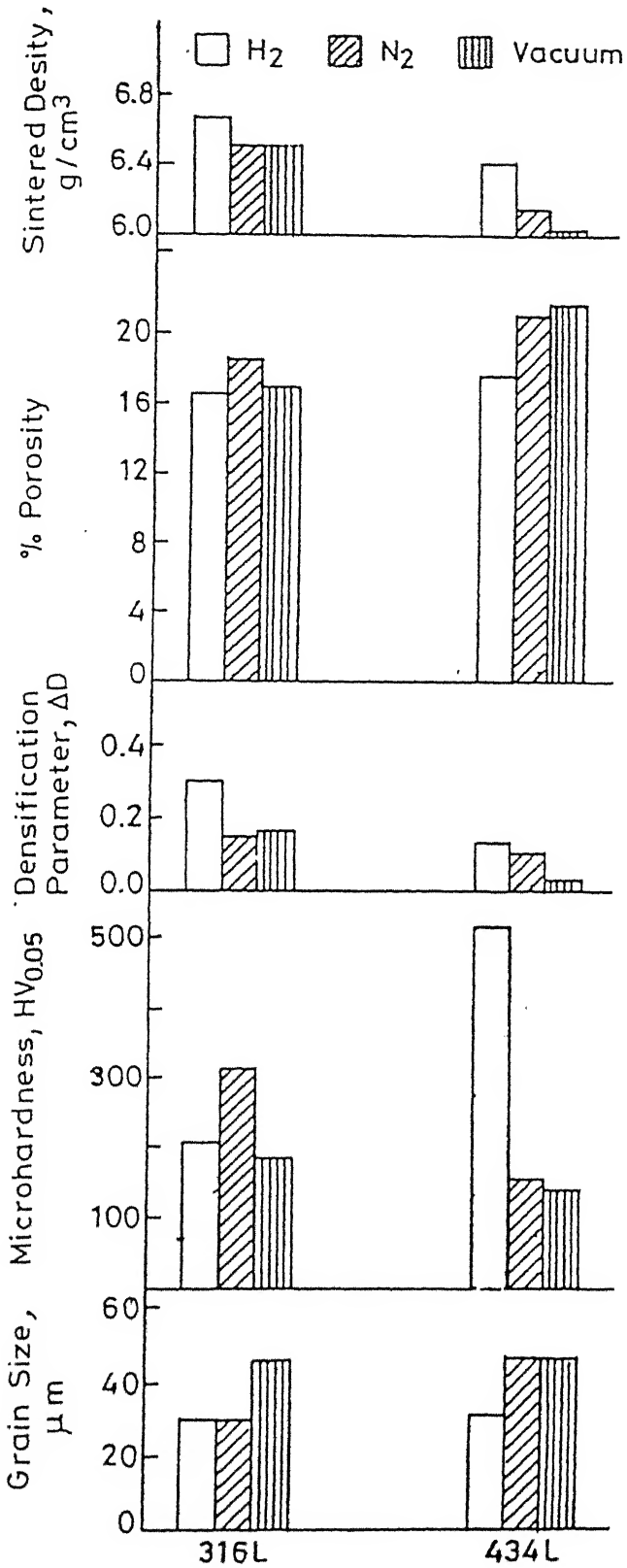

Fig. 3.4 Properties variation of 316L and 434L stainless steels sintered at 1250°C in different atmospheres.

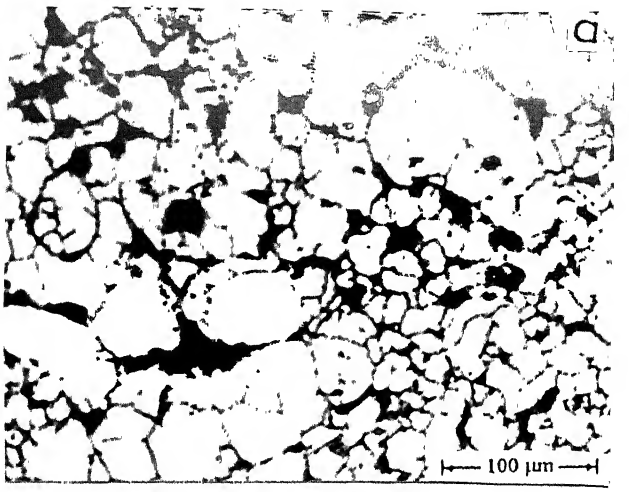
a
100 µm

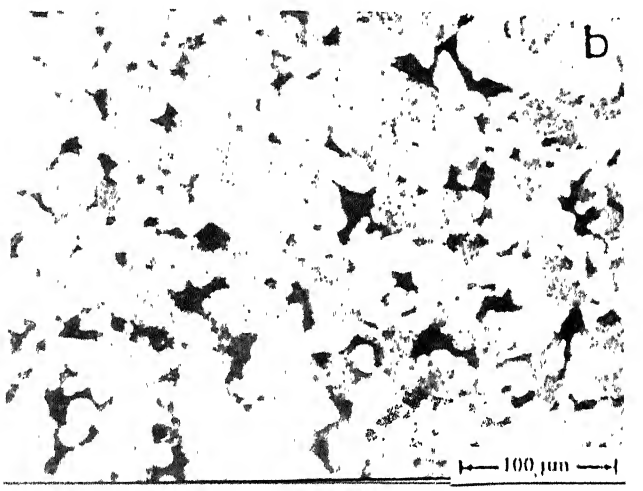
b
100 µm

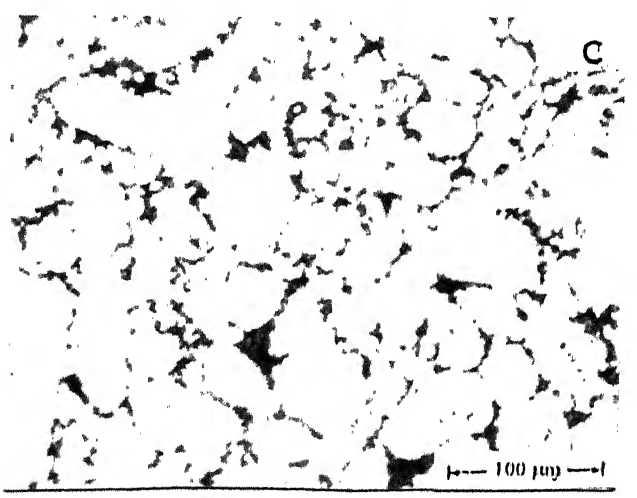
c
100 µm

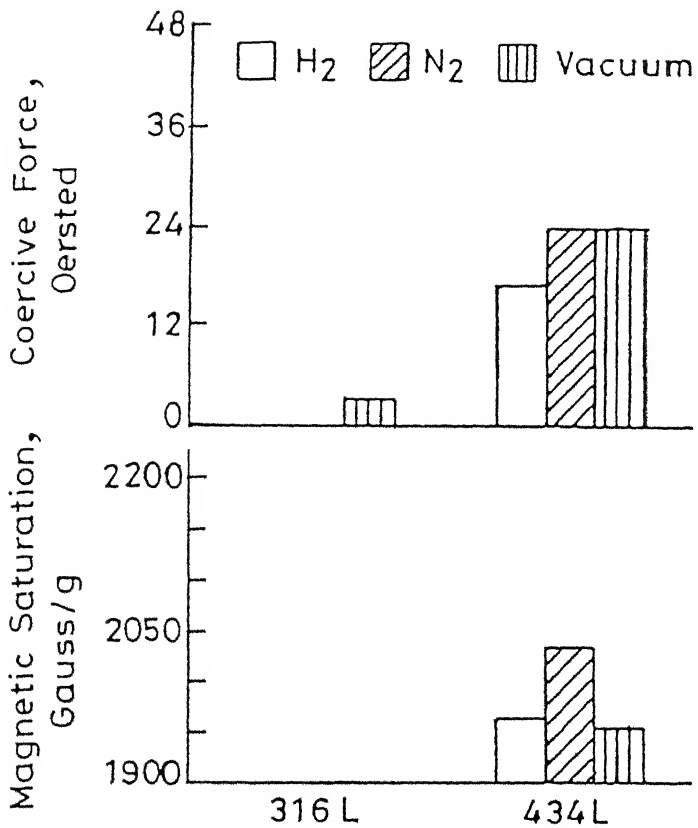

Fig. 3.6 Magnetic properties variation of 316L and 434L stainless steels sintered at 1250°C in different atmospheres.

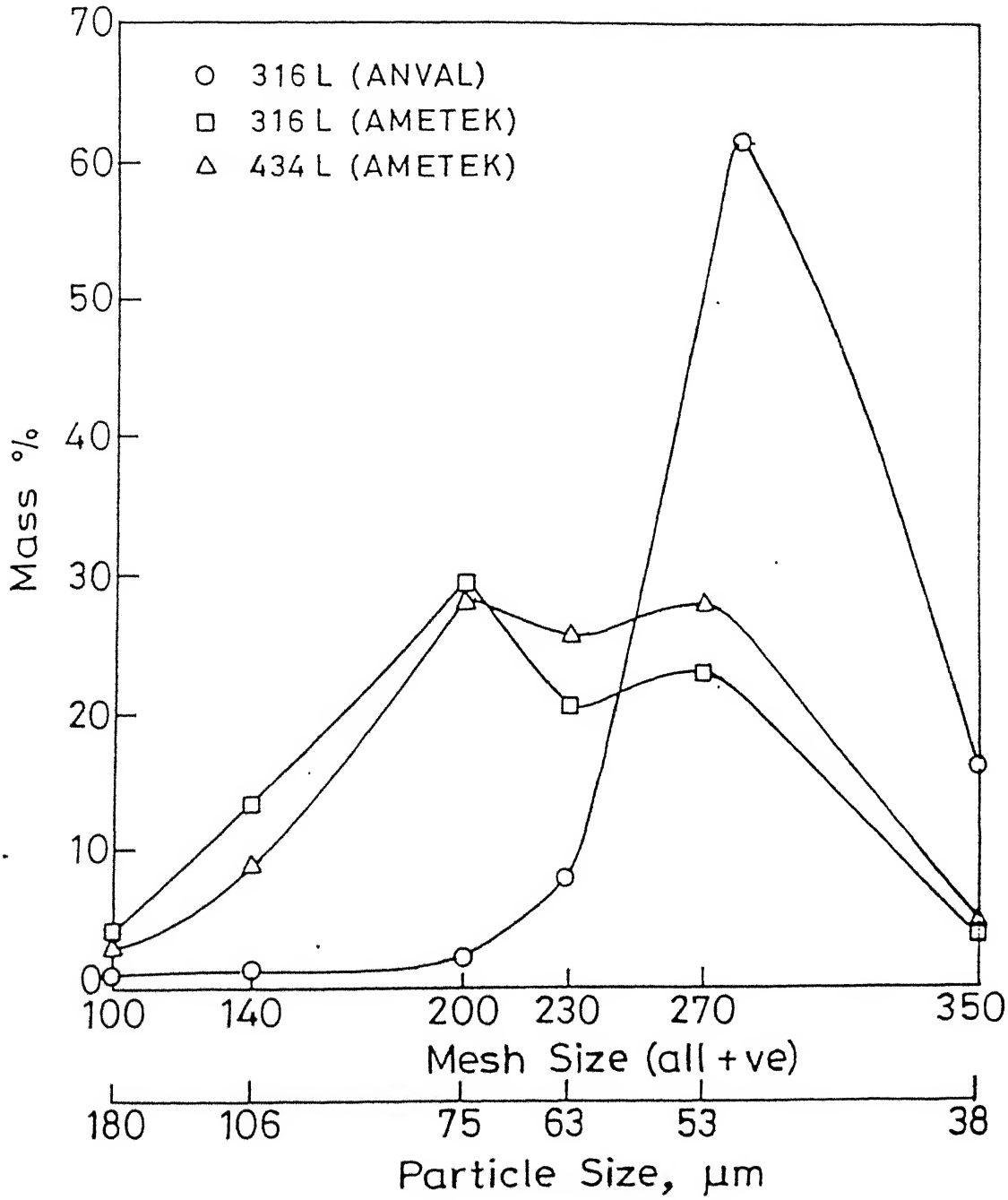

Fig. 3.7 Particle size distribution of various stainless steel powders.

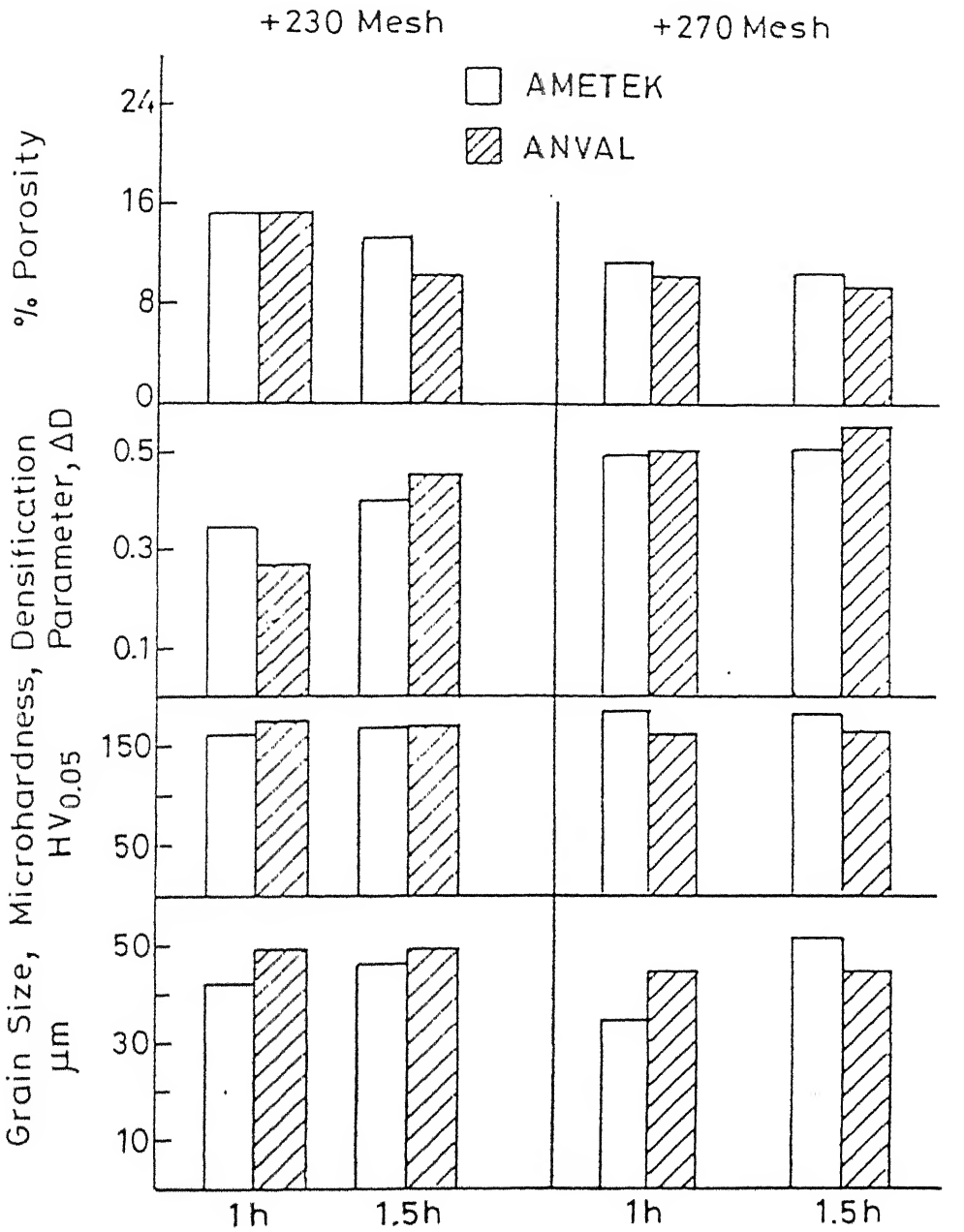

Fig. 3.8 Properties of 316L (AMETEK) and 316L(ANVAL) sintered at 1350°C in H_2 for different periods.

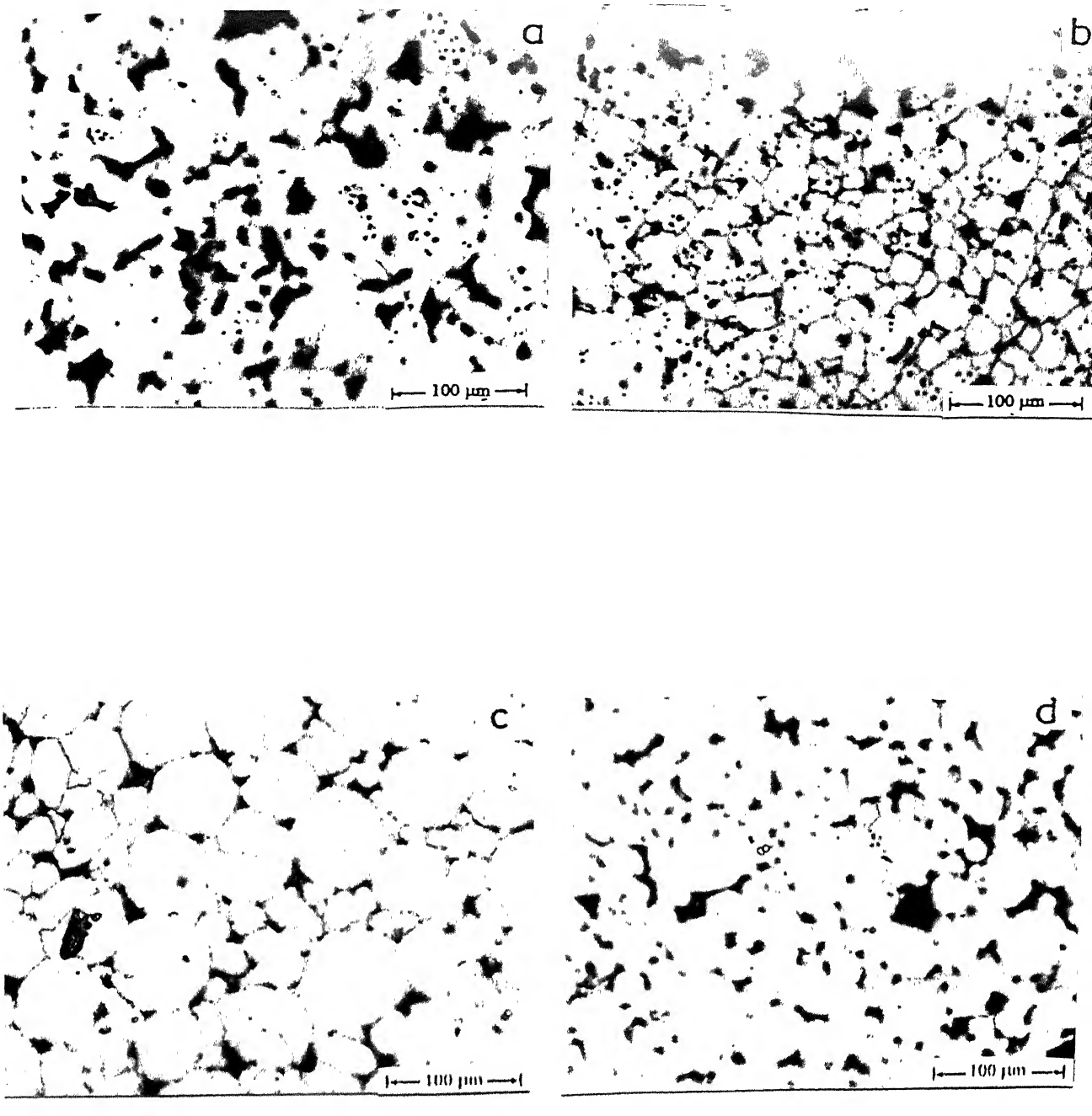

Fig. 3.9 Optical microstructures of 316L (AMETEK) and 316L(ANVAL) sintered at 1350°C for 1 hr in H_2. AMETEK - (a) + 230 mesh, (a) + 270 mesh; ANVAL - (c) + 230 mesh, (d) + 270 mesh.

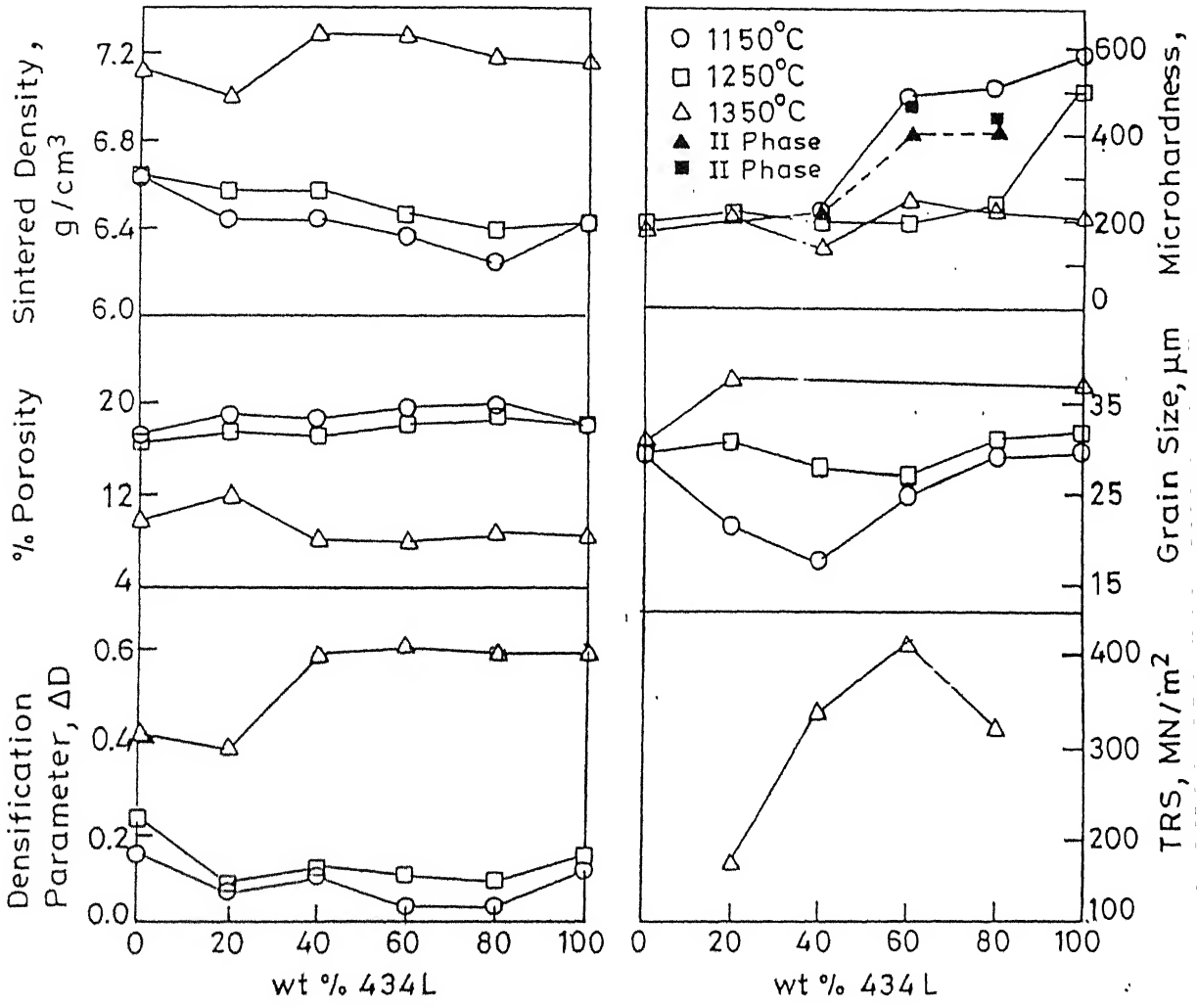

Fig. 3.10 Properties variation of 316L-434L composites sintered in H_2 at different temperatures.

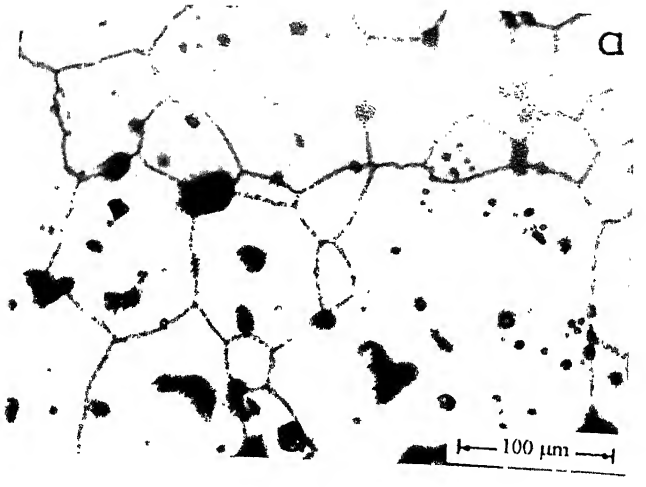
a
100 μm

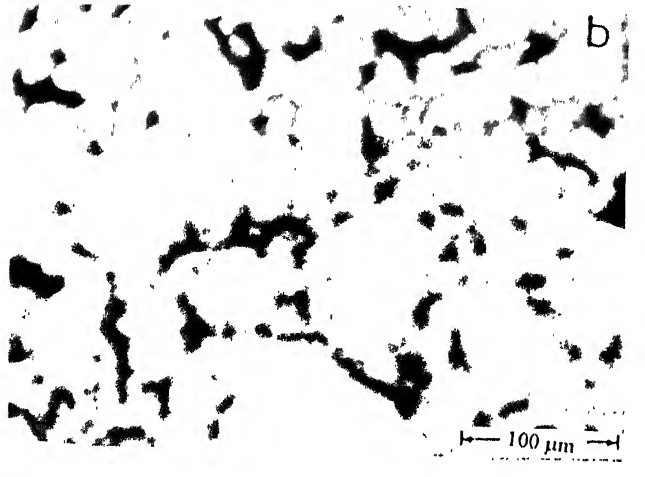
b
100 μm

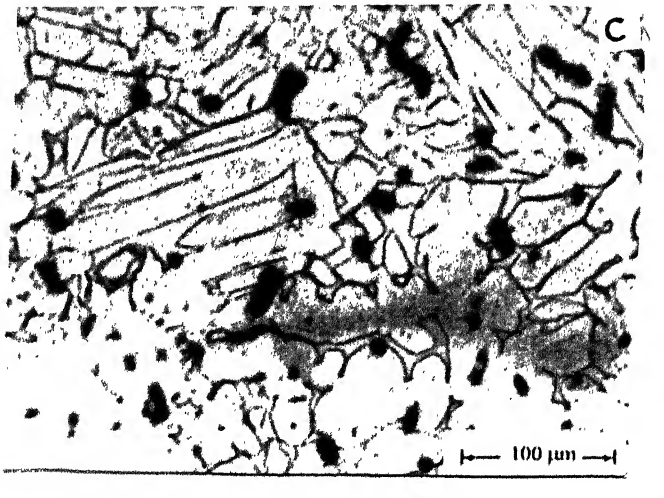
c
100 μm

Fig. 3.11 Optical microstructures of 316L-434L composites sintered at 1350°C in H_2. (a) 0w/o 434L, (b) 20w/o 434L, (c) 40w/o 434L, (d) 60w/o 434L, (e) 80w/o 434L, (f) 100w/o 434L.

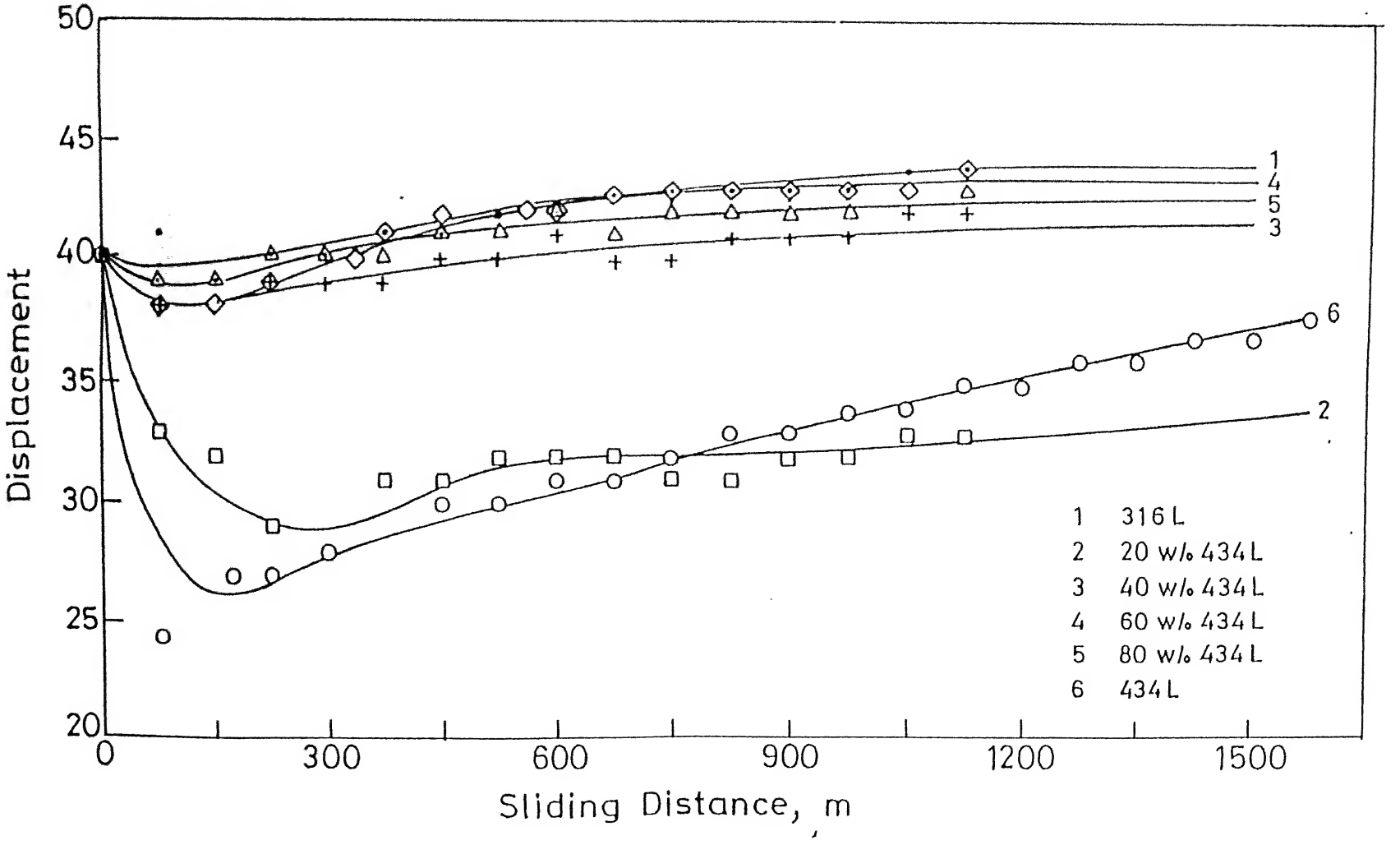

Fig. 3.12 Sliding wear loss of 316L-434L composites sintered at 1350°C in H_2 with respect to sliding distance.

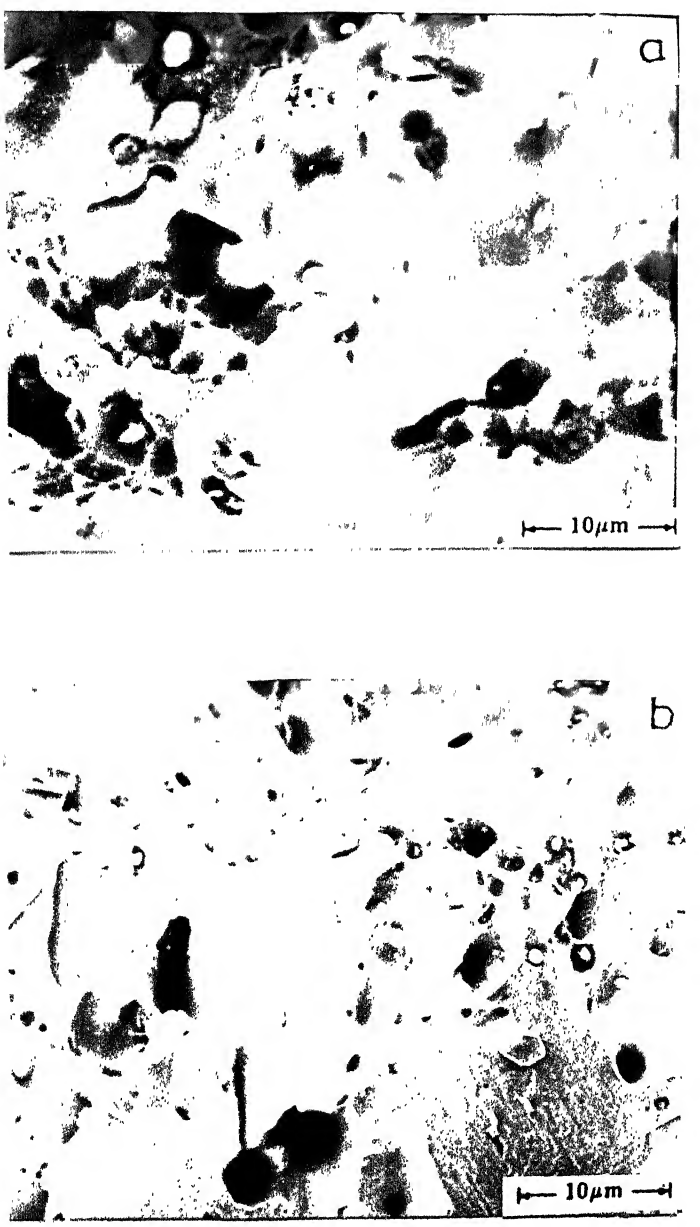

Fig. 3.13 Scanning fractographs of 316L-434L composites sintered at 1350°C in H_2. (a) 60w/o 434L and (b) 80w/o 434L.

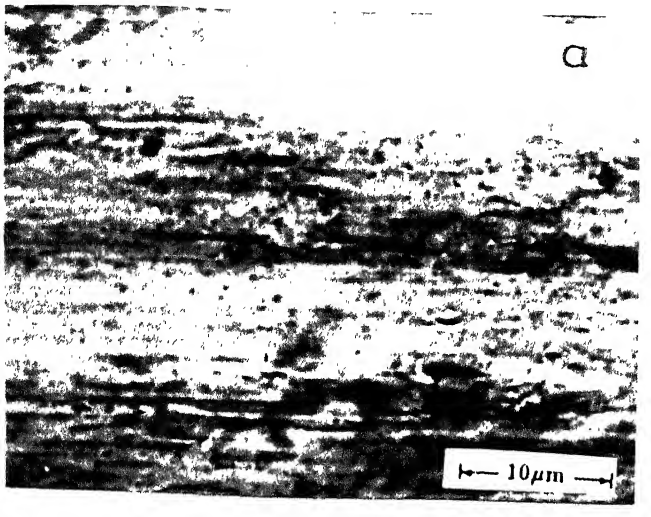
a
10μm

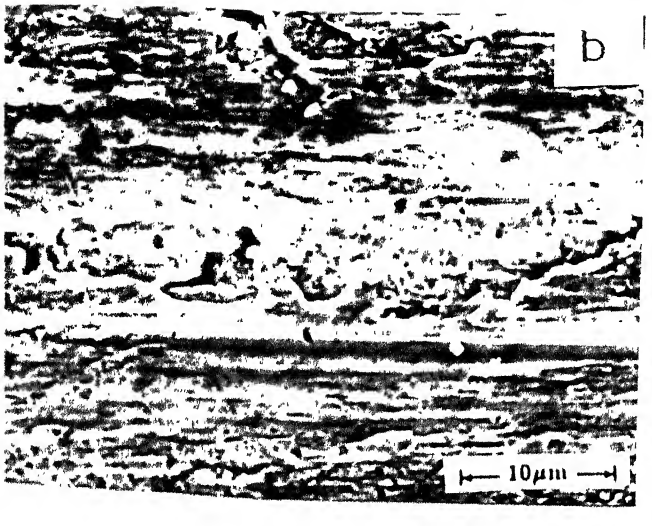
b
10μm

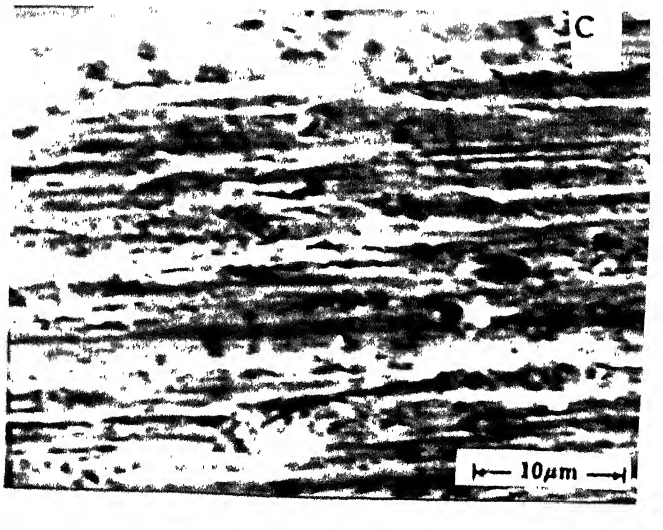
c
10μm

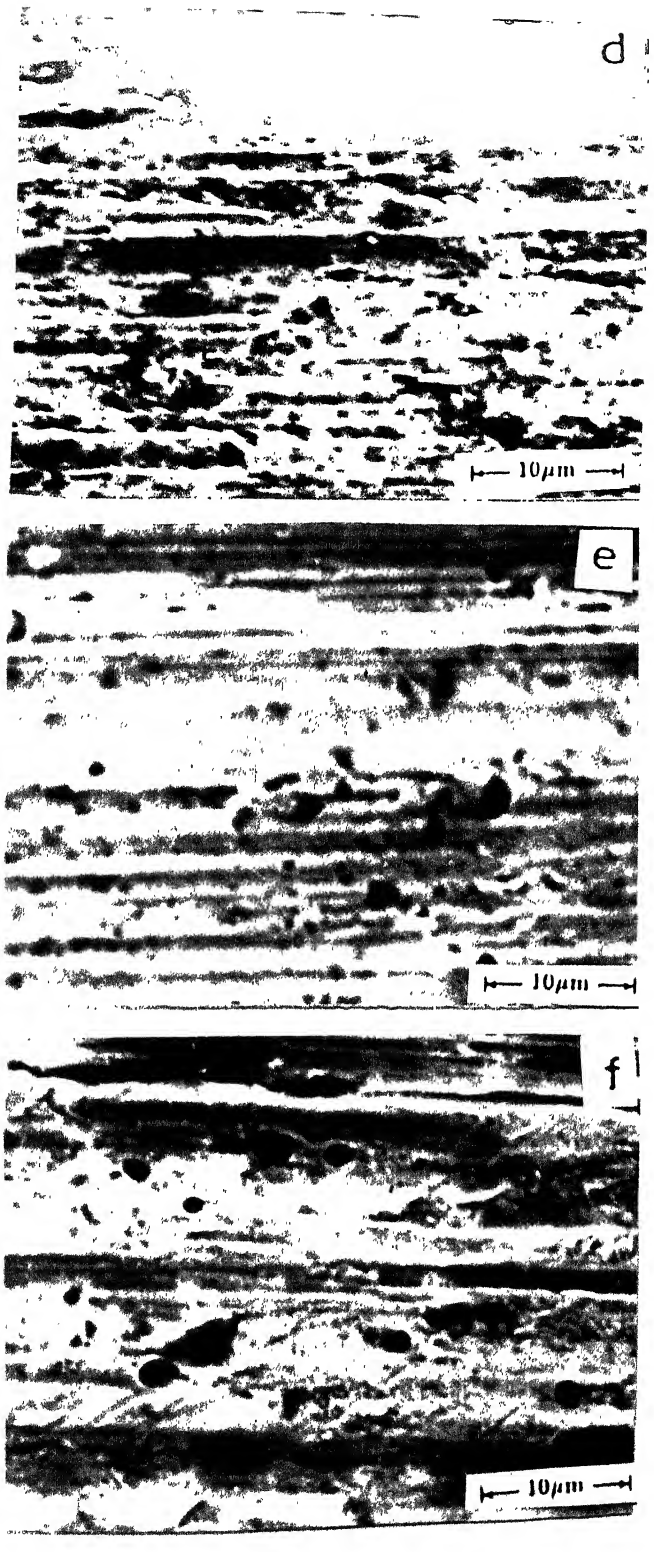

Fig. 3.14 SEM pictures of worn out surfaces of sintered stainless steels and their composites after sliding wear testing for 1650 m. (a) 0w/o 434L, (b) 20w/o 434L, (c) 40w/o 434L, (d) 60w/o 434L, (e) 80w/o 434L, (f) 100w/o 434L.

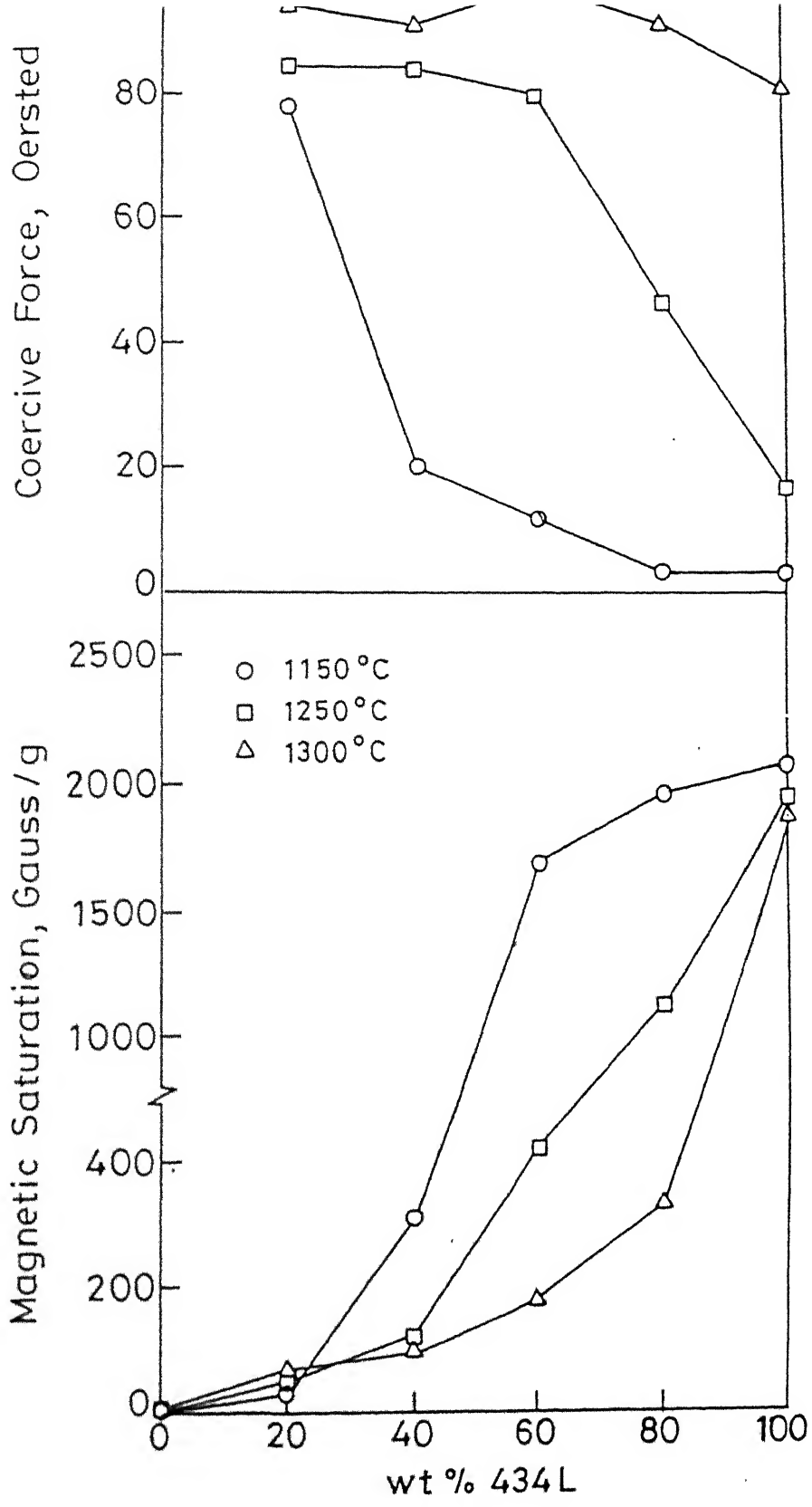

Fig. 3.15 Magnetic properties variation of 316L-434L composites sintered at different temperatures in H_2.

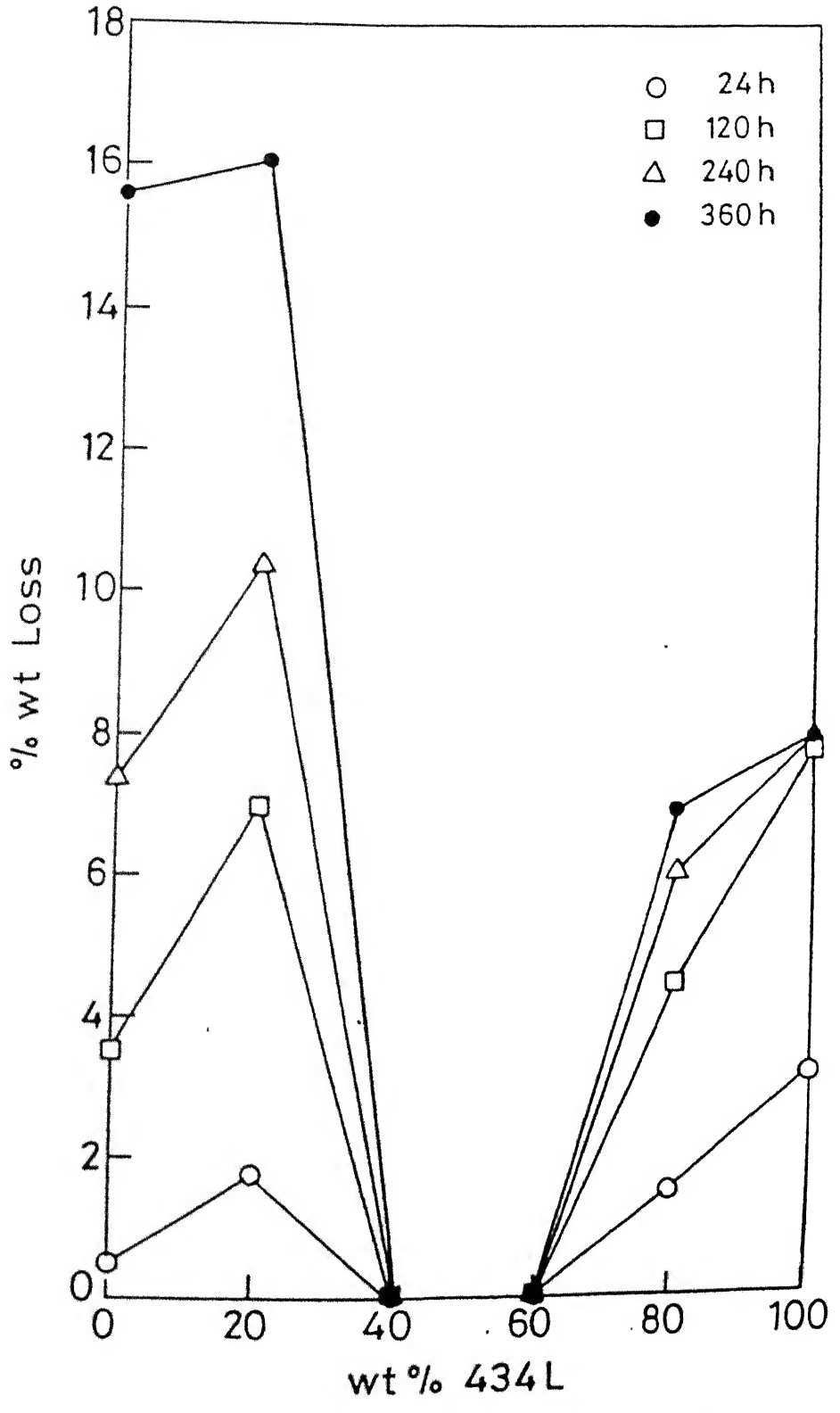

Fig. 3.16 Corrosion weight loss variation of 316L-434L composites in 1(N) H_2SO_4 after various exposure times. Sintered at 1350°C for 1 hr in H_2.

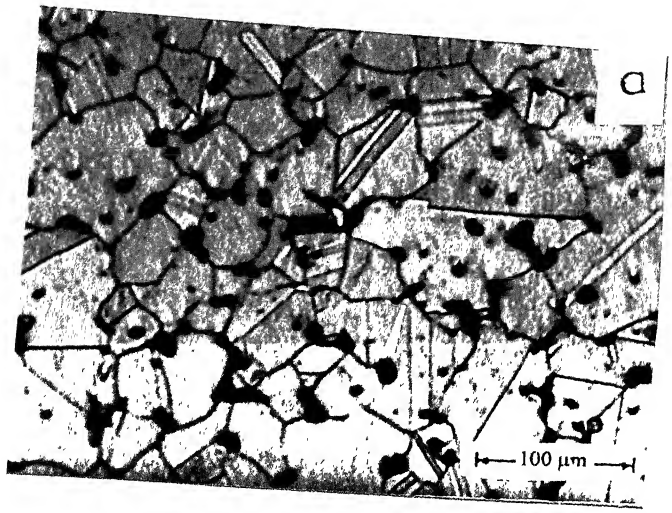
a
100 µm

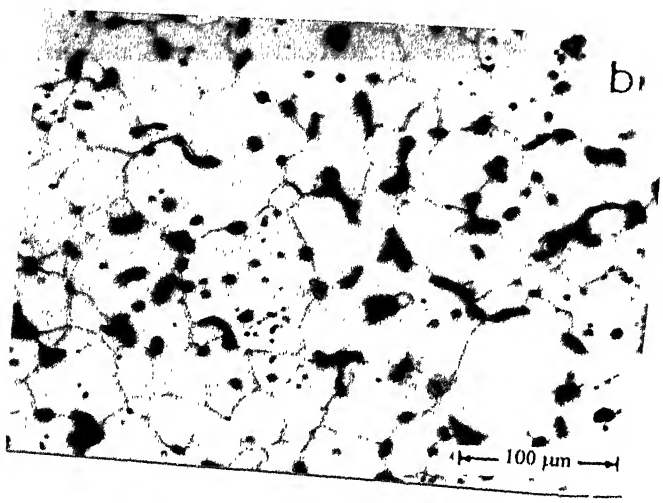
b
100 µm

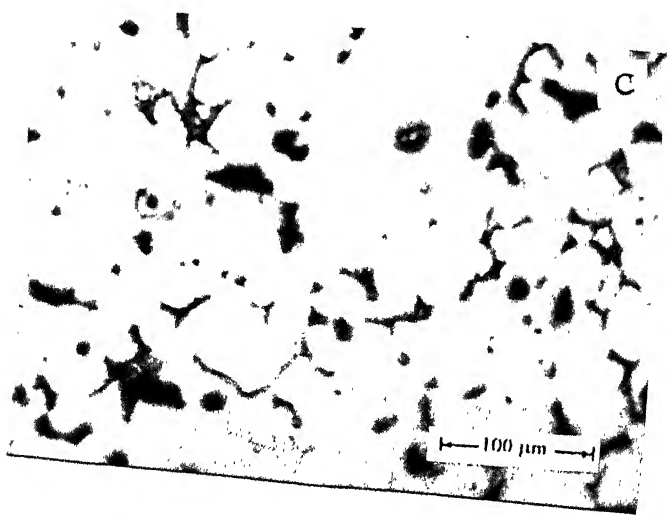
c
100 µm

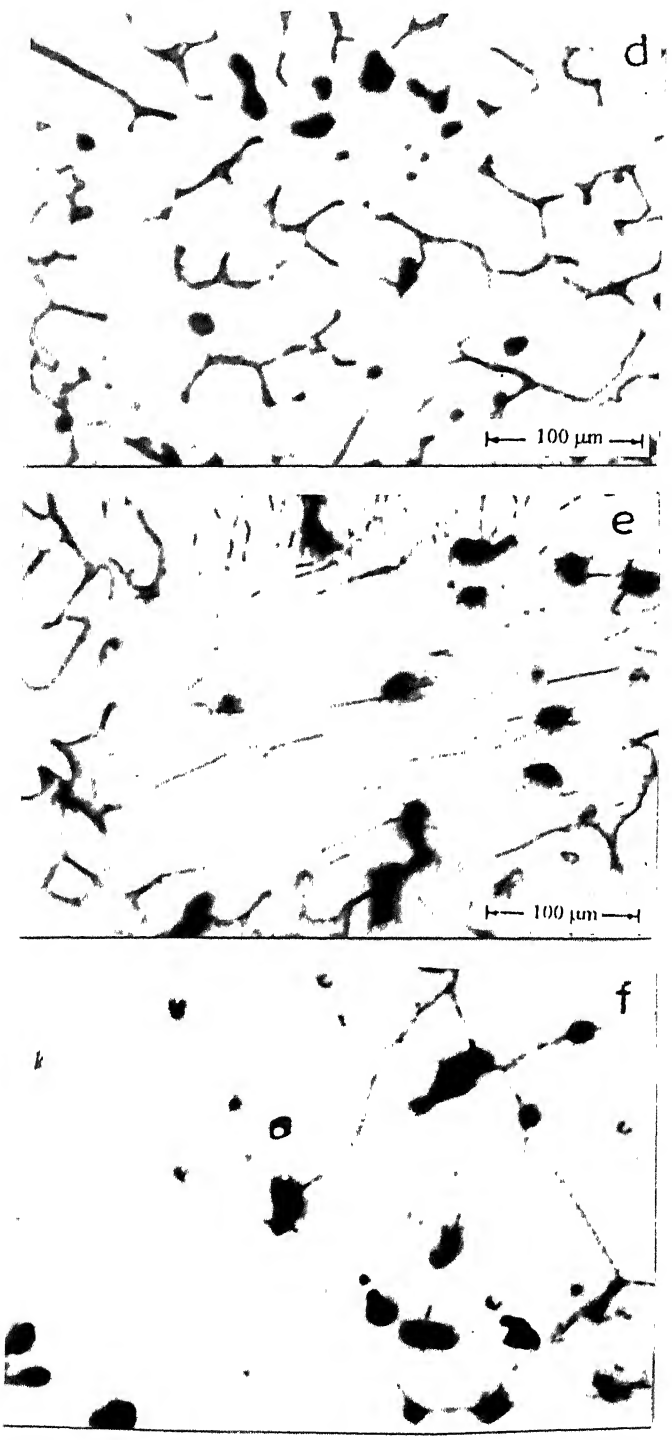

Fig. 3.18 Optical microstructures of 316L-434L composites with 2 mass % copper sintered at 1350°C in H_2 for 1 hr. (a) 0w/o 434L, (b) 20w/o 434L, (c) 40w/o 434L, (d) 60w/o 434L, (e) 80w/o 434L, (f) 100w/o 434L.

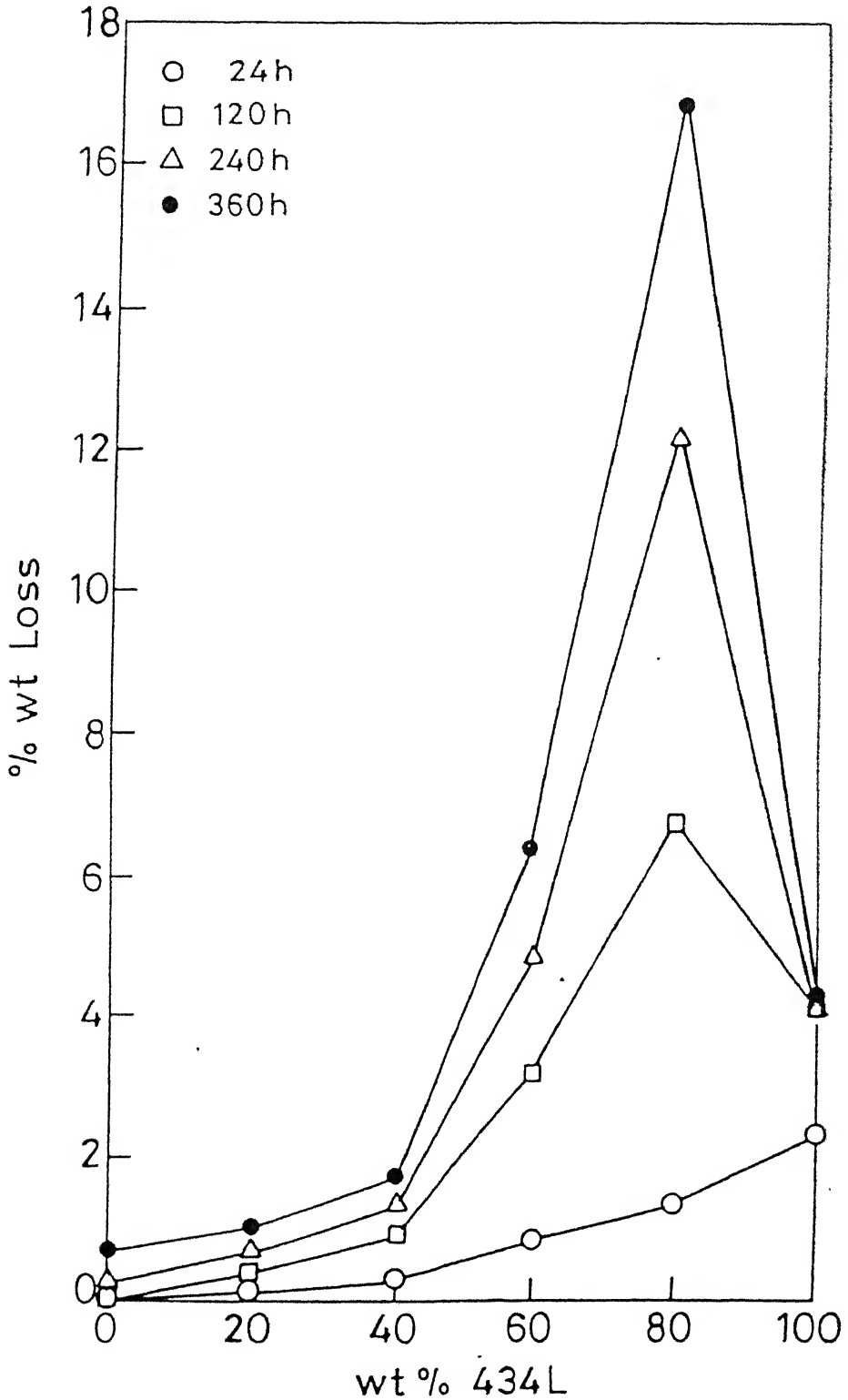

Fig. 3.19 Corrosion weight loss variation of copper containing 316L-434L composites in 1(N) H_2SO_4 after various exposure times (sintered at 1350°C in H_2 for 1 hr).

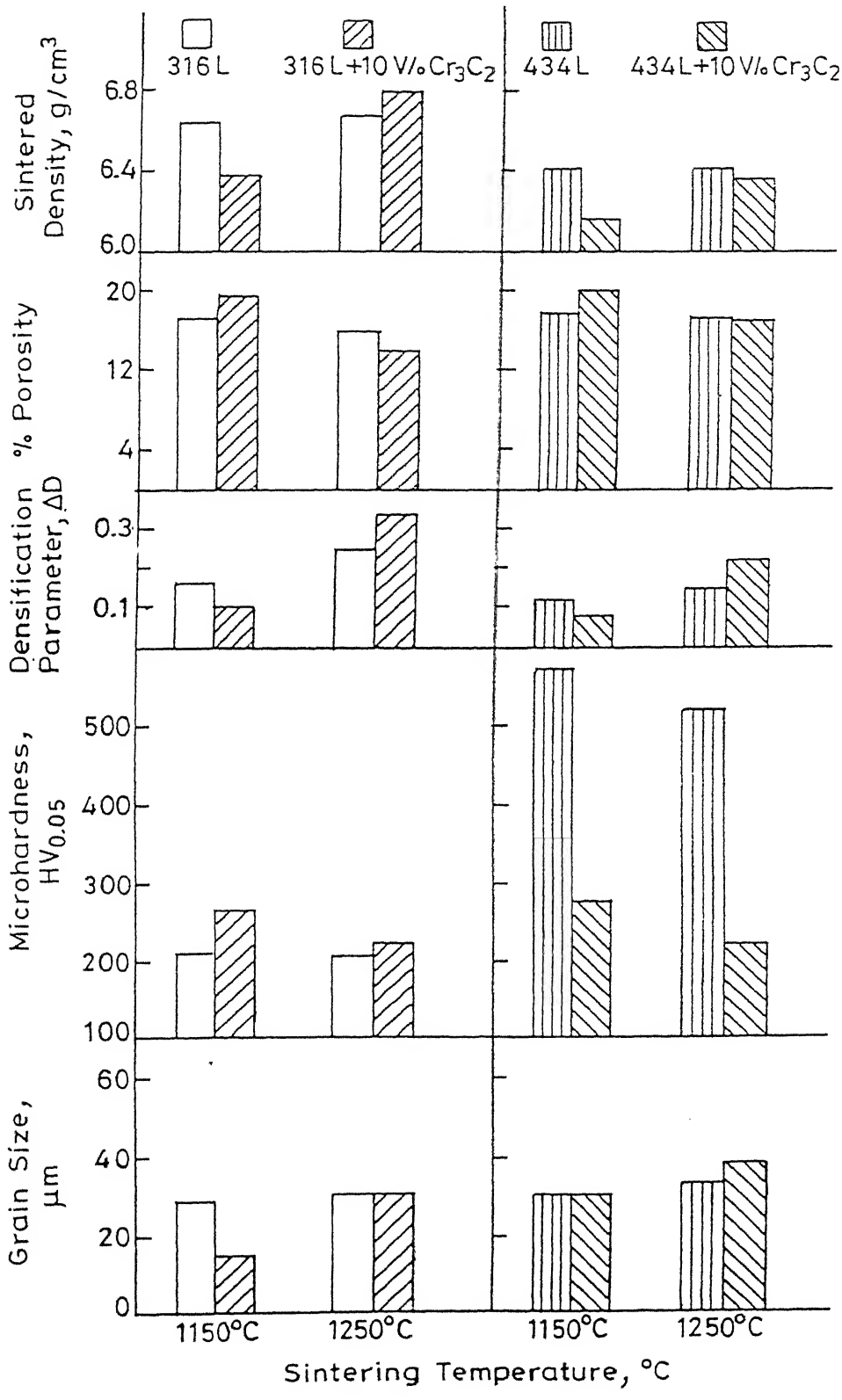

Fig. 3.20 Properties variation of 316L and 434L stainless steels containing 10v/o Cr_3C_2 sintered at different temperatures in H_2.

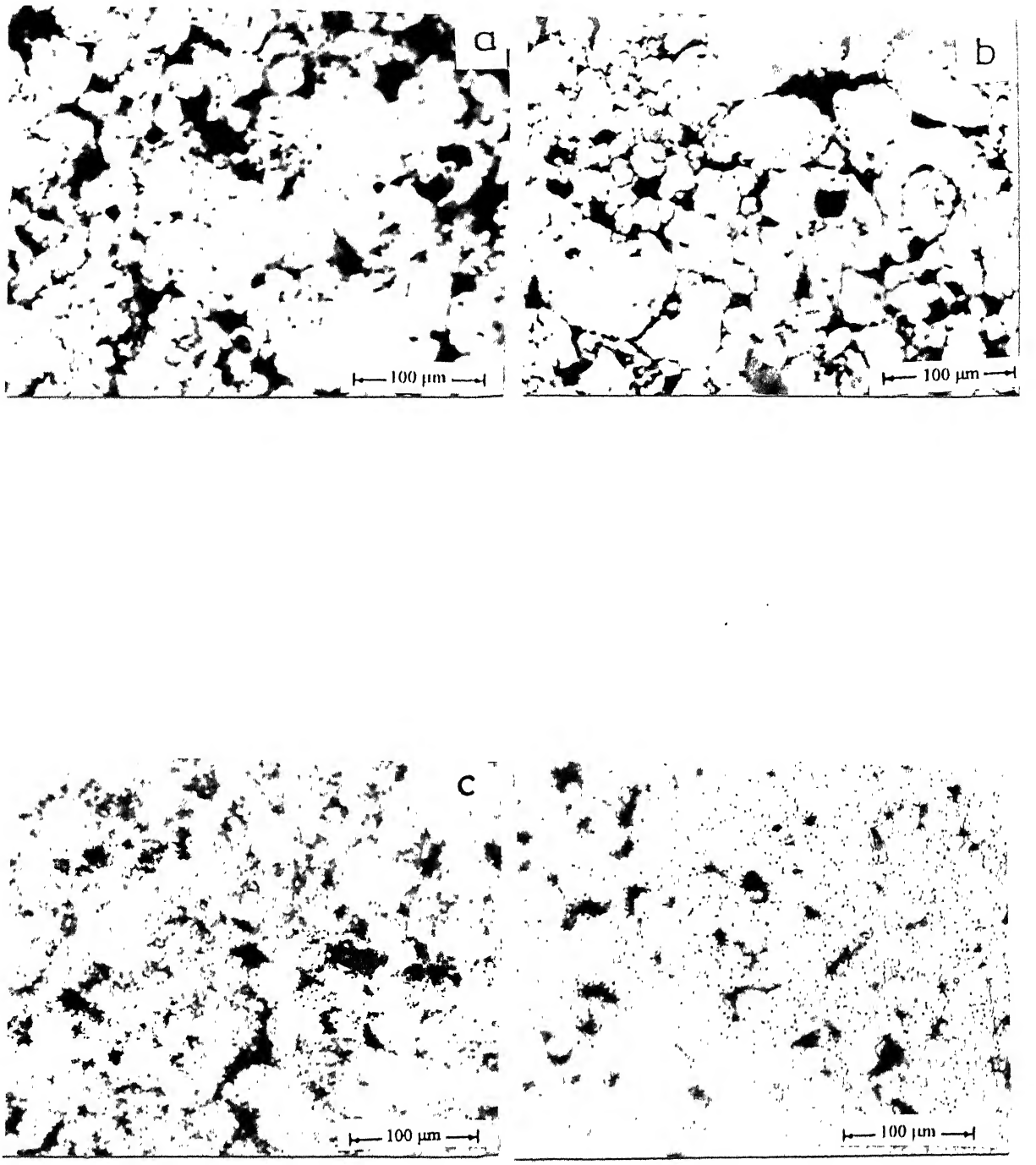

Fig. 3.21A Optical microstructures of 316L-10v/o Cr_3C_2 composites sintered at different temperatures in H_2. 316L - (a) 1150°C, (b) 1250°C, composite (c) 1150°C, (d) 1250°C.

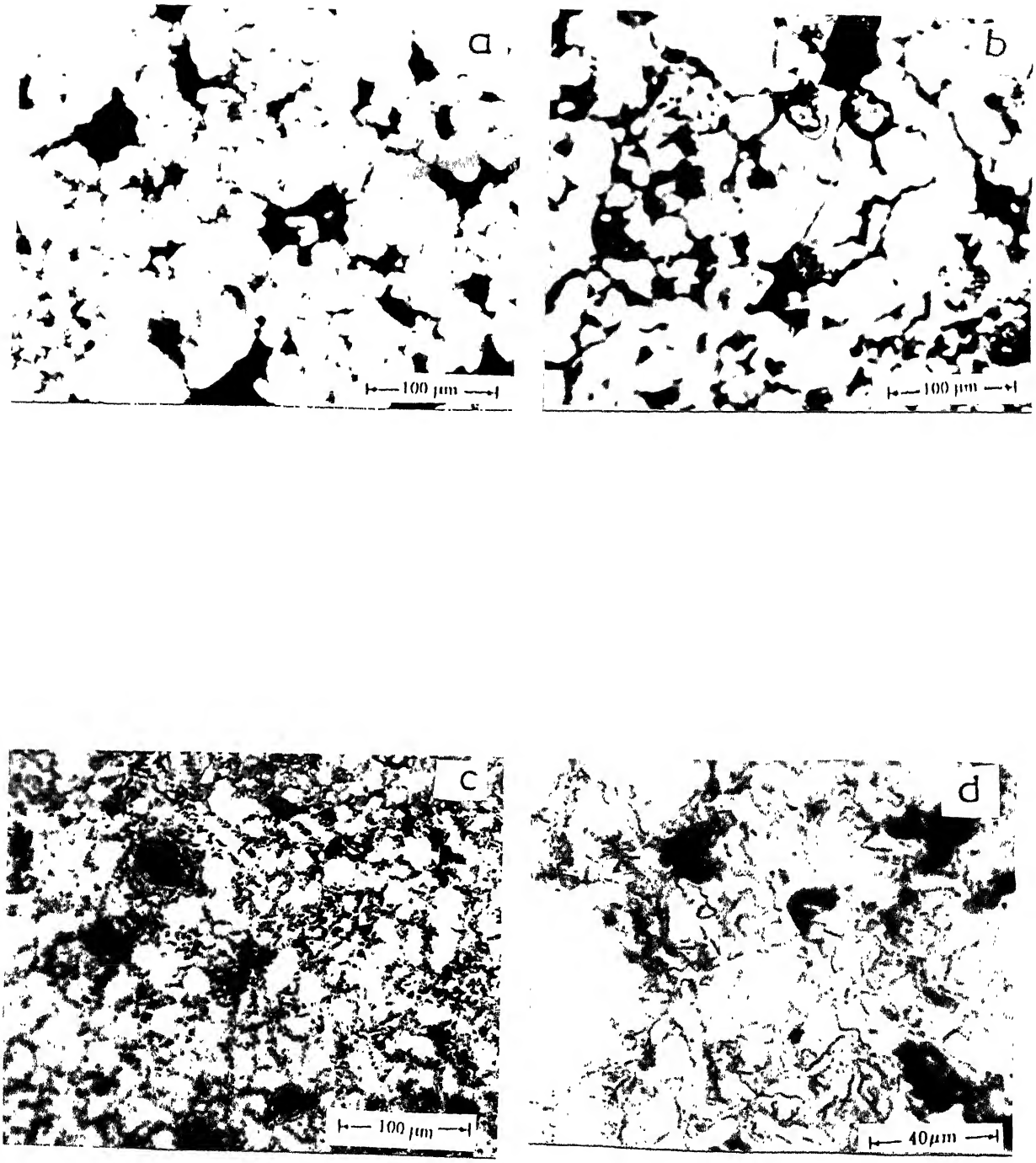

Fig. 3.21B Optical microstructures of 434L-10v/o Cr_3C_2 composites sintered at different temperatures in H_2. 434L - (a) 1150°C, (b) 1250°C, composite (c) 1150°C, (d) 1250°C.

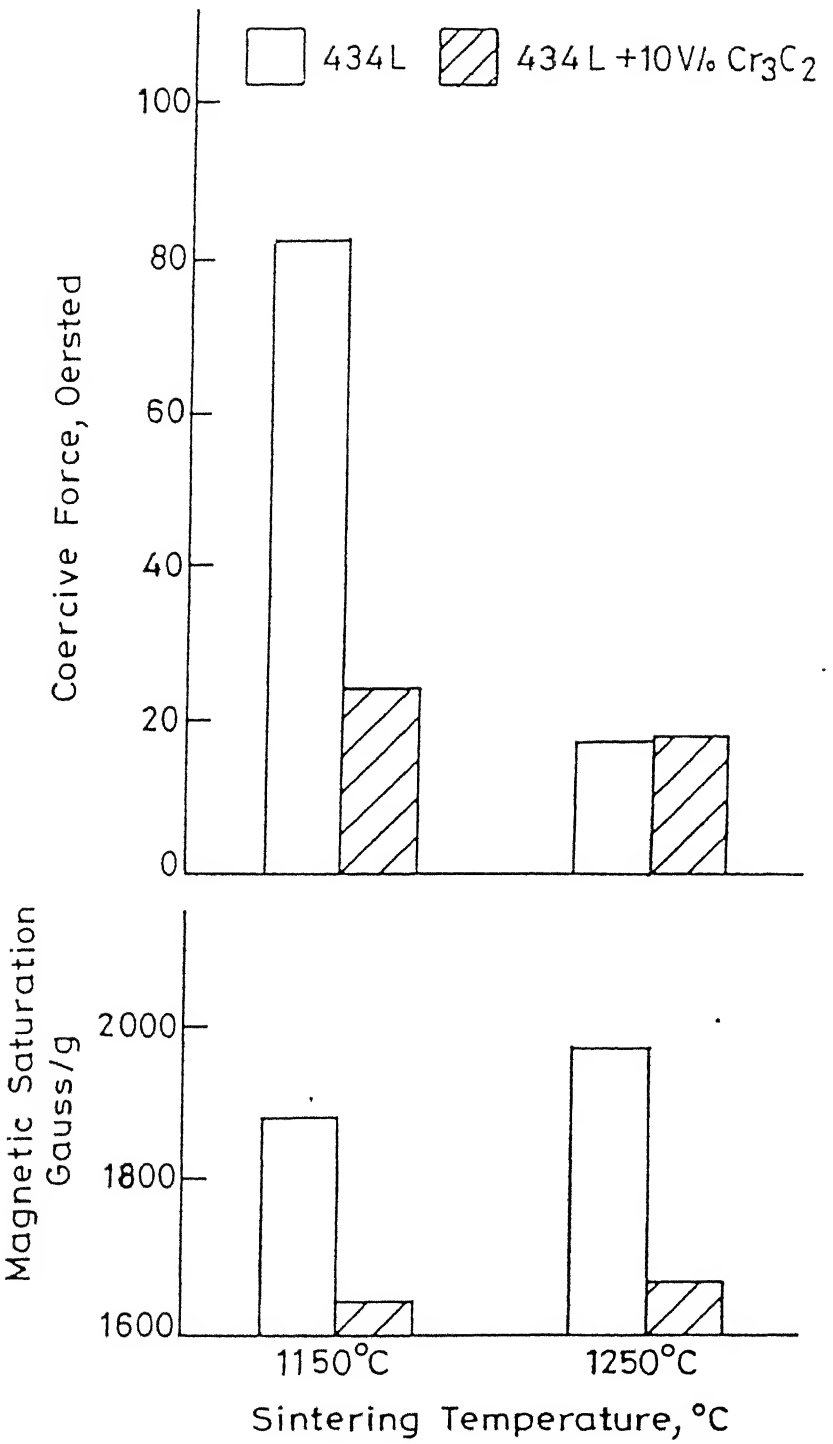

Fig. 3.22 Magnetic properties of 434L-10v/o Cr_3C_2 composites sintered at different temperatures in H_2.

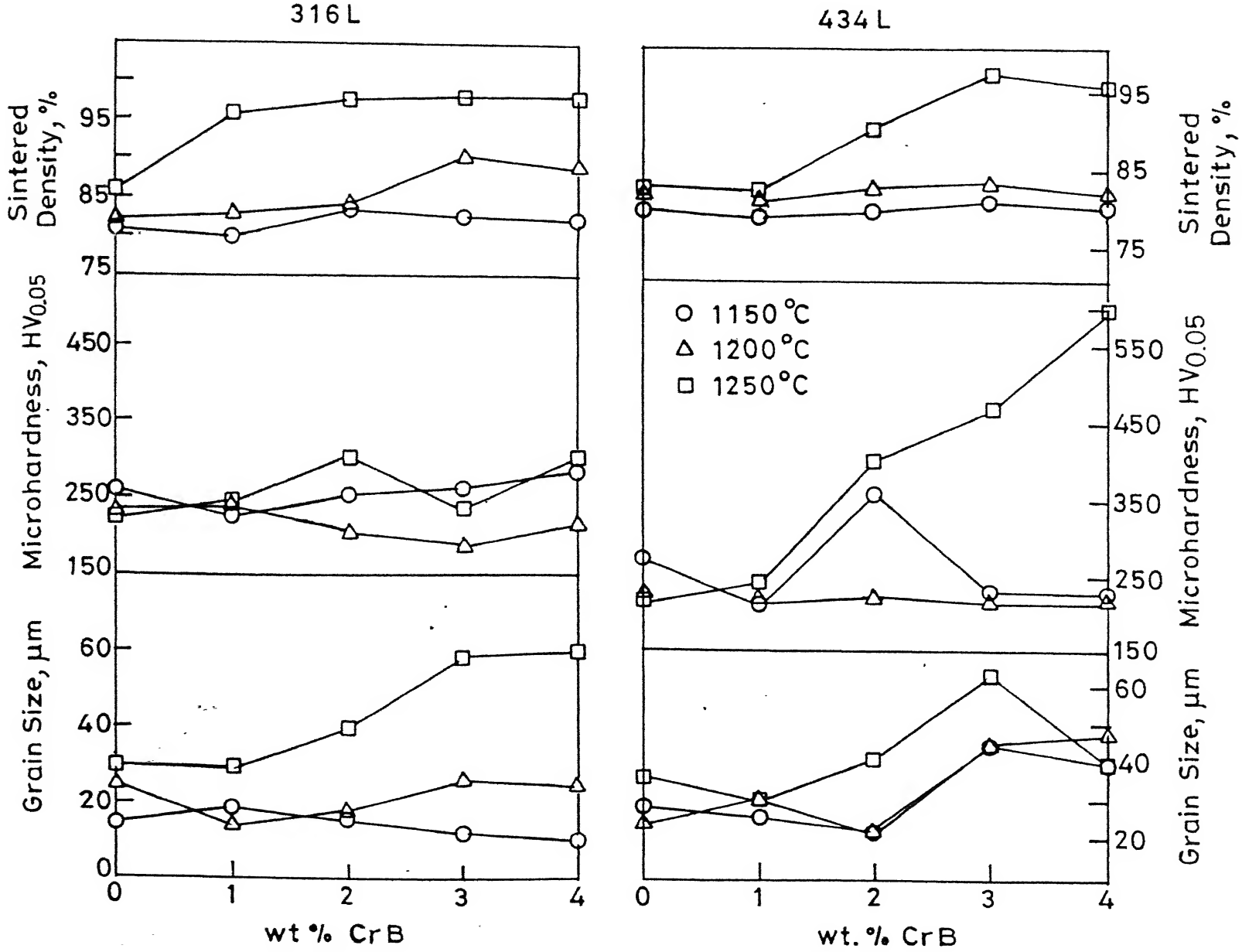

Fig. 3.23 Properties variation of 316L and 434L stainless steels containing Cr_3C_2/CrB sintered at different temperatures in H_2.

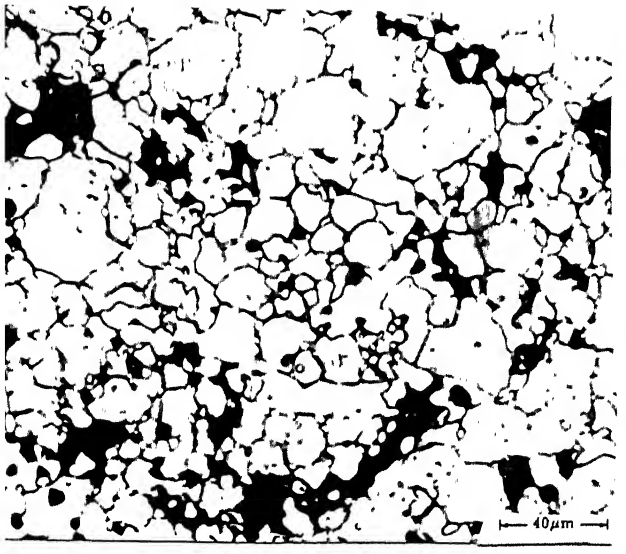
40μm

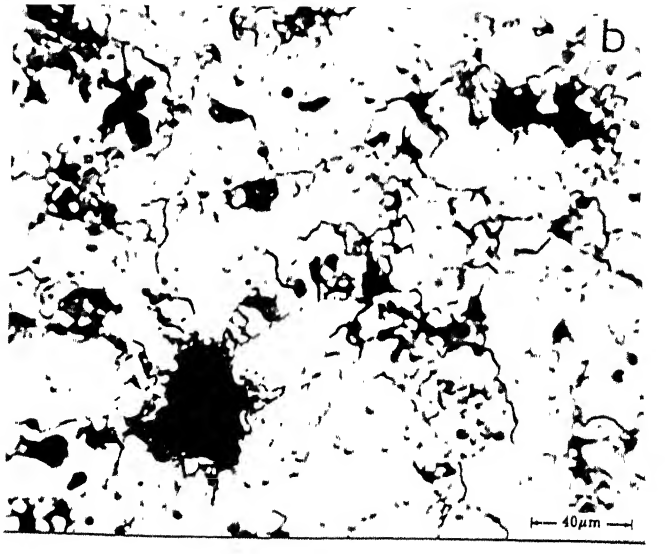
b
40μm

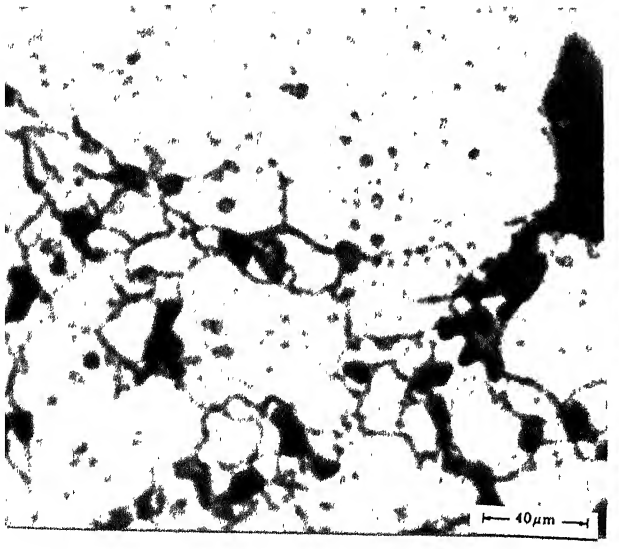
40μm

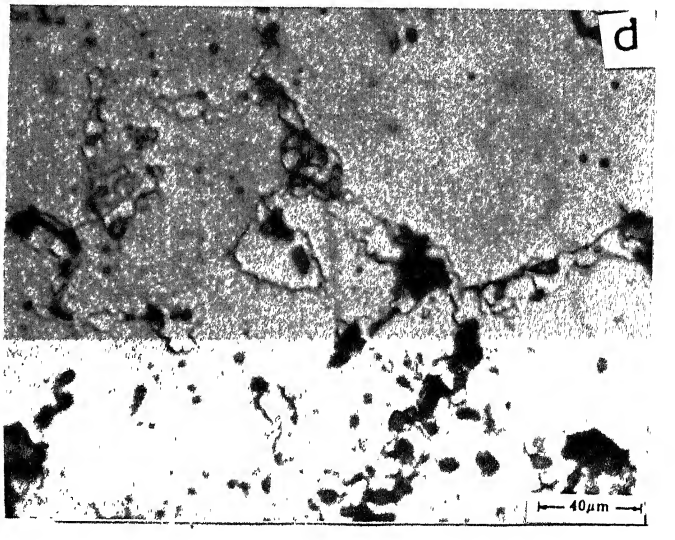
d
40μm

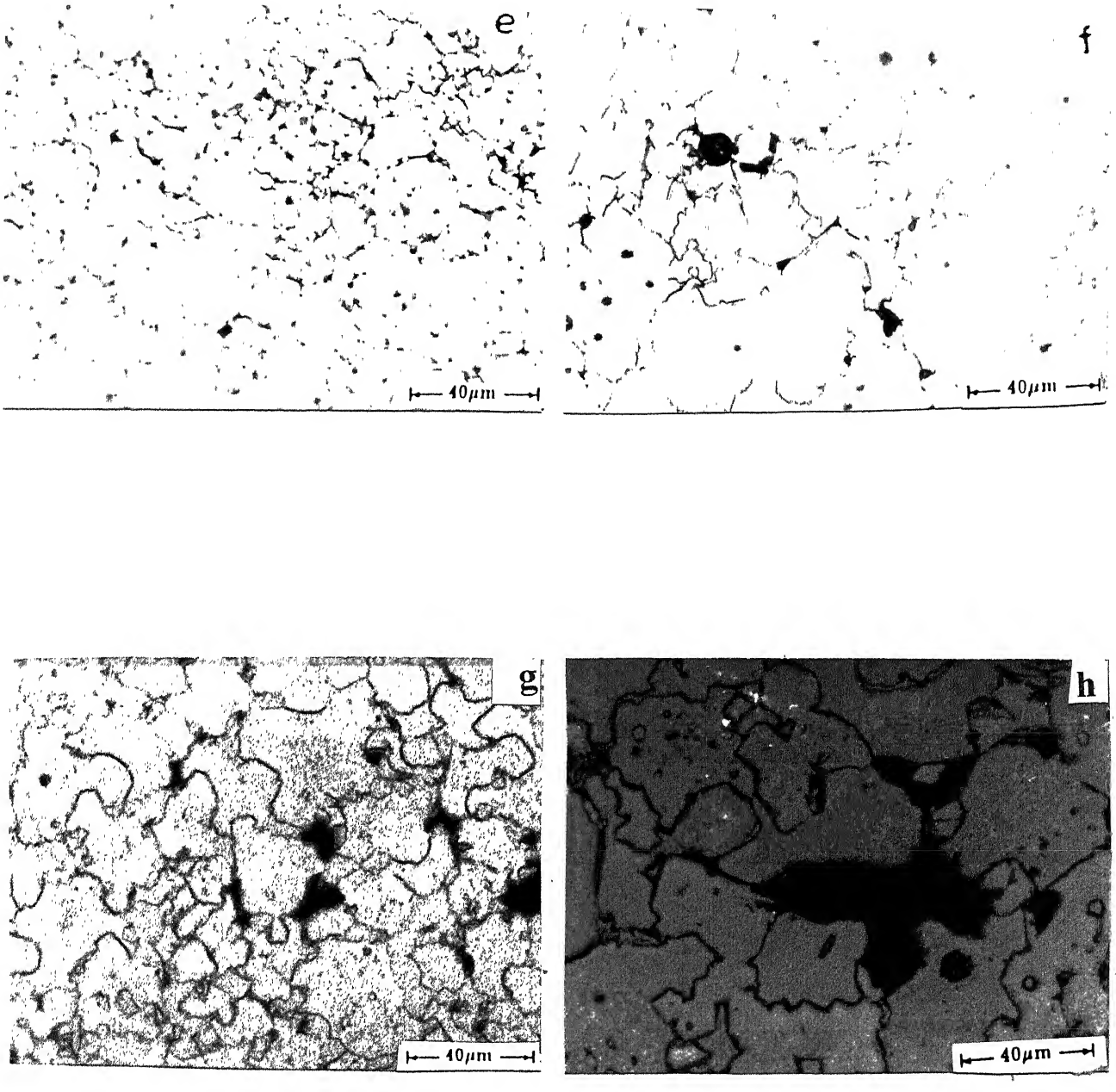

Fig. 3.24 Optical microstructures of 316L-10v/o Cr_3C_2 composites containing different amounts of CrB; sintered at 1200°C and 1250°C respectively in H_2.
1200°C - (a) 1w/o CrB, (b) 2w/o CrB, (c) 3w/o CrB, (d) 4w/o CrB
1250°C - (e) 1w/o CrB, (f) 2w/o CrB, (g) 3w/o CrB, (h) 4w/o CrB

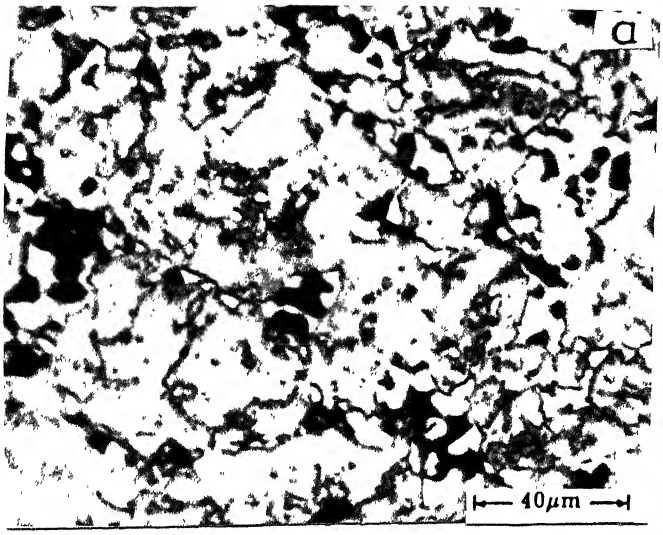
a
40μm

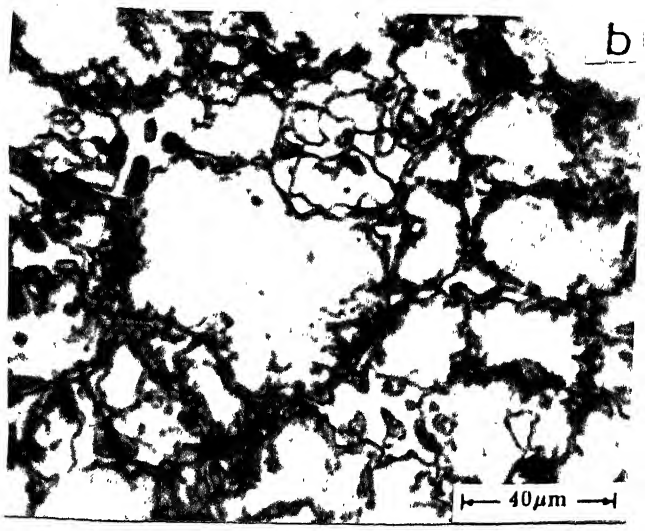
b
40μm

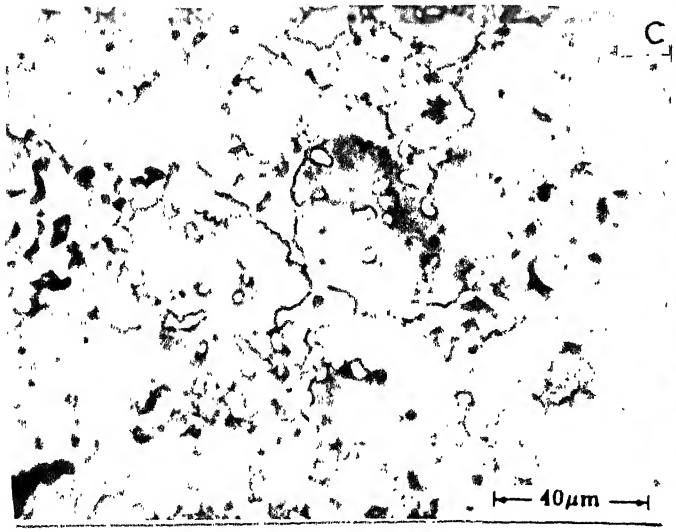
c
40μm

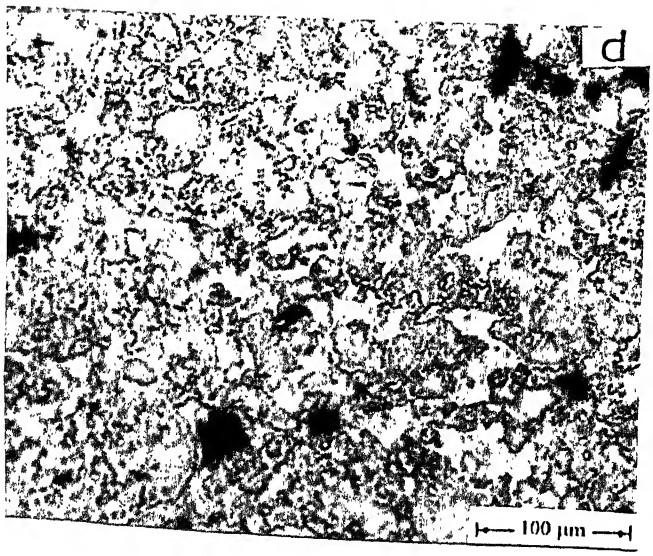
d
100 μm

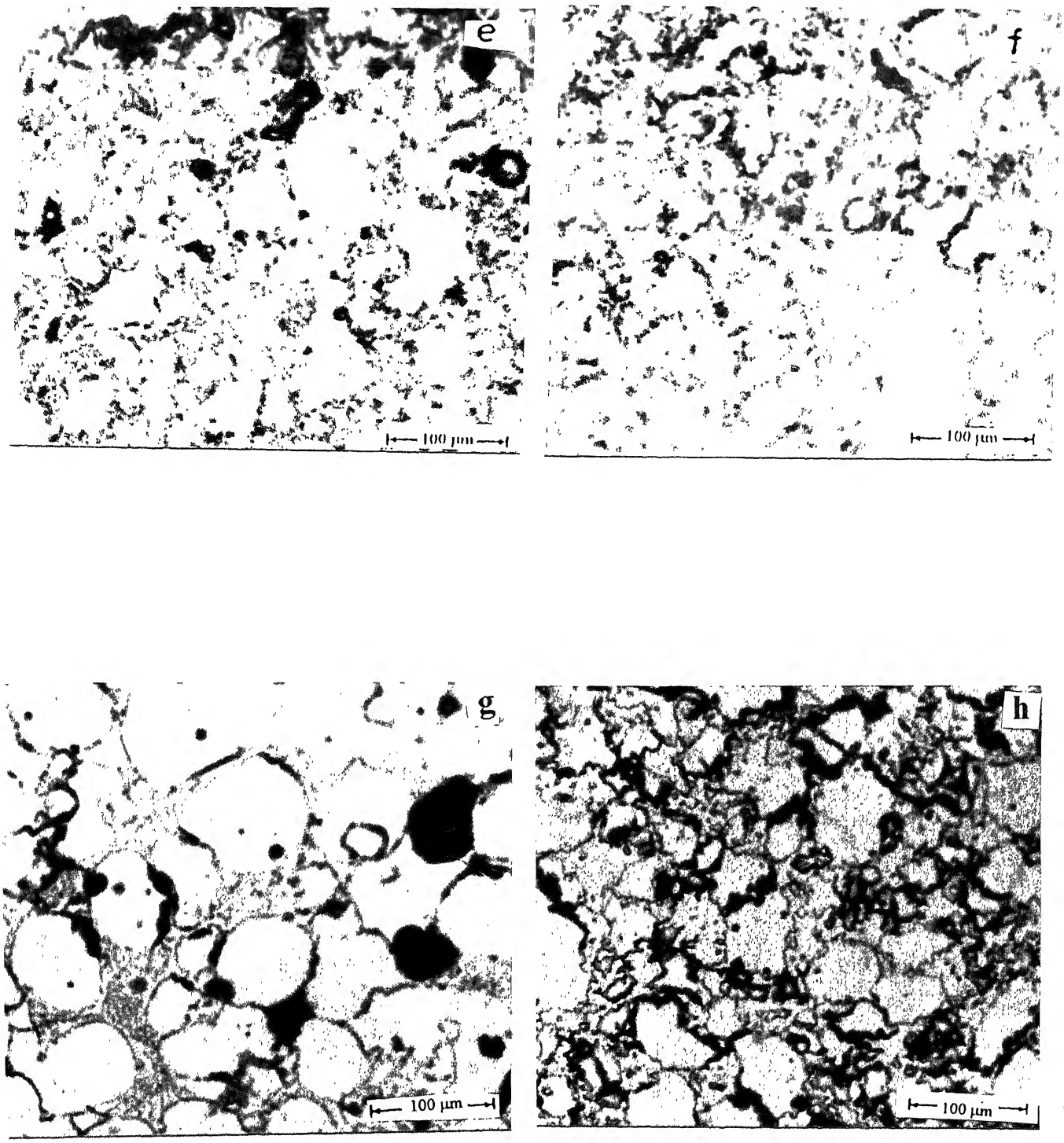

Fig. 3.25 Optical microstructures of 434L-10v/o Cr_3C_2 composites containing different amounts of CrB; sintered at 1200°C and 1250°C respectively in H_2.
1200°C - (a) 1w/o CrB, (b) 2w/o CrB, (c) 3w/o CrB, (d) 4w/o CrB
1250°C - (e) 1w/o CrB, (f) 2w/o CrB, (g) 3w/o CrB, (h) 4w/o CrB

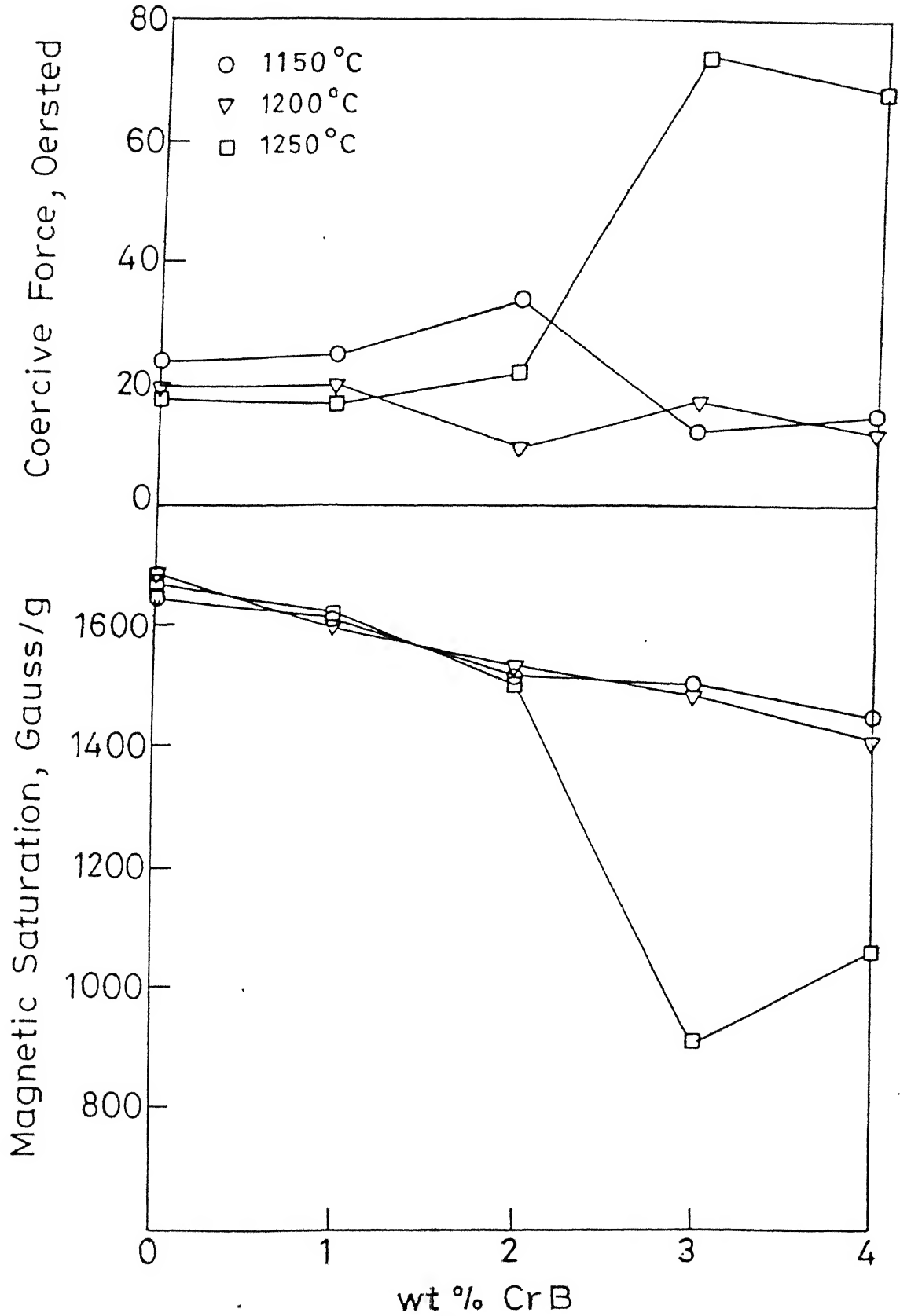

Fig. 3.26 Magnetic properties variation of 434L stainless steel containing Cr_3C_2 (10v/o) and CrB (0 - 4w/o) at different temperatures in H_2.

Chapter 4

Discussion

The results obtained in the present investigation are discussed in this chapter. The entire discussion has been divided into three parts. The sintered properties of 316L and 434L are discussed in part I. In part II sintered properties of 316L-434L composites with or without copper addition are discussed. Finally, part III describes the role of Cr_3C_2 and CrB additions on the sintered properties of 316L and 434L.

PART I

Sintering of 316L/ 434L Stainless Steels

4.1 Effect of Sintering Temperature

The increase in sintering temperature from 1150°C to 1350°C shows positive results such as an increase in sintered density, densification parameter and decrease in % sintered porosity (Figure 3.1). This is the natural consequence of higher diffusivity at elevated temperature resulting in better particle bond. Earlier workers [26,29] also obtained similar results though the levels of sintered densities were not same. Lal [26] got higher sintered density for 316L stainless steel powder under identical sintering conditions as compared to the present case due to the fact that his 316L powder was finer than the present one. However, Mukherjee [29] for 434L stainless steel obtained lower sintered density than the present case because of

lower green densites of the compacts prepared from the powder having different particle size distribution than the presently investigated one.

In the present investigation, sinterability of 316L is greater than 434L up to 1250°C sintering temperature but at 1350°C the same is higher for the later (Fig. 3.1). This is directly related with powder chemistry. In the selected 434L oxygen content is higher than 316L as revealed in the chemical compositions given in section 2.1. The prevalent dew point (-35°C) is not sufficient enough to remove the oxides of silicon and chromium up to 1250°C. But when the temperature is raised to 1350°C, required dew point of gas is also raised for reduction of oxides (Fig. 1.6). Thus the existing dew point *i.e* -35°C is sufficient enough to reduce the oxides mentioned earlier. Additional reason may be better diffusivity of 434L due to its bcc structure.

Coming to microhardness, it is observed that microhardness decreases with increasing sintering temperature. This is attributed to grain growth at higher temperature. Earlier workers [26,29] obtained opposite trend i.e higher hardness after higher temperature sintering but their measurements were on macrohardness. Their results were explained in terms of densification, as higher densification minimizes interference of porosity during hardness tests.

From literature [59] it is known that the microhardness of 434L is higher than 316L. This feature is reflected in the present investigation. Higher microhardness of 316L in N_2 sintering atmosphere than the same in H_2 may be explained on the basis of austenite stability in the former. However, due to limited solubility of N_2 in 434L as compared to 316L, matrix of the former softens due to probable depletion of Chromium to form Cr_2N precipitates at grain boundaries.

Grains of 434L are bigger than 316L (Fig. 3.1) as a result of higher diffusivity of 434L due to its more open structure (bcc) than fcc 316L.

Coming to magnetic properties, coercivity is zero for 316L because austenetic stainless steel is a paramagnetic material. Coercivity of 434L is highest after 1150°C sintering in H_2 atmosphere (Fig. 3.3). This is because of small grain size and relatively high hardness value. As the sintering temperature increases, coercivity decreases with increase in permeability as a consequence of higher density coupled with grain growth. As sintering temperature increases magnetic saturation also increases, the reason being similar to above.

4.2 Effect of Sintering Atmosphere

It is an established fact that water atomized stainless steel powders contain some oxygen in the form of Cr_2O_3. Sintering in hydrogen reduces surface oxide to some extent. The reduction of Cr_2O_3 promotes a greater degree of bonding in the sintered compacts. But this reduction is not possible either in N_2 or in vacuum. So sintered density and densification parameter is higher in H_2 than other two sintering atmospheres (Fig.3.4). % porosity level of 434L is higher than 316L at sintering temperature of 1250°C. This is because of the fact that in this case dew point of the sintering atmosphere is not sufficient enough to reduce Cr_2O_3. During vacuum sintering the extent of vacuum was not adequate for oxide reduction.

Microhardness of 316L is highest in N_2 sintering because of strengthening effect of N_2 but for 434L it is highest in H_2 atmosphere (Fig.3.4). This is mainly because of small grain size compared to other two atmospheres.

Grain size is smaller in N_2 sintering for 316L as N_2 prevents grain growth. In case of 434L small grains are found after H_2 sintering (Fig.3.4) because of the presence of large amount of alloying elements in the matrix, whereas there is no restriction of grain growth in N_2 or in vacuum due to alloying element loss either by Cr_2N precipitation or by vaporization.

Coming to magnetic properties, coercivity of 316L is zero in all sintering atmospheres except in vacuum (Fig.3.6). This may be due to formation of some martensite because of the probable variation in the overall composition as a result of vaporization loss. Coercivity for 434L is lowest in H_2 sintering atmosphere, in spite of smaller grain size in this atmosphere compared to other two atmospheres. The reason appears to be better reduction of oxides which minimizes coercivity. Magnetic saturation of 434L is highest when sintered in N_2 because of the reasons already stated earlier.

4.3 Effect of N_2 Content and Particle Size in 316L

Several studies reported that many properties of austenetic stainless steel are improved by increasing the interstitial nitrogen concentration [41-45] for example, high N_2 content increases tensile strength both at cryogenic and at elevated temperature. Fine powder size and extended time temperature cycles used in P/M permits N_2 concentration to be enhanced during thermal treatment. Some of the above observations are reflected in the present study.

% porosity decreases with the increase in fineness of powder (Fig.3.8). This is because sinterability increases as particle size decreases. As a result densification of +270($> 53\mu$m) is greater than +230($> 63\mu$m). Densification of 316L(ANVAL) is more because of higher green density of powder due to round shape with better apparent density in contrast to 316L(AMETEK).

Coming to microhardness, it is higher for +230 mesh powder based compacts of 316L (ANVAL) due to their higher N_2 content which strengthens the matrix. But for +270 mesh size based compacts, microhardness is higher for 316L AMETEK make than that of ANVAL make (Fig.3.8). The reason may be that the former being irregular in shape with larger surface area contains larger amount of impurities which aid in increasing microhardness.

Coming to grain size, increasing sintering period has no effect in grain coarsening for 316L (ANVAL) because of its higher N_2 content which prevents grain growth. Grain coarsening of 316L(AMETEK) is noticeable (Fig.3.8) due to larger driving force associated with irregular shape.

PART II

Sintering of 316L-434L Composites with or without Copper Addition

4.4 Sintering of 316L-434L Composites

It is well known fact that ferritic stainless steel increases yield strength and provides resistance to stress corrosion cracking, whereas austenitic steel imparts toughness along with good corrosion resistance. Keeping this in view, a mixed structure of ferrite and austenite would offer good corrosion resistance along with high strengths and reasonable toughness. The attention of stainless steel powder manufacturers has not yet gone to produce commercial grade ferrite-austenite duplex stainless steels. A reasonable way is, therefore, to study 316L-434L premix sintered compacts.

As evident from the result (Fig. 3.10), densification increases with increase in sintering temperature. This is a natural consequence of higher degree of driving force at higher sintering temperatures. % Sintered porosity after 1350°C sintering is much less when 434L

content in 316L is 40w/o or more. This is because of the introduction of bcc ferrite phase which enhances sinterability due to greater diffusivity. Above 40w/o of 434L no noticeable change in densification is observed.

Results of microhardness variation show that after 1150°C sintering, with increase in 434L addition microhardness increases (Fig.3.10). This is attributed to intrinsic higher hardness of 434L due to higher chromium content, as it gives rise to a number of intermetallic phases (ki. σ etc). It is also observed from microstructures (Fig.3.11) that some of the composites have two distinct phases. Those phases have been tentatively lebeled with the help of well known Shaeffler Diagram shown in Figure 4.1. Chromium and Nickel equivalent have been calculated for each composition using following formulae: [49]

Cr_{eqv} = Cr + 2 Si + 1.5 Mo + 5 V + 5.5 Al + 1.75 Nb + 1.5 Ti + 0.75 W

Ni_{eqv} = Ni + Co + 0.5 Mn + 0.3 Cu + 25 N + 30 C.

Calculated values and ratio of Cr_{eqv} and Ni_{eqv} are given in Table 4.1. Points for each composition of the composite have been marked in the diagram. This plot suggests ferrite austenite two field up to 40w/o 434L in the composite but above that it suggests phase mixture of ferrite + austenite + martensite. Phase stability, when confirmed with the microstructural results. reveals that in the composite systems containing 40 and 60w/o are invariably two phases i.e α and γ whereas for the border line compositions i.e 20 and 80w/o 434L containing composites, only single phase is revealed. The divergence in microhardness values in case of 80w/o 434L composite indicates the possibility of two phase existence. However, such features are not observed in case of 20w/o 434L composite. Metallographical investigation does not confirm presence of martensite. This can be attributed to inadequate homogenization of the alloys prepared by premix route. In other words, the use of Shaeffler diagram in the present case is mere indicative one. It is further interesting to note that the revealation of two phases is only in those cases where the composites were sintered at high temperature i.e 1350°C.This confirms that such phases are not microstructurally detectable in porous compacts.

The largest grain size of pure 434L among all composites after any sintering (Fig.3.10) can be attributed to greater atomic mobility due to its open bcc ferrite structure.

Coming to TRS variation, increase in TRS with 434L addition in austenitic stainless steel may be due to alloy strengthening effect. TRS of 60w/o 434L containing composite is higher than its 80w/o 434L containing counterpart as the former has larger share of tough austenite phase. This is also confirmed from SEM fractographs (Fig.3.13), which shows dimples in 60w/o 434L-316L composite suggesting ductile fracture whereas in a still ferrite

rich composite (80w/o 434L-316L) presence of both dimples and cleavage fractures exist.

Coming to wear behaviour it is noticed that wear loss is minimum for 316L and maximum for 434L (Fig.3.12). Minimum wear loss of 316L is attributed to its high work hardening rate compared to 434L. Among straight stainless steels the wear loss in 434L ferritic stainless steel is significant, while in case of 316L austenitic stainless steel, there is no wear. It appears that addition of 434L in 316L optimizes hardening and toughening, with a result that the material removal during wear is absent. However the only exception is 20w/o 434L containing composite, which has wear response more or less similar to 434L. Reason for such behaviour is not clear.

The decrease in coercivity of the composites with increase in sintering temperature (Fig.3.16) is an outcome of grain coarsening. Magnetic saturation of 316L-434L composites increases with increase in sintering temperature due to greater amount of densification at higher temperature because less pore density increases magnetic permeability. The deviation from linearity in magnetic saturation variation with respect to composition suggests the effect of phase mixture.

It was reported earlier [118] that the main mechanism affecting the low corrosion resistance of the sintered austenitic stainless steel in 1(N) H_2SO_4 is the evolution of hydrogen concentration cells due to electrolytic stagnation in the interconnected pores. In addition, Chromium depletion processes due to carbide or other phases precipitation such as Cr_2N, σ etc act synergistically with morphological factor and reduce the corrosion resistance. Pohl [119] observed better corrosion resistance of ferrite-austenite duplex stainless steel in media which otherwise tend to selective corrosion attack on one phase. The typical 'pancake' microstructure of such steels has been attributed to microstructural blocking effect resulting in higher corrosion resistance [119]. In the present investigation % weight loss increases rapidly for either 316L or 20w/o 434L in it (Fig.3.16). This is attributed to the larger porosity in those two materials compared to others (Fig.3.10) and also due to the other phenomenon, as stated earlier. No weight loss in 1(N) H_2SO_4 solution after an exposure time of 360 hours for 40 and 60w/o 434L containing composites may be due to the same effect as observed by Pohl [119] because the above mentioned composites also posses 'pancake' structure (Fig.3.11).

4.5 Effect of 2 mass % Copper Addition in 316L-434L Composites

Addition of copper forms liquid phase during sintering in the presently selected sintering temperature of 1350°C. Such an addition markedly increases the sinterability because of faster material transport. This is evident from higher sintered density for the copper containing composites (Fig.3.17) compared to that for composites without any copper (Fig.3.10). Effect of copper addition in reducing porosity is higher for 434L rich composites because of combined effect of liquid phase sintering and enhanced diffusivity in ferrite phase.

The lower microhardness value of copper containing composites can be interpreted from the variation of Cr_{eqv}/Ni_{eqv} ratio with respect to composite composition (Fig.4.2). It reveals that in austenitic stainless steel rich composites, the variation is sluggish in contrast to ferritic stainless steel rich composites. Similar plot for composites containing 2 mass% Cu, shows lower position than the corresponding Cu free composites. Uniform lowering of this ratio is reflected in mechanical properties variation such that the hardness values are invariably lower for any copper containing composites. It is well known fact that hardness of ferritic stainless steel with higher Cr_{eqv}/Ni_{eqv} is higher than that for austenitic stainless steel. Besides, coarse grain size of copper containing composites due to liquid phase sintering also contributes in lowering the hardness. Copper free composites show two phase ferrite-austenite structure when 434L content is 40w/o or more. But for Cu containing composites, the two phases are observed only when 434L content of the composites is 80w/o. Possible reason for this may be copper's ability to stabilize austenite phase.

Coming to magnetic properties, coercivity of 40w/o 434L containing composite is maximum because of its smaller grains (Fig.3.17). Coercivity is directly related with grain size, such that it is reduced for 434L due to large grain sizes. In general coercivity is lower for copper containing composites than composites without copper, because such addition imparts grain coarsening in the composites. Copper addition in composites also causes lowering of magnetic saturation compared to their counterpart without copper, because a diemagnetic material like copper pins down domain wall movement.

Effect of copper addition on the corrosion behaviour of 316L in 1(N) H_2SO_4 has been reported [120]. Improved corrosion resistance after copper addition has been attributed to the enhancement of the passivation process of sintered austenitic stainless steel due to cathodic depolarization effect of hydrogen evolution and oxygen reduction. Copper inhibits the attack of 316L in H_2SO_4 by shifting the corrosion potential from an active to a passive state. In

another study [121] it is confirmed that copper has a detrimental effect on the passivity of the ferritic stainless steel. It is suggested that anodic dissolution of metallic copper would produce a small surface fraction of active sites from which local dissolution of passive film starts which leads to complete breakdown. Copper in conjunction with molybdenum appears to promote the repassivation of steel because of significant suppression of active dissolution current. Role of copper has been labeled highly controversial for two phase ferrite-austenite wrought stainless steels particularly because Cu-rich precipitates could be pit initiation sites [122]. Combrade [123] *et.al* suggested copper to be beneficial because of the synergism between copper and moybdenum in the ferrite and copper and nitrogen in the austenite. Some of the above observations are reflected in the present results such that % weight loss in 1(N) H_2SO_4 is lowered after 2 mass% copper addition in either 316L or 434L (Fig.3.16&3.19)

. Reason may be the same as stated earlier [120,121]. But the impairment of corrosion resistance of 316L-434L composites with copper addition observed in the present study may be, therefore, due to chemical heterogeneity of the structure.

PART III

316L and 434L Composites Containing Cr_3C_2 and CrB

4.6 Effect of Cr_3C_2

In case of 1150°C sintering, lowering of sintered density and densification parameter occurs after Cr_3C_2 addition in either 316L or 434L stainless steel. This is mainly due to inhibition of sintering in the presence of hard Cr_3C_2 particles. The increase in sintering temperature from 1150°C to 1250°C shows an improvement in densification for both the composites (Fig.3.20). This is a natural consequence of higher diffusivity at elevated temperature, resulting in better composite bonding. This is confirmed from the microstructural study (Fig.3.21A and Fig.3.21B).

Coming to microhardness, it is observed that microhardness of 316L based composite is higher than that of straight 316L. This is attributed to intrinsic higher hardness value of Cr_3C_2. But microhardness of 434L based composite is lower than that of straight 434L stainless steel. This appears to be the consequence of depletion of chromium atoms from the steel and getting combined with Cr_3C_2 to form other lower carbides.

Coming to magnetic properties, coercivity of both 316L and 316L based composites is zero because of the reasons stated in earlier part of the discussion. Reasons, for higher coercivity of 434L after 1150°C sintering and higher magnetic saturation of straight 434L stainless steel are discussed in earlier part of forgoing discussion.

4.7 Effect of CrB Addition

Processing of stainless steel via press and sinter route generally results in porosity greater than 10%. Any attempt to decrease porosity level demands higher sintering temperature (>1350°C) and time (>1h). Significant cost savings are possible if sintering is carried out at lower sintering temperature, for achieving densification. This is possible if sintering aids are used. CrB has been used as an additive by various researchers [100,101] as it forms an eutectic liquid phase at around 1240°C [101]. In the present investigation, it is observed that after 1250°C 2w/o CrB containing composite attains a high density (~97%) (Fig.3.23).

This is the natural consequence of liquid phase sintering. However, no further improvement in sintered density is observed beyond 2w/o CrB. Above 2w/o CrB slumping of 316L composites occurs. However, formation of liquid phase at 1200°C may not be ruled out because 3w/o CrB containing composite attains a sintered density as high as 90% of the theoretical density at that temperature. Such a feature is due to lowering of solidus because of boron addition in the form of CrB.

Coming to microhardness, 2w/o CrB with 316L based composite has highest value when sintering temperature was 1250°C. This may be due to formation of eutectic melt. For 434L composites microhardness increases with increase in CrB addition after 1250°C sintering, which may be due to enrichment of matrix by chromium as a result of its diffusion from CrB.

Coming to grain size variation, relatively large grains of 316L based composites are observed when CrB additive was 3w/o or more and sintering temperature was 1250°C(Fig.3.24). This is attributed to the formation of extra liquid as 2w/o CrB gives enough liquid for significant densification (Fig.3.23). For 434L based composites largest grain is observed with 3w/o additive after 1250°C sintering (Fig.3.25), which may be attributed to liquid phase sintering. However, why grains of 4w/o CrB containing 434L based composites are smaller than its 3w/o CrB containing counterpart after 1250°C sintering is not clear.

Coming to magnetic properties, it is observed that all composites of 316L, irrespective of CrB content, have zero coercivity. The reason has been discussed earlier. For 434L based composites, coercivity is highest for 3w/o CrB containing composite sintered at 1250°C because of its higher hardness (Fig3.26). Since, in case of 4w/o CrB containing composites the grain size is similar to that of straight 434L, the role of hardness appears to be predominating factor in achieving high coercivity. Generally magnetic saturation increases with increase in sintering temperature. The present opposite trend may be attributed to probable evolution of some phases which could not be confirmed.

le 4.1 Chromium and nickel equivalents of investigated 316L - 434L composites with or without Cu.

Materials	Cr_{eqv}	Ni_{eqv}	Ni_{eqv} (Cu)	$\frac{Cr_{eqv}}{Ni_{eqv}}$	$\frac{Cr_{eqv}}{Ni_{eqv}}$ (Cu)
316L	22.09	14.925	15.525	1.48	1.42
316L-20 w/o 434L	21.642	12.222	12.822	1.77	1.68
316L-40 w/o 434L	21.194	9.519	10.119	2.22	2.09
316L-60 w/o 434L	20.744	6.816	7.416	3.04	2.79
316L-80 w/o 434L	20.238	4.113	4.713	4.93	4.30
434L	19.85	1.41	2.01	14.07	9.87

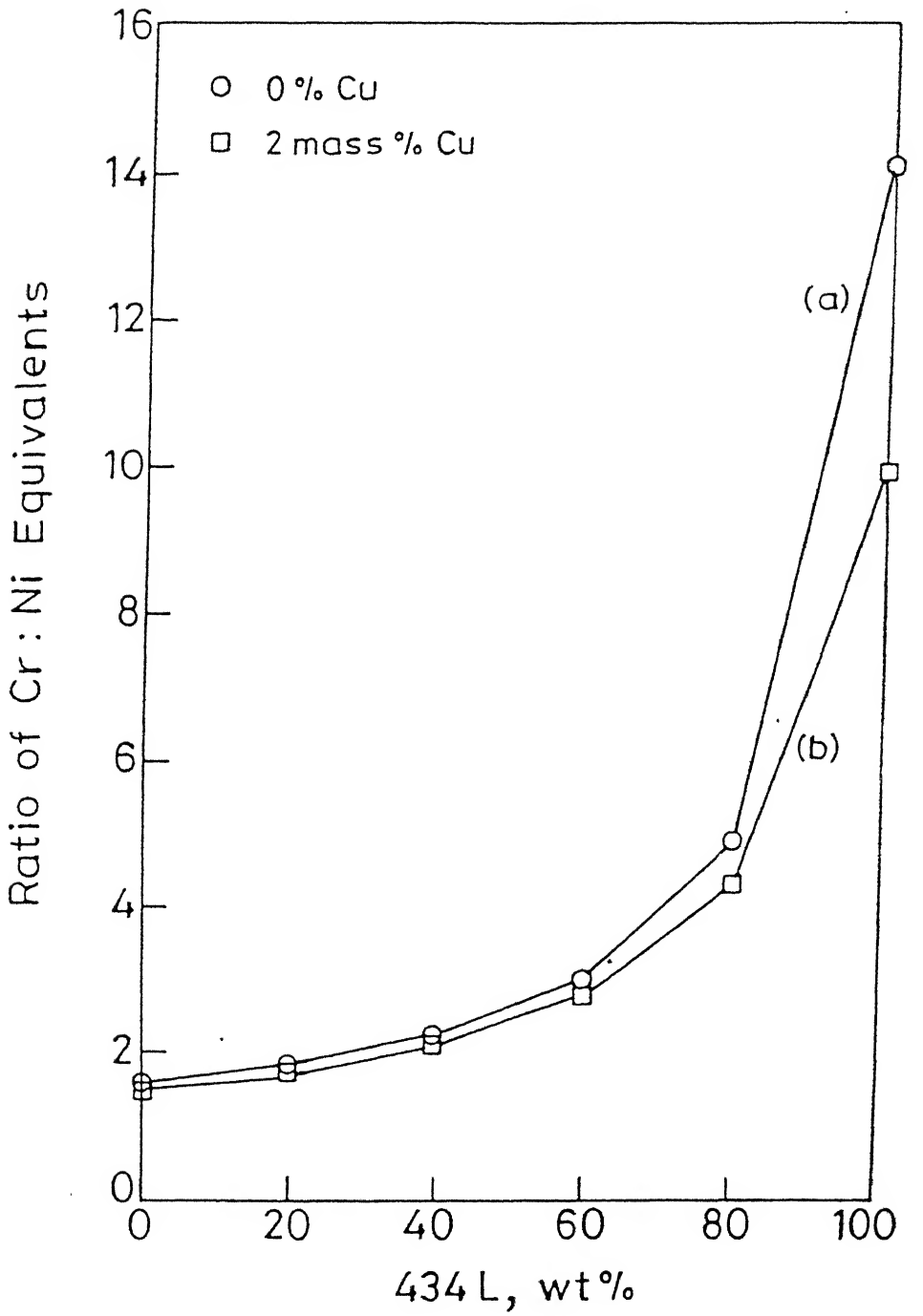

Fig. 4.2 Ratio of Cr_{eqv} to Ni_{eqv} vs. compositions of 316L-434L composites containing (a) 0 mass % Copper and (b) 2 mass % Copper.

Chapter 5

Conclusion

Considering the results and discussion of the present investigation, the following conclusion can be drawn:

PART I

1. Sinterability of 316L is greater than 434L up to 1250°C, but after 1350°C the same i higher for the latter. The sintered 434L steels exhibit bigger grain sizes as compare to 316L.

2. Microhardness decreases with increasing sintering temperature for both 316L and 434I stainless steels. The values for 434L are higher than those for 316L irrespective of sin tering temperature. However for 316L it is higher in N_2 atmosphere than H_2 atmospher whereas the same is opposite for 434L.

3. Magnetic coercivity of 316L is zero irrespective of sintering temperature and atmo sphere. Magnetic saturation of 316L is negligible as compared to 434L. But for 434L coercivity is highest after low temperature sintering. Magnetic saturation of 434L in creases with increasing sintering temperature.

4. Microhardness of 316L (ANVAL) with higher N_2 content is higher when particle size is coarse. But for 316L (AMETEK) with lower N_2, it is higher as fineness of particles increases. Increasing sintering period has no effect in grain coarsening of 316L with higher N_2 content.

PART II

5. Densification increases with increasing sintering temperature for 316L-434L composites. % Porosity decreases with increase in 434L content only after 1350°C sintering. Copper addition promotes densification.

6. Ferrite-austenite two phase structure is observed for 40 and 60w/o 434L containing composites after 1350°C. Divergence of microhardness in 80w/o 434L containing composite also suggests possibility of two phases. Copper addition stabilizes austenite phase in 316L-434L composites. Only 316L-80w/o 434L composite shows two phase ferrite austenite structure.

7. 316L-60w/o 434L composite exhibit maximum TRS value. Addition of copper lowers microhardness of composites and increases grain size of the same.

8. Wear loss during sliding wear is minimum for straight 316L and maximum for straight 434L. For composites, the values are intermediate.

9. Corrosin weight loss in 1(N) H_2SO_4 is maximum for 316L or 316L with 20w/o 434L after any exposure time. 40 and 60w/o 434L containing composites remain immune to the same after any exposure time. Copper addition lowers corrosion weight loss for straight stainless steels and 20w/o 434L containing composite but above that it increases corrosion weight loss.

10. Coercivity of 316L-434L composites decreases with increase in sintering temperature whereas magnetic saturation increases with increase in sintering temperature. Copper addition impairs coercivity and magnetic saturation of the composites.

PART III

11. Cr_3C_2 addition in 316L stainless steel increases microhardness but the reverse is true for 434L.

12. After 1250°C, 316L based composites attain near by full density with 2w/o CrB whereas 434L based composites attain similar densification level with 3w/o CrB. Relatively large grains are observed after 1250°C for both 316L and 434L composites with 3w/o CrB.

13. No improvement in microhardness of 316L based composites with more than 2w/o CrB is observed after 1250°C sintering. But for 434L based composites microhardness increases with increase in CrB content after 1250°C sintering.

14. Magnetic coercivity or magnetic saturation of 316L based composite with any amount of CrB content is not different than that of straight 316L stainless steel irrespective of sintering temperature. 434L based composites with 3w/o CrB show highest magnetic coercivity and lowest saturation after 1250°C sintering.

References

1. (Ed.) J.R. Davis, Introduction to Stainless Steel , Davis & Associates, 1994, ASM International, Materials Park, p.89.

2. Vicente Chiaverni In 'Advances in Powder Metallurgy & Particulate Materials', eds. J.M. Capus and R.M. German, Vol.5, 1992, Metal Powder Industries Federation, Princeton, NJ, p.359

3. C.R. Mayne In 'Proceedings of Stainless Steel Powder Seminar', Detroit, February, 1965, Hoganas Corporation, NJ, p.13.

4. J.M. Ruiz, Prieto, W. Moriera, J.M. Torralba and L.E.G. Cambro, Powder Metallurgy, Vol.37, No.1, 1994, 57

5. J. Charles In 'Duplex Stainless'91 Steels', eds. J. Charles and S. Bernhardsson, Vol.1 Beaune, France, Oct. 1991, p.3

6. P. Beiss, Powder Metallurgy, Vol.34, No.4, 1991, 259

7. L. Nyborg and I. Olefjord, Powder Metallurgy, Vol.31, No.1, 1988, 33

8. Metals Handbook, Ninth Edition, Vol.7, Powder Metallurgy, ASM International, Ohio, 1984, p.100.

9. C. Molins, J.A. Bas and J. Planas In 'Advances in Powder Metallurgy & Particulate Materials', eds. J.M. Capus and R.M. German, Vol.5, 1992, Metal Powder Industries Federation, Princeton, NJ, p.345.

10. N. Deutzenberg and H. Gesell, Powder Metallurgy International, Vol.8, No.1, 1976, 14.

11. K.H. Moyer, International Journal of Powder Metallurgy and P/T, Vol.7, No.3, 1971, 9.

12. G.L. Pearson, Technical Bulletin Hoeganaes Corporation, Riverton, NJ, 1969, p.9

13. G.H. Reinshagen and R.P. Mason In 'Advances in Powder Metallurgy & Particulate Materials', eds. J.M. Capus and R.M. German, Vol.5, 1992, Metal Powder Industries Federation, Princeton, NJ, p.385.

14. D.L. Dyke and H.D. Ambs In 'Powder Metallurgy Applications, Advantages and Limitations', ed. Erhard klar, ASM, Ohio, 1983, p.123.

15. A. Stousy In 'Proceedings of Stainless Steel Powder Seminar', Detroit, Feb. 1965, Hoeganaes Corporation, NJ, p.27.

16. H.D. Ambs and A. Stousy In 'Handbook of Stainless Steel', Mc graw Hill, New York.

17. N.B. Shaw and R.W.K. Honeycombe, Powder Metallurgy International, Vol.9, 1977. 191.

18. Y. Imai and H. Hirotani, 'Powder Metallurgy', ed. W.Leszynsski, Interscience, New York,London, 1961, p.359.

19. R.P.H. Fleming, International Conference on Mechanical Behaviour and Nuclear Applications of Stainless Steel at Elevated Temperature, Varsee, Italy, 20-22 May, 1981.

20. R.M. German, Powder Metallurgy Science, 2nd edition, MPIF, Princeton, N.J, 1994, p.271.

21. S.K. Mukherjee and G.S. Upadhyaya, Oxidation of Metals, Vol.23, No.3/4, 1985, 177.

22. D.H. Rao and E. Klar In 'Modern Development in Powder Metallurgy', ed. H.H. Hausner et.al, MPIF, Princeton, Newjersy, Vol.13, 1980, p.247.

23. S. Lal and G.S. Upadhyaya In 'Modern Development in Powder Metallurgy', eds., P.U. Glusamseon and D.A. Gustafson, Vol.18, 1988, MPIF, Princeton, p.581.

24. H.S. Nayar, R.M. German and W.R. Johnson In 'Progress in Powder Metallurgy', Vol.37, 1981, p.1.

25. Howard I. Sanderow, International Journal of Powder Metallurgy, Vol.27, No.4, 1991, 309.

26. S. Lal, Ph.D Thesis, IIT Kanpur, June, 1988.

27. E. Klar, Metal Powder Report, March, 1988, 160.

28. I.D. Radomysel'skii, V.V. Shil'don and V.F. Tkachenko, Soviet P/M and Metal Ceramics, Vol.20, No.7, July, 1981, 448.

29. S.K. Mukherjee, Ph.D Thesis, IIT Kanpur, March 1984.

30. W.A. Kassyer and W.J. Huppmann In 'Proceedings of P/M'86', Dusseldorf, 7-11 July, 1986, p.325.

31. P.M. French and P.G. Mardon, International Journal of Powder Metallurgy & P/T, Vol.3, No.4, 1967, 65.

32. A. Stousy, Technical Bulletin Hoeganaes Corporation, Riverton, N.J, 1969, p.13.

33. A. Stousy and R.R. Holmes, Metal Progress, Vol.91, May 1967, 81.

34. George Otto In 'Modern Developments in Powder Metallurgy', eds. H.H. Hausner and W.E. Smith, Vol.6, 1974, MPIF, APMI, Princeton, N.J, p.293.

35. G. Lei, R.M. German and H.S. Nayer In 'Progress in Powder Metallurgy', Vol.39, 1984, MPIF, N.J, p.391.

36. C. Toennes and R.M. German, Powder Metallurgy International, Vol.24, No.3, 1992, 151.

37. W.D.Jones, Fundamental Principles of Powder Metallurgy, Edward Arnold (Publishers) Limited, 1960, London.

38. Eugene Andreotti In 'Proceedings of Stainless Steel Powders Seminar', Detroit, 25 February, 1965, Hogaenaes Corporation, N.J, p.57.

39. J. Rawers, F. Croydon, R. Krable and N. Duttlinger, The International Journal of Powder Metallurgy, Vol.32, No.4, 1996, 319.

40. J.H. Reinshagen and T.J. Bockiles In 'Advances in P/M & Particulate Materials', eds. M. Philips and J. Porter, Vol.3, NO.11, 1995, p.19.

41. J.W. Simons, G.S. Slavens and J.S. Dunning In 'Advances in P/M & Particulate Materials', eds. M. Philips and J. Porter, Vol.3, No.10, 1995, p.63.

42. H.I. Sanderow and T. Prucher, 'Advances in P/M & Particulate Materials', eds. M. Philips and J. Porter, Vol.3, No.10, 1995, p.13.

43. H.S. Nayer and B. Wasiezko, Metal Powder Report, Sept. 1990, 611.

44. G. Lei, R.M. German and H.S. Nayer, Powder Metallurgy International, Vol.15, No.2, 1983, 70.

45. T. Tunberg and L. Nyborg, Powder Metallurgy, Vol.38, No.2, 1995, 120.

46. W.F. Wang, Powder Metallurgy, Vol.37, No.1, 1994, 33.

47. D.B. Goldman and S. Hart, Materials Science and Engineering, 1985, 191.

48. M.A. Pao and E. Klar at the Meeting of APMI, New Orlans, 1983.

49. F.B. Pickering, Physical Metallurgy and the Design of Steels, Applied Science Publishers, London and New York, 1983, p.166.

50. W.C. Leslie, Physical Metallurgy of Steels, McGraw Hill, New York, 1983.

51. I.V. Nel'zind and I.D. Radomysel'skii, Soviet P/M and Metal Ceramics, Vol.20, No.12, 1981, 854.

52. T. Katoh, K. Kusada and T. Hisada, Metal Powder Report, June, 1984, 351.

53. A. Sharon, N. Melman and D. Itzhak, Powder Metallurgy, Vol.37, No.1, 1996, 67.

54. S.K. Chaterjee and M.E. Warwick In 'Modern Developments in Powder Metallurgy', eds. E.N. Aqua and C.I. Wlitman, Vol.16, 1985, MPIF, Princeton, p.277.

55. K. Kusada, T. Kato and T. Hisada 'Modern Developments in Powder Metallurgy', eds. E.N. Aqua and C.I. Wlitman, Vol.16, 1985, MPIF, Princeton, p.247.

56. A. Molinari, B. Tesi, A. Tiziani, L. Ferizzi and G. Straffelni, International Journal of Powder Metallurgy, Vol.27, No.1, 1991, 15.

57. A. Tiziani, A. Mollinari and J. Kazikor, Powder Metallurgy International, Vol.22, No.4, 1990, 17.

58. A. Sharon and D. Itzhak In 'Powder Metallurgy & Particulate Materials', eds. J.M. Capus and R.M. German, Vol.5, 1992, MPIF, Princeton, N.J, p.373.

59. W.F. Wang and Y.L. Su, Powder Metallurgy, Vol.29, No.3, 1986, 177.

60. W.F. Wang, Y.L. Su and D.C. Lo, Powder Met. Int. Vol.19, No.4, 1987, 15.

61. C. Lall In 'Advances in Powder Metallurgy and Particulate Composites', Vol.3, 1992, MPIF, p.135.

62. K.H. Moyer and J.B. Ryan In 'Modern Development in Powder Metallurgy', Vol.18, 1988, MPIF, p.757.

63. F.H. Hanejko, H.G. Rutz and C.J. Oliver In 'Advances in Powder Metallurgy and Particulate Composites', Vol.6, 1992, MPIF, p.375.

64. L.I. Frayman, D.R. Ryan and J.B. Ryan, Metal Powder Report, May, 1997, 44.

81. G.H. Lei and R.M. German In 'Proceedings of P/M-84', June 17-22, Toronto, Canada, 1984.

82. S.K. Mukherjee and G.S. Upadhaya, International Journal of P/M and Powder Tech., Vol.19, No.4, 1983, 283.

83. D. Itzhak and E. Aghion, Corrosion Science, Vol.23, No.23, 1983, 1085.

84. C. Ranninger, A. Torres, M.L. Aparicio et.al. In 'Sintering' 87', eds S. Somiya, M. Shimada, M. Voshimuva and R. Watanabe, Elsevier Applied Science, Barking (U.K), 1988, p.689.

85. S.H. Avner, Introduction to Physical Metallurgy, Second Edition, McGraw Hill New York, 1994, p.190.

86. G.E. Dieter, Mechanical Metallurgy, Third Edition, McGraw Hill, New York, 1988, p.212.

87. E.A. Bloch, Metals Review, Vol.6, 1961, 193.

88. D.L. Wood, Trans. AIME, Vol.215, 1959, 925.

89. A. Gatti, Trans. AIME, Vol.215, 1959, 753.

90. J.A. Lund, et.al., Lead Powder Metal Project, LM8, 1969, p.16.

91. R. Murphy and N.J. Grant, Powder Met.,Vol.10, 1962, 18.

92. K.M. Pwisky and N.J. Grant, Trans. AIME, Vol.221, 1961, 371.

93. J.S. Benjamin, Sci. Am., Vol.5, 1976, 234.

94. J.S. Benjamin and T.E. Volin, Metall. Trans., Vol.5, 1974, 1927.

95. A.N. Patel and W.E. Kuhn In 'Modern Development in Powder Met.', Vol.12-14, MPIF, Princeton, NJ, 1980, p.27.

96. Ibid, p.195.

97. Y.Imai and H. Hirotani In 'Powder Metallurgy', ed. W. Lezynski, Interscience Publishers, N.W., 1961, p.158.

98. R.L. Sands, D.A. Philps and W.R. Morgan, Powder Metallurgy, No.10, 1962, 158.

99. S. Lal and G.S. Upadhaya, Materials Science Letter, Vol.6, 1987, 761.

100. N. Petersen In 'Proceedings of 12th Riso International Sysposium on Materials Science', eds. N. Hansen, D. Juuljensen, T. Leffers, T. Lorentzen, A.S. Pedersen, O.B. Pedersen and B. Ralh, 2-6 Sept., 1991, Roskilde, Denmark, p.581.

101. R.Tandon and R.M. German, International Journal of Powder Met, Vol.34, No.1, 1998, 40.

102. T. Oda and T. Daikoku, In 'Modern Development in P/M', Vol.5, MPIF, Princeton, 1971, p.159.

103. T. Doikoku and M.Ikenoga, J. Japan Soc. of Powders and Powder Met., Vol.18, 1972, 307.

104. B.A. Borok, et.al., Soviet Powder Met. and Metal Ceramics, Vol.59, 1967, 876.

105. E.T. Dnisenku and P. Van Asbrocek, Soviet Powder Met. and Metal Ceramics, No.9, 1972, 25.

106. R.E. Allen, General Electrical Co. and Contract, N00019-69-C0149, Jan., 1970.

107. Ibid N00019-70C-0232, Jan, 1971.

108. R.E. Allen and R.J. Perkins, ibid, N00019-71C-0232, April, 1972.

109. Ibid, N00019-72C-0271, May, 1973.

110. Ibid, N00019-72-0397, Nov., 1973.

111. R.L. Sands, et.al., Powder Met., Vol.3, 1981, 141.

112. S.K. Mukherjee and G.S. Upadhaya, The International Journal of Powder Met and Powder Tech. vol.19, 1989, 289.

113. S.K. Mukherjee and G.S. Upadhaya, Trans Powder Met. Ass. of India, Vol.10, 1983, 27.

114. J. Arthur, J. Inst. of Metals, 84 (1956), 327.

115. (Ed) C.J. Smithells, Metals Reference Book, Butterworth & Co. Ltd. Washington, 1962, p.695.

116. G.V. Samonov and I.M. Vinitskii, Handbook of Refractory Compounds, 2nd edition, Metallurgia, Moscow, 1976, p.102. (In Russian)

117. Metals Hand Book, Eight Edition, Vol.8, 1973, ASM International, Metals Park, Ohio, p.98.

118. D. Itzhak and E. Aghion, Corrosion science, Vol.24, No.2, 1984, 145.

119. Michael Pohl, Z.Metallkd., 86 (1995), 97.

120. D. Itzhak and P. Peled, Corrosion Science, Vol.26, No.1, 1986, 49.

121. M. Seo, G. Hultquist, C. Leygraf and N. Sato, Corrosion science, Vol.26, No.1, 1986, 949.

122. L.F. Garifas-Mesias and J.M. Sykes, Corrosion, Vol.54, No.1, 1998, 40.

123. P. Combrade and S.P. Audobard In 'Duplex Stainless'91 Steels', eds. J. Charles and S. Bernhardsson, 28-30 Oct., 1991, Beaune, France, p.257.